SCUOLA DI DOTTORATO
UNIVERSITÀ DEGLI STUDI DI MILANO-BICOCCA

Department of Earth and Environmental Sciences (DISAT)

PhD program in Chemical, Geological and Environmental Sciences
Cycle XXXV

Curriculum in Terrestrial and Marine Environmental Sciences

INTEGRATING NUMERICAL MODELLING AND 3D OPEN DATA DATABASES FOR GROUNDWATER MANAGEMENT IN MILAN METROPOLITAN CITY

Sartirana Davide

Registration number: 762798

Tutor: Prof. Franzetti Andrea

Supervisor: Prof. Bonomi Tullia

Prof. De Amicis Mattia

Coordinator: Prof. Malusà Marco Giovanni

ACADEMIC YEAR 2021/2022

Table of Contents

Abstract

Cities are intricate areas, where a multitude of elements interact. A change in the paradigm towards sustainability goals, as the limit of soil consumption, is determining a greater use of the subsurface, thus abandoning the urban horizontal sprawl. This results in increasing interactions between groundwater (GW) and the underground infrastructures (UIs). Thus, it is reasonable to think that in the next years a huge effort will be allocated to research in urban hydrogeology. Among the cities that worldwide have been affected by this issue, the city of Milan (Northern Italy, Lombardy Region) experienced a strong water table rise in the last decades, leading to flooding episodes for different categories of UIs. Considering that a future subsurface development has been already planned, this highlights the importance of adopting integrated strategies in the framework of both underground development and GW management.

Within this general scheme, the present PhD project has been divided into three parts, to provide a detailed definition of the urban conceptual model for the city of Milan, that could play a pivotal role and support decision-making processes in urban planning policies.

More specifically, the first part of the project deals with the reconstruction of a 3D geodatabase (3D GDB) for urban UIs. Using Open Data databases as the primary, but not unique source of information, three categories of subsurface elements (private and public car parks, subway lines) have been gathered within the 3D GDB. This information has been then combined with water table reconstructions of GW minimum and maximum conditions to identify the areas where the UIs were submerged by the water table.

In the second part, data-driven techniques have been applied to analyse GW time-series of the shallow aquifer, occupied by the UIs. Statistical and geospatial techniques were used to reach a better understanding of the hydrogeologic system, pinpointing the main potential variables influencing the water table levels. Consequently, four management areas have been identified to act as future geographic units, defining specific GW management strategies in relation to UIs.

In the third part, a local scale numerical model was implemented for the western part of the city to further evaluate GW/UIs interactions. In particular, GW infiltrations into UIs were quantified, leading to a better definition of the urban conceptual model. The numerical model was developed using MODFLOW-USG, and combining the HFB and the DRN packages to model the UIs.

The results of this project pointed out that the combination of these different tools could be beneficial to manage the interactions between GW and the UIs and to support the decision makers in urban GW management. In this way, proper strategies could be adopted to sustainably design the future subsurface development of the city.

Acknowledgments

First and foremost, I would like to express my gratitude to the two persons that helped and supported me since the beginning of my master thesis, and for the opportunity of this PhD. To Prof. Tullia Bonomi, for giving me the possibility of working on Milan city, thus getting more in touch with a familiar place, learning a lot about how complex but fascinating can be dealing with urban areas. Thanks also for helping me to understand how it is important to be rigorous when working with environmental data, otherwise it would be difficult to understand things, obtain reliable results and properly communicate them. Thanks for the continuous help in the last months, and for giving me the possibility of being part of such a multidisciplinary and talented group. An immense thank goes to Prof. Mattia De Amicis, for his continuous support, for sharing with me all his knowledge about GIS and Milan, and for giving me plenty of opportunities: from the summer school in Kazakhstan, to the possibility of working on Civil Protection themes, a topic that always fascinated me and useful to improve the way of communicating with people. Thanks also for always talking of themes that exceed from the university, and for being a good goalkeeper when playing football together.

Thanks also to Prof. Letizia Fumagalli, for her continuous interest and support during all my PhD, and for always sharing a lot of geological experience about the clay lenses in Milan subsurface, helping me to understand how it is important to properly deal with geological heterogeneities.

All my gratitude goes to Prof. Daniel Feinstein. Thanks for hosting me during my abroad period at UWM, and for all the nice time we spent together when I was in Milwaukee. Most of all, thanks for your teachings and for being a huge example of hard work, dedication, passion and humbleness. You are a great source of inspiration, because you reached a lot during your life, but you are always curious and ready for new challenges. Finally, the name of a genius is contained in your last name, and I firmly believe that it’s not by chance.

Thanks also to Rose Ann, for your extreme kindness and availability, for giving me a lot of information about Milwaukee and for sharing a lot of your memories. We're waiting for you to come to Italy to collect even more together.

A warm thank goes to Bill and Cathy: you hosted me and I will always be grateful for this. But, most of all, I enjoyed a lot the time we spent together: thanks for teaching me a lot about US, its politics, and for sharing with me a lot of the incredible experiences that you lived throughout your life. Thanks also for letting me know part of your family and friends: all of you taught me something that I will always try to bring with me. As for Rose Ann, I'm waiting for you to come to Milan.

Thanks to Dr. Marco Rotiroti for sharing his knowledge and for always playing the role of the internal reviewer of my articles during this period, trying to teach me which is the most effective way to write all the parts of a paper, thus helping the international reader to follow the thread of the speech.

A sincere thank goes to Dr. Veronica Nava, for all her kindness, the enthusiasm and the time she spent helping me with R, adjusting scripts to make them work effectively. It was a really challenging experience for me.

Thanks also to my office mates: to Dr. Mariachiara Caschetto, for her humanity, kindness and availability when asking for an advice. Thanks also for sharing with us all your funny experiences on public transport!

To Dott. Agnese Redaelli, for all the laughs and funny moments in this year and a half. I think that in the next years you'll become expert to understand jokes. I hope, but I'm also sure, that your PhD experience will be challenging and full of success.

A huge thank goes to Dr. Alberto Stefania: thanks for helping me since day one in the office, when I was travelling along all the subway lines to count steps to check how deep are the stations. Thanks for all the funny moments we shared and for reminding me that sometimes being practical is useful when working with models. You always teach me something new.

To Dr. Chiara Zanotti, for the plenty of laughs and for her scientific support: you are probably not fully aware, but you pushed me out of my comfort zone, as I have always been reluctant to statistics, but thanks to you now I have learnt a bit more how useful it can be when dealing with environmental data. Without your intuition, probably I would have not developed a part of my project. It was also nice to support you during your lessons, hoping to share even more experiences in the next years.

To my dear friend Dott. Luca Toscani, for all the moments we shared together during these years. I have learnt a lot from you, because you have a huge problem solving attitude and every time you know some new information to share. It's always stimulating to work with you, to try to find the best solutions to prepare an image, or to solve issues in our everlasting battle against the computer. But, mostly, thanks for you sincere friendship.

Thanks also to my friends and mates, Crive, Tommy, Roby and Teo, for all the memories we collected during our university journey: if I decided to keep on studying, it's also because of the nice time we spent together within these walls, that always make me think to the University as a nice place to stay.

I would like to thank my uncles, for always being a positive example to follow. In particular, a huge thank goes to Dario, for his continuous support and interest during all my life, for the thousands of moments shared together, including lots of holidays and suffered football matches.

Thanks to Alessandra, for all the unconditional love, happiness and thousands of moments that we shared together over our life journey, hoping to share many more in the next years; thanks for your continuous support especially in this last period, that was quite difficult and tiring: you were there trying to make me feel confident and not to go out of track. Life gave you some lemons, but you have been always able to make lemonade: this is just because you are strong and have a huge capability to overcome difficulties. I hope that you'll always keep your enthusiasm when doing everything.

Thanks to my sister, Chiara, for sharing all the aspects of our daily life. We have grown together and in these last years we are sharing even more about University, passions, and things to discuss. Now that your studies are almost over, I hope that you'll be able to find your way, whatever it is. I'll always try to be there if you need an advice or some support.

Finally, thanks to my parents, for all the continuous support and teaching throughout all my life. You've always been there to give me an advice if needed, leaving me the freedom to do thousands of experiences, try, fail, improve. Thanks for always reminding me to behave politely: it is something I'll always try to do. You're simply the best example me and Chiara could have asked for.

Chapter 1: Introduction

Urban areas are complex systems, where different topics get in touch. In particular, subsurface is one of the most profitable parts of these environments; here, four main resources can be considered basics for liveability: materials, energy, space and water (Vázquez-Suñé et al. 2005; Parriaux et al. 2007; Vähäaho 2014). GW represents globally the most important source of freshwater (Li et al. 2013a); its importance is related to its links with scientific, economic, social, legal and political aspects (Vázquez-Suñé et al. 2005; Hunt et al. 2016). For this reason, researchers and stakeholders constantly pay attention to overexploitation, depletion and pollution problems. In urban areas, among the various needs, it is exploited for drinking, sanitary, thermal, industrial, and also recreational purposes (Danielopol et al. 2003; Afonso et al. 2020). In the last decades, urban transformations and intense human activities have progressively determined an intense use of this valuable resource, threatening both its quality and availability (Schirmer et al. 2013; La Vigna 2022). Nowadays, space hunting has moved towards a three dimensional trend, limiting the urban sprawl in the horizontal direction. This increased tendency to "go underground" (Bobylev 2009) has determined a strong interaction between GW and the growing number of UIs (Koziatek and Dragićević 2017). Mostly, these situations took place worldwide as a direct consequence of a water table rising triggered by an intense industrial decommissioning phase (Wilkinson 1985; Vazquez-sune and Sanchez-vila 1999; Hayashi et al. 2009; Lamé 2013; Gattinoni and Scesi 2017).

These interactions can introduce risks and disturbances both for GW and the infrastructural elements: a) GW flow can be impacted, and a fragmentation of the aquifer can occur, with an influence on GW mass balance (Attard et al. 2015); UIs can also be damaged, with flooding of lower levels, corrosion of foundations (Vázquez-Suñé et al. 2005; Attard et al. 2016) and stability issues determined by an intense water pressure (Liu et al. 2022); b) GW temperature can be impacted, due to the high density of UIs that can alter the geothermal potential of the shallow GW system, combined with the increase use of shallow geothermal installations (Epting and Huggenberger 2013; Bayer et al. 2019; Noethen et al. 2022); consequently, c) GW quality can be affected, as the formation of the subsurface urban heat island (SUHI) can alter the chemical-physical properties and the bacterial community of GW (Blum et al. 2021; Previati et al. 2022). Moreover, other direct (materials used for UIs) and indirect reasons (i.e. inflow of pollutants due to GW drawdown) (Chae et al. 2008; Attard et al. 2015) can determine a risk for water quality.

All these considerations highlight the importance of a coordinate management of all the resources in underground urbanism (Li et al. 2013b; Li et al. 2013c). In this sense, the adoption of centralized data platforms gathering all the information about the underground elements could properly support decision makers (Admiraal and Cornaro 2016; Di Salvo et al. 2020). Through a deep knowledge of the subsurface, city planners must operate to give the right value to each topic, trying to create resilient, sustainable and liveable cities (Bricker et al. 2017). To do so, the development and application of different tools (i.e. numerical modelling) is needed to assess the current variability and how to relate it with possible changes in the underground framework, thus supporting the stakeholders in their decision-making processes (Attard et al. 2017).

References

Admiraal H, Cornaro A (2016) Engaging decision makers for an urban underground future. Tunn Undergr Sp Technol 55:221–223. https://doi.org/10.1016/j.tust.2015.08.009

Afonso MJ, Freitas L, Marques JM, Carreira PM, Pereira AJSC, Rocha F, Chaminé HI (2020) Urban groundwater processes and anthropogenic interactions (Porto region, nw portugal). Water (Switzerland) 12(10):1–26. https://doi.org/10.3390/w12102797

Attard G, Cuvillier L, Eisenlohr L, Rossier Y, Winiarski T (2016) Deterministic modelling of the cumulative impacts of underground structures on urban groundwater flow and the definition of a potential state of urban groundwater flow: example of Lyon, France. Hydrogeol J 24(5):1213–1229. https://doi.org/10.1007/s10040-016-1385-z

Attard G, Rossier Y, Winiarski T, Eisenlohr L (2017) Urban underground development confronted by the challenges of groundwater resources: Guidelines dedicated to the construction of underground structures in urban aquifers. Land use policy 64:461–469. https://doi.org/10.1016/j.landusepol.2017.03.015

Attard G, Winiarski T, Rossier Y, Eisenlohr L (2015) Review: Impact of underground structures on the flow of urban groundwater. Hydrogeol J 24(1):5–19. https://doi.org/10.1007/s10040-015-1317-3

Bayer P, Attard G, Blum P, Menberg K (2019) The geothermal potential of cities. Renew Sustain Energy Rev 106(February):17–30. https://doi.org/10.1016/j.rser.2019.02.019

Blum P, Menberg K, Koch F, Benz SA, Tissen C, Hemmerle H, Bayer P (2021) Is thermal use of groundwater a pollution? J Contam Hydrol 239(February):103791. https://doi.org/10.1016/j.jconhyd.2021.103791

Bobylev N (2009) Mainstreaming sustainable development into a city's Master plan: A case of Urban Underground Space use. Land use policy 26(4):1128–1137.

https://doi.org/10.1016/j.landusepol.2009.02.003

Bricker SH, Banks VJ, Galik G, Tapete D, Jones R (2017) Accounting for groundwater in future city visions. Land use policy 69(July):618–630. https://doi.org/10.1016/j.landusepol.2017.09.018

Chae GT, Yun ST, Choi BY, Yu SY, Jo HY, Mayer B, Kim YJ, Lee JY (2008) Hydrochemistry of urban groundwater, Seoul, Korea: The impact of subway tunnels on groundwater quality. J Contam Hydrol 101(1–4):42–52. https://doi.org/10.1016/j.jconhyd.2008.07.008

Danielopol DL, Griebler C, Gunatilaka A, Notenboom J (2003) Present state and future prospects for groundwater ecosystems. Environ Conserv 30(2):104–130. https://doi.org/10.1017/S0376892903000109

Di Salvo C, Mancini M, Cavinato GP, Moscatelli M, Simionato M, Stigliano F, Rea R, Rodi A (2020) A 3d geological model as a base for the development of a conceptual groundwater scheme in the area of the colosseum (Rome, Italy). Geosci 10(7):1–26. https://doi.org/10.3390/geosciences10070266

Epting J, Huggenberger P (2013) Unraveling the heat island effect observed in urban groundwater bodies - Definition of a potential natural state. J Hydrol 501:193–204. https://doi.org/10.1016/j.jhydrol.2013.08.002

Gattinoni P, Scesi L (2017) The groundwater rise in the urban area of Milan (Italy) and its interactions with underground structures and infrastructures. Tunn Undergr Sp Technol 62:103–114. https://doi.org/10.1016/j.tust.2016.12.001

Hayashi T, Tokunaga T, Aichi M, Shimada J, Taniguchi M (2009) Effects of human activities and urbanization on groundwater environments: An example from the aquifer system of Tokyo and the surrounding area. Sci Total Environ 407(9):3165–3172. https://doi.org/10.1016/j.scitotenv.2008.07.012

Hunt DVL, Makana LO, Jefferson I, Rogers CDF (2016) Liveable cities and urban underground space. Tunn Undergr Sp Technol 55:8–20.

https://doi.org/10.1016/j.tust.2015.11.015

Koziatek O, Dragićević S (2017) iCity 3D: A geosimualtion method and tool for three-dimensional modeling of vertical urban development. Landsc Urban Plan 167(June):356–367. https://doi.org/10.1016/j.landurbplan.2017.06.021

La Vigna F (2022) Review: Urban groundwater issues and resource management, and their roles in the resilience of cities. Hydrogeol J 30(6):1657–1683. https://doi.org/10.1007/s10040-022-02517-1

Lamé A (2013) Modélisation hydrogéologique des aquifères de Paris et impacts des aménagements du sous-sol sur les écoulements souterrains [Hydrogeological modeling of the Paris aquifers and impacts of subsoil development on underground flows]

Li F, Feng P, Zhang W, Zhang T (2013a) An Integrated Groundwater Management Mode Based on Control Indexes of Groundwater Quantity and Level. Water Resour Manag 27(9):3273–3292. https://doi.org/10.1007/s11269-013-0346-8

Li HQ, Parriaux A, Thalmann P, Li XZ (2013b) An integrated planning concept for the emerging underground urbanism: Deep City Method Part 1 concept, process and application. Tunn Undergr Sp Technol 38:559–568. https://doi.org/10.1016/j.tust.2013.04.010

Li HQ, Li X, Parriaux A, Thalmann P (2013c) An integrated planning concept for the emerging underground urbanism: Deep City Method Part 2 case study for resource supply and project valuation. Tunn Undergr Sp Technol 38:569–580. https://doi.org/10.1016/j.tust.2013.04.009

Liu JQ, Sun YK, Li C jun, Yuan H liang, Chen WZ, Liu XY, Zhou XS (2022) Field monitoring and numerical analysis of tunnel water inrush and the environmental changes. Tunn Undergr Sp Technol 122(June 2021):104360. https://doi.org/10.1016/j.tust.2021.104360

Noethen M, Hemmerle H, Bayer P (2022) Sources, intensities, and implications of subsurface warming in times of climate change. Crit Rev Environ Sci Technol 0(0):1–23. https://doi.org/10.1080/10643389.2022.2083899

Parriaux A, Blunier P, Maire P, Tacher L (2007) The DEEP CITY Project: A Global Concept for a Sustainable Urban Underground Management. 11th ACUUS Int Conf Sp Expand Front Athens, Greece :255–260

Previati A, Epting J, Crosta GB (2022) The subsurface urban heat island in Milan (Italy) - A modeling approach covering present and future thermal effects on groundwater regimes. Sci Total Environ 810:152119. https://doi.org/10.1016/j.scitotenv.2021.152119

Schirmer M, Leschik S, Musolff A (2013) Current research in urban hydrogeology - A review. Adv Water Resour 51:280–291. https://doi.org/10.1016/j.advwatres.2012.06.015

Vähäaho I (2014) Underground space planning in Helsinki. J Rock Mech Geotech Eng 6(5):387–398. https://doi.org/10.1016/j.jrmge.2014.05.005

Vázquez-Suñé E, Sánchez-Vila X (1999) Groundwater modelling in urban areas as a tool for local authority management : Barcelona case study (Spain). Impacts Urban Growth Surf Water Groundw Qual Proc IUGG 99 Symp HS5 (259):65–72

Vázquez-Suñé E, Sánchez-Vila X, Carrera J (2005) Introductory review of specific factors influencing urban groundwater, an emerging branch of hydrogeology, with reference to Barcelona, Spain. Hydrogeol J 13(3):522–533. https://doi.org/10.1007/s10040-004-0360-2

Wilkinson W (1985) Rising groundwater levels in London and possible effects on engineering structures. Proc 18th Congr Int Assoc Hydrogeol Cambridge :145–157

Chapter 2: Aims of the PhD project

The main aim of the present PhD project is to conduct research activity on urban hydrogeology. More in detail, this project deals with the development of methodologies and tools in order to provide a deep understanding of the interactions between GW and the UIs in the complex and evolving reality of Milan metropolitan city. In addition, the project aims at looking for effective solutions to define an urban GW management plan.

To reach this goal, three different tasks have been developed on specific topics. In particular:

1. **Implementation of a 3D Geodatabase (GDB) for urban underground infrastructures (UIs):** this topic was addressed using Open Data as the primary source of information. The information on different categories of UIs has been then digitized and stored by means of GIS tools. Once gathered, this information has been then applied and examined in the subsequent parts of the work.
2. **Hydrodynamic characterization of the shallow aquifer to support underground management:** this part of the project was developed through the application of data-driven and geospatial techniques to detect the potential variables influencing the water table behaviour.
3. **GW/UIs interactions:** this issue was investigated through the realization of a local scale numerical model for the western portion of the city. In particular, the model aimed at estimating GW infiltrations into UIs.

2.1. Implementation of a 3D Geodatabase (GDB) for urban underground infrastructures (UIs)

Transition to sustainable development implies the urban governance to combine environmental protection and economic growth (Li et al. 2013a; Li et al. 2013b). To do so, a rational management of all the urban resources should be a priority.

Favouring the tendency of a vertical development, to limit the urban sprawl, means to consider also the subsurface in urban planning policies (Parriaux et al. 2006; Blunier et al. 2007; Koziatek and Dragićević 2017). Using this hidden, yet valuable asset is crucial to further develop in a sustainable way (Admiraal and Cornaro 2016). However, planning underground strategies took place in the past with a lack of long-term vision (Parriaux et al. 2004; Sterling 2007; Delmastro et al. 2016); the historic top-down development was made on the basis of a first come first served approach (Bobylev 2009), considering only the element to be constructed and not the subsurface as a whole to be sustainably managed. Consequently, in highly urbanized areas, finding space in the first subsurface layers has become nearly impossible for new infrastructures (Bobylev 2009; Sterling et al. 2009). This saturation in the shallow portions from the ground acts as a constrain for new infrastructures, that are progressively built more in depth (Li 2011). Thus, it is necessary to shift from a sectorial strategy, where the resources are considered independently, to a combined approach, evaluating the interactions between the various applications of the underground resources (materials, energy, space and water) (Blunier et al. 2007) . Through this change of paradigm, urban underground should be addressed as a valuable opportunity, rather than as an afterthought (Doyle et al. 2016).

Despite this, data collection and visualization for the different resources still occurs separately, evidencing a lack of communication between stakeholders (Li et al. 2012; Doyle et al. 2016; Hunt et al. 2016). Hence, sometimes a lack of data quality continues to persist for the present (Metje et al. 2007; Sterling et al. 2009; Baiden et al. 2014). As an integrated strategy is necessary to handle all the subsurface assets, 3D geodatabase (GDB) research figures as an interesting field to support urban underground management (Breunig and Zlatanova 2011; Di Salvo et al. 2020). 3D information is the first step to ensure and define a long-term multi-use potential of the resources, avoiding jeopardizing them below the city (Parriaux et al. 2007). A complete catalogue of the existing structures and assets is in fact necessary to act as a reference point to define a management plan (Hunt et al. 2016).

Usually, a large amount of information is available in urban areas, also as historical data (Carneiro and Carvalho 2010; Culshaw and Price 2011; Vázquez-Suñé et al. 2016). Notwithstanding, as previously mentioned, much of this information is not stored in standardized or ordered formats but rather is dispersed among the various institutions and stakeholders that generated and collected them using different protocols and criteria (Vázquez-Suñé et al. 2016). A more profitable collaboration between the administrations could positively influence the development of management plans in urban underground policies, through enabling the realization of a more comprehensive database. In fact, archiving and standardizing this amount of information into accessible formats requires a lot of administrative effort and time. However, the creation of a centralized platform is needed as this data, after being pre-processed, are translated into 3D GW numerical models (Vázquez-Suñé et al. 2005; Li 2011). To facilitate this achievement, the opening of data could be beneficial: on the one side, sometimes Open Data contain incomplete or obsolete information; beyond that, through Open Data the creation of new information could be favoured, avoiding also to collect the same information repetitively, thus improving the policy-making process (Arzberger et al. 2004; Zurada and Karwowski 2011; Janssen et al. 2012).

In urban areas, the GDB serves as a toolbox to access the geometries of UIs, as the volumes of buildings (Breunig and Zlatanova 2011). Information on the location and depth of UIs are useful to evaluate the interactions with the water table and identify their spatial distribution. A 3D GDB should be simple and flexible, collecting the necessary information to be integrated into models. Moreover, a database should be easily upgradable, thus considering future urban planning modifications (Frigerio et al. 2013).

All these procedures of realizing, managing and integrating a 3D GDB can be aided by the adoption of Geographic Information Systems (GIS) (Delmastro et al. 2016). GIS tools could be useful also for their flexibility in visualizing, interpreting and sharing this information, thus actively contributing to the adoption of proper urban planning strategies (Marker 2009). Their application allows to raise awareness in both thinking 3D and "long-term": this is fundamental as urban underground constitutes the last space of liberty for cities (Parriaux et al. 2007), thus requiring the implementation of well-coordinated planning policies.

This topic was addressed in this first part of the PhD project through the implementation of a 3D GDB for UIs for the city of Milan, adopting Open Data as the primary source of information.

2.2. Hydrodynamic characterization of the shallow aquifer to support underground management

Environmental datasets are growing in size, complexity and resolution; as a consequence, applying data science becomes an opportunity in different fields of research (Kanevski et al. 2008; Gibert et al. 2018). However, the potential value of this stored amount of information is not often properly exploited (Zanotti et al. 2019a).

As regards GW, possible threats from pollution, overexploitation or climate change issues impose the need of a detailed monitoring of both qualitative and quantitative status of the resource. In this sense, the spatial distribution of monitoring networks and the frequency of measures are key factors to reveal the phenomena related to the availability and the behaviour of the resource.

Within this scope, the application of data-driven techniques represents a valid approach to pinpoint the main factors influencing the aquifer processes (Chae et al. 2010; Obergfell et al. 2013).

Dealing with qualitative aspects, the availability of information on different variables favours the application of multivariate analysis. Different techniques, as cluster analysis, allow to identify the relationships between variables, grouping samples with similar chemical features. This enables evidencing the main sources affecting the resource, unravelling the presence of anthropogenic or natural pressures (Tziritis et al. 2016;

Rotiroti et al. 2019; Pollicino et al. 2021). In this way, targeted management strategies can be adopted to preserve GW quality.

The adoption of data-driven tools is increasing also as regards GW quantity. One of the main fields of application is related to GW levels forecasting (Almedeij and Al-Ruwaih 2006; Zanotti et al. 2019b; Tao et al. 2022). In this case, the amount of information available is exploited to train mathematical models to make future projections. Different techniques, ranging from univariate to multivariate analysis, have been recently adopted to deal with GW time-series analysis (Patle et al. 2015; Pathak and Dodamani 2019; Naranjo-Fernández et al. 2020; Sottani et al. 2020; Meggiorin et al. 2021). In fact, as a time-series contains information on the evolution of an environmental phenomenon over time, these tools can be applied to look for the presence of an internal structure revealing seasonality, random components or trends; these latter can evidence how past values influence the current state of a variable, thus providing an idea of the memory of the GW system. At the same time, the application of bivariate analysis, as cross-correlation, can reveal the relation of two variables as a function of the displacement of one with respect to the other. Thus, the response of GW to precipitations can be investigated over time.

The main advantage deriving from their application is that information can be extracted from the available data without requiring a deep knowledge of the subsurface parameters of the aquifer (Chae et al. 2010; Obergfell et al. 2013; Bakker and Schaars 2019). This means that their implementation is generally more agile than developing distributed numerical models, that require a huge quantity of data and an extensive approximation of geological parameters. Considering the frequent data fragmentation within the institutions described in the previous section, using a data-driven approach could lead to obtain at least preliminary results at specific locations, while information on the system and its structures is still limited. Subsequently, this information can be integrated with the realization of numerical models.

In fact, GW numerical models have peculiar capabilities, as valuable information can be gained regarding mass balance and GW flow directions (Spitz and Moreno 1996). To reach this goals, models should make maximum use of the existing data and their information content (Lotti et al. 2021b; Lotti et al. 2021a), that can also positively drive the calibration process (Bakker and Schaars 2019).

In this sense, a combination of GW time-series analysis and numerical models could offer wide opportunities to plan effective GW management strategies, thus bringing valuable information to planners and decision makers .

This topic was addressed in the second part of this PhD project through an hydrodynamic characterization of the shallow aquifer for the city of Milan. Different data-driven techniques, supported by geospatial techniques, have been applied to identify the main factors governing the aquifer behaviour; subsequently, these results have been adopted to elaborate management proposals for the construction of new UIs.

2.3. GW/ UIs interactions

Urban GW has emerged as a specific branch of research within hydrogeology, due to the interaction of GW with many urban aspects (Vázquez-Suñé et al. 2005; Schirmer et al. 2013). Flow and transport processes governing urban GW do not differ from other areas, while time and spaces involved in urban processes are different from other domains, as rural areas (Vázquez-Suñé et al. 2005; Fletcher et al. 2007; La Vigna 2022). This also happens because shallow urban networks are an intricate network of sewers, tunnels and infrastructures that make GW/UIs management challenging (La Vigna 2022). One of the most significant aspects of urban GW models is the immense amount of information that must be processed. However, as previously stated, information is scattered among many sources (local authorities/suppliers, private consumers, historical archives, etc.), and often becomes available at different stages during model development. This requires the conceptual model to be revised frequently (Vázquez-Suñé et al. 2005). This is mainly due to the few interactions that administrations have, in addition to a poor understanding of the other underground domains (Parriaux et al. 2007). Once again, this evidences the importance of structuring standardized 3D GDBs to gather and store the information on UIs to be used in numerical models.

GW models can be designed and solved by means of two main approaches: the finite difference method (FDM) and the finite element method (FEM). The main difference between these approaches is the solving method of the flow equation. The FDM approximates the flow equation through a differentiation, while the FEM solves the flow equation by means of an integral approach.

In the FDM approach, the model is subdivided into rectangular subdomains through a regular grid. In each cell, constant system parameters are assigned and the differential equation is solved calculating the unknown variable (i.e. hydraulic head) at the central points of the cells (Spitz and Moreno 1996). In case the geometry of the system is irregular, the application of the FDM could result more arduous and computational demanding. MODFLOW is the main FDM code: it is a free code developed by the United States Geological Survey (USGS). It is organized with a modular structure, with a main program supported by highly independent subroutines called “packages”. Each package deals with a specific feature of the hydrologic system which is to be simulated, such as flow from rivers or flow into drains, or with a specific method of solving linear equations that describe the flow system. The modular division allows the user to analyze independently specific hydrologic elements of the model. In this way, the development of new modules or packages is facilitated, as the already existing modules are not modified (McDonald and Harbaugh 1988; Harbaugh 1990; Harbaugh 2005). With the exception of MODFLOW-USG, previous versions of MODFLOW supported only “regular” grids composed of rows, columns, and layers of rectangular-prismatic cells. The development of MODFLOW 6 also supports “unstructured” grids whose cells need not to be rectangular and whose connectivity is not restricted to rows, columns, or layers. This unstructured connectivity allows the user a wider flexibility in constructing grids that conform also with irregular geometry and complex geology (Langevin et al. 2017), thus overcoming previous difficulties of FDM.

As for the FEM, almost no restrictions on the elements shape are present; this determines a wider flexibility in the model discretization with respect to the FDM. Usually, the model is divided into subareas, called elements, having triangular, or also tetrahedral and hexahedral shapes. These shapes allow to adapt FEM to solve complex geologic problems, and can support the development of complex fluid and transport processes (Previati et al. 2022). FEM usually approximates the solution of the hydraulic head through piecewise linear functions and its distribution is approximated for each element by a linear function (Spitz and Moreno 1996). FEFLOW, a proprietary and not freely available numerical code, is the main FEM code.

FEM does not guarantee the local mass conservation, while on the contrary FDM provides a mass conservative solution. This situation, and the modular structure that allows a certain flexibility in modelling and analyzing the hydrogeologic elements, makes MODFLOW the international standard to develop GW flow models.

In urban areas, many GW management models have been realized, through different modelling approaches (Attard et al. 2015); despite this, a recent study (Bricker et al. 2017) stated that GW management is still lacking in future city visions, although water is included in future cities assessment (Rojas-Torres et al. 2014). This means that ecosystem services provided by urban underground space (as GW) are not yet fully appreciated by most city representatives (Parriaux et al. 2007). In this framework, numerical models figure as important tools to enhance the understanding of the system behaviour, thus making GW more visible also for non-experts (La Vigna 2022). In urban domain, evaluating topics as the relation between GW and the UIs, the thermal effect induced by geothermal systems and the subsurface elements, or possibly related contamination effects is possible. Thus, their implementation can enable stakeholders to elicit their preferences for different management options (Wu and Lee 2015).

In this third part of the PhD project, the topic of GW/UIs interactions was addressed testing a methodology to quantify GW infiltrations into UIs, through the combined use of HFB and DRN packages and MODFLOW-USG.

References

Admiraal H, Cornaro A (2016) Engaging decision makers for an urban underground future. Tunn Undergr Sp Technol 55:221–223. https://doi.org/10.1016/j.tust.2015.08.009

Almedeij J, Al-Ruwaih F (2006) Periodic behavior of groundwater level fluctuations in residential areas. J Hydrol 328(3–4):677–684. https://doi.org/10.1016/j.jhydrol.2006.01.013

Arzberger P, Schroeder P, Beaulieu A, Bowker G, Casey K, Laaksonen L, Moorman D, Uhlir P, Wouters P (2004) Policy forum. 303(March):1777–1779

Attard G, Winiarski T, Rossier Y, Eisenlohr L (2015) Review: Impact of underground structures on the flow of urban groundwater. Hydrogeol J 24(1):5–19. https://doi.org/10.1007/s10040-015-1317-3

Baiden G, Bissiri Y, Luoma S, Henrich G (2014) Mapping utility infrastructure via underground GPS positioning with autonomous telerobotics. Tunn Undergr Sp Technol 39:6–14

Bakker M, Schaars F (2019) Solving Groundwater Flow Problems with Time Series Analysis: You May Not Even Need Another Model. Groundwater 57(6):826–833. https://doi.org/10.1111/gwat.12927

Blunier P, Tacher L, Parriaux A (2007) Systemic approach of urban underground resources exploitation. 11th ACUUS Int Conf - Undergr Sp Expand Front :43–48

Bobylev N (2009) Mainstreaming sustainable development into a city's Master plan: A case of Urban Underground Space use. Land use policy 26(4):1128–1137. https://doi.org/10.1016/j.landusepol.2009.02.003

Breunig M, Zlatanova S (2011) 3D geo-database research: Retrospective and future directions. Comput Geosci 37(7):791–803. https://doi.org/10.1016/j.cageo.2010.04.016

Bricker SH, Banks VJ, Galik G, Tapete D, Jones R (2017) Accounting for groundwater in future city visions. Land use policy 69(September):618–630. https://doi.org/10.1016/j.landusepol.2017.09.018

Carneiro J, Carvalho JM (2010) Groundwater modelling as an urban planning tool: Issues raised by a small-scale model. Q J Eng Geol Hydrogeol 43(2):157–170. https://doi.org/10.1144/1470-9236/08-028

Chae GT, Yun ST, Kim DS, Kim KH, Joo Y (2010) Time-series analysis of three years of groundwater level data (Seoul, South Korea) to characterize urban groundwater recharge. Q J Eng Geol Hydrogeol 43(1):117–127. https://doi.org/10.1144/1470-9236/07-056

Culshaw MG, Price SJ (2011) The 2010 Hans Cloos lecture. Bull Eng Geol Environ 70(3):333–376. https://doi.org/10.1007/s10064-011-0377-4

Delmastro C, Lavagno E, Schranz L (2016) Underground urbanism: Master Plans and Sectorial Plans. Tunn Undergr Sp Technol 55:103–111. https://doi.org/10.1016/j.tust.2016.01.001

Di Salvo C, Mancini M, Cavinato GP, Moscatelli M, Simionato M, Stigliano F, Rea R, Rodi A (2020) A 3d geological model as a base for the development of a conceptual groundwater scheme in the area of the colosseum (Rome, Italy). Geosci 10(7):1–26. https://doi.org/10.3390/geosciences10070266

Doyle MR, Thalmann P, Parriaux A (2016) Underground potential for urban sustainability: Mapping resources and their interactions with the Deep City method. Sustain 8(9). https://doi.org/10.3390/su8090830

Fletcher TD, Mitchell VG, Deletic A, Ladson TR, Seven A (2007) Is stormwater harvesting beneficial to urban waterway environmental flows? Water Sci Technol 55(4):265–272

Frigerio I, Roverato S, De Amicis M (2013) A Proposal for a Geospatial Database to Support Emergency Management. J Geogr Inf Syst 05(04):396–403. https://doi.org/10.4236/jgis.2013.54037

Gibert K, Horsburgh JS, Athanasiadis IN, Holmes G (2018) Environmental Data Science. Environ Model Softw 106:4–12. https://doi.org/10.1016/j.envsoft.2018.04.005

Harbaugh AW (1990) A computer program for calculating subregional water budgets using results from the U.S. Geological Survey Modular Three-Dimensional Finite-Difference Ground-Water Flow Model

Harbaugh AW (2005) MODFLOW-2005, the US Geological Survey modular ground-water model: the ground-water flow process. US Department of the Interior, US Geological Survey Reston, VA

Hunt DVL, Makana LO, Jefferson I, Rogers CDF (2016) Liveable cities and urban underground space. Tunn Undergr Sp Technol 55:8–20. https://doi.org/10.1016/j.tust.2015.11.015

Janssen M, Charalabidis Y, Zuiderwijk A (2012) Benefits, Adoption Barriers and Myths of Open Data and Open Government. Inf Syst Manag 29(4):258–268. https://doi.org/10.1080/10580530.2012.716740

Kanevski M, Pozdnukhov A, Timonin V (2008) Machine learning algorithms for geospatial data. Applications and software tools

Koziatek O, Dragićević S (2017) iCity 3D: A geosimualtion method and tool for three-dimensional modeling of vertical urban development. Landsc Urban Plan 167(June):356–367. https://doi.org/10.1016/j.landurbplan.2017.06.021

La Vigna F (2022) Review: Urban groundwater issues and resource management, and their roles in the resilience of cities. Hydrogeol J 30(6):1657–1683. https://doi.org/10.1007/s10040-022-02517-1

Langevin CD, Hughes JD, Banta ER, Niswonger RG, Panday S, Provost AM (2017) Documentation for the MODFLOW 6 Groundwater Flow Model: U.S. Geological Survey Techniques and Methods. B 6, Model Tech :197

Li HQ (2011) Sustainable 3D Urban Governance: Creating a “ Deep City ” for Our

Modern City. Swiss Fed Inst Technol Lausanne (EPFL), Switz :1–14

Li HQ, Parriaux A, Thalmann P, Li XZ (2013a) An integrated planning concept for the emerging underground urbanism: Deep City Method Part 1 concept, process and application. Tunn Undergr Sp Technol 38:559–568. https://doi.org/10.1016/j.tust.2013.04.010

Li HQ, Li X, Parriaux A, Thalmann P (2013b) An integrated planning concept for the emerging underground urbanism: Deep City Method Part 2 case study for resource supply and project valuation. Tunn Undergr Sp Technol 38:569–580. https://doi.org/10.1016/j.tust.2013.04.009

Li HQ, Parriaux A, Thalmann P (2012) The way to plan a sustainable "deep city": the strategic framework and economic model. 13th ACUUS Conf "undergr Sp Dev – Oppor Challenges" (November):12

Lotti F, Borsi I, Guastaldi E, Barbagli A, Basile P, Favaro L, Mallia A, Xuereb R, Schembri M, Mamo JA, Demichele F, Sapiano M (2021a) NECoM (Numerically Enhanced COnceptual Modelling) of two small Maltese Aquifers: Mizieb and Pwales. Acque Sotter - Ital J Groundw 10(1):7–21. https://doi.org/10.7343/as-2021-496

Lotti F, Borsi I, Guastaldi E, Barbagli A, Basile P, Favaro L, Mallia A, Xuereb R, Schembri M, Mamo JA, Sapiano M (2021b) Numerically enhanced conceptual modelling (NECoM) applied to the Malta Mean Sea Level Aquifer. Hydrogeol J 29(4):1517–1537. https://doi.org/10.1007/s10040-021-02330-2

Marker BR (2009) Geology of megacities and urban areas. Geol Soc Eng Geol Spec Publ 22(1):33–48. https://doi.org/10.1144/EGSP22.3

McDonald MG, Harbaugh AW (1988) A modular three-dimensional finite-difference ground-water flow model. US Geological Survey

Meggiorin M, Passadore G, Bertoldo S, Sottani A, Rinaldo A (2021) Techical report Assessing the long-term sustainability of the groundwater resources in the

Bacchiglione basin (Veneto , Italy) with the Mann – Kendall test: suggestions for higher reliability. :35–48. https://doi.org/10.7343/as-2021-499

Metje N, Atkins PR, Brennan MJ, Chapman DN, Lim HM, Machell J, Muggleton JM, Pennock S, Ratcliffe J, Redfern M, Rogers CDF, Saul AJ, Shan Q, Swingler S, Thomas AM (2007) Mapping the Underworld - State-of-the-art review. Tunn Undergr Sp Technol 22(5–6):568–586. https://doi.org/10.1016/j.tust.2007.04.002

Naranjo-Fernández N, Guardiola-Albert C, Aguilera H, Serrano-Hidalgo C, Montero-González E (2020) Clustering groundwater level time series of the exploited almonte-marismas aquifer in southwest Spain. Water (Switzerland) 12(4). https://doi.org/10.3390/W12041063

Obergfell C, Bakker M, Zaadnoordijk WJ, Maas K (2013) Deriving hydrogeological parameters through time series analysis of groundwater head fluctuations around well fields. Hydrogeol J 21(5):987–999

Parriaux A, Blunier P, Maire P, Tacher L (2007) The DEEP CITY Project: A Global Concept for a Sustainable Urban Underground Management. 11th ACUUS Int Conf Sp Expand Front Athens, Greece :255–260

Parriaux A, Tacher L, Joliquin P (2004) The hidden side of cities - Towards three-dimensional land planning. Energy Build 36(4):335–341. https://doi.org/10.1016/j.enbuild.2004.01.026

Parriaux A, Tacher L, Kaufmann V, Blunier P (2006) Underground resources and sustainable development in urban areas

Pathak AA, Dodamani BM (2019) Trend Analysis of Groundwater Levels and Assessment of Regional Groundwater Drought: Ghataprabha River Basin, India. Nat Resour Res 28(3):631–643. https://doi.org/10.1007/s11053-018-9417-0

Patle GT, Singh DK, Sarangi A, Rai A, Khanna M, Sahoo RN (2015) Time series analysis of groundwater levels and projection of future trend. J Geol Soc India 85(2):232–242

Pollicino LC, Colombo L, Alberti L, Masetti M (2021) PCE point source apportionment using a GIS-based statistical technique combined with stochastic modelling. Sci Total Environ 750:142366. https://doi.org/10.1016/j.scitotenv.2020.142366

Previati A, Epting J, Crosta GB (2022) The subsurface urban heat island in Milan (Italy) - A modeling approach covering present and future thermal effects on groundwater regimes. Sci Total Environ 810:152119. https://doi.org/10.1016/j.scitotenv.2021.152119

Rojas-Torres MG, Nápoles-Rivera F, Ponce-Ortega JM, Serna-González M, El-Halwagi MM (2014) Optimal design of sustainable water systems for cities involving future projections. Comput Chem Eng 69:1–15. https://doi.org/10.1016/j.compchemeng.2014.05.026

Rotiroti M, Zanotti C, Fumagalli L, Taviani S, Stefania GA, Patelli M, Nava V, Soler V, Sacchi E, Leoni B (2019) Multivariate statistical analysis supporting the hydrochemical characterization of groundwater and surface water: A case study in northern Italy. Rend Online Soc Geol Ital 47(March):90–96. https://doi.org/10.3301/ROL.2019.17

Schirmer M, Leschik S, Musolff A (2013) Current research in urban hydrogeology - A review. Adv Water Resour 51:280–291. https://doi.org/10.1016/j.advwatres.2012.06.015

Sottani A, Meggiorin M, Ribeiro L, Rinaldo A (2020) Comparison of two methods for optimizing existing groundwater monitoring networks: application to the Bacchiglione Basin , Italy. :8759

Spitz K, Moreno J (1996) A practical guide to groundwater and solute transport modeling. John Wiley and sons

Sterling RL (2007) Urban underground space use planning: a growing dilemma. Urban Plan Int 6(004)

Sterling RL, Anspach JH, Allouche EN, Simicevic J, Rogers CDF, Weston KE, Hayes

K (2009) Encouraging innovation in locating and characterizing underground utilities

Tao H, Hameed MM, Marhoon HA, Zounemat-Kermani M, Heddam S, Kim S, Sulaiman SO, Tan ML, Sa'adi Z, Mehr AD, Allawi MF, Abba SI, Zain JM, Falah MW, Jamei M, Bokde ND, Bayatvarkeshi M, Al-Mukhtar M, Bhagat SK, Tiyasha T, Khedher KM, Al-Ansari N, Shahid S, Yaseen ZM (2022) Groundwater level prediction using machine learning models: A comprehensive review. Neurocomputing 489:271–308. https://doi.org/https://doi.org/10.1016/j.neucom.2022.03.014

Tziritis E, Skordas K, Kelepertsis A (2016) The use of hydrogeochemical analyses and multivariate statistics for the characterization of groundwater resources in a complex aquifer system. A case study in Amyros River basin, Thessaly, central Greece. Environ Earth Sci 75(4):1–11. https://doi.org/10.1007/s12665-015-5204-y

Vázquez-Suñé E, Marazuela MÁ, Velasco V, Diviu M, Pérez-Estaún A, Álvarez-Marrón J (2016) A geological model for the management of subsurface data in the urban environment of Barcelona and surrounding area. Solid Earth 7(5):1317–1329. https://doi.org/10.5194/se-7-1317-2016

Vázquez-Suñé E, Sánchez-Vila X, Carrera J (2005) Introductory review of specific factors influencing urban groundwater, an emerging branch of hydrogeology, with reference to Barcelona, Spain. Hydrogeol J 13(3):522–533. https://doi.org/10.1007/s10040-004-0360-2

Wu JS, Lee JJ (2015) Climate change games as tools for education and engagement. Nat Clim Chang 5(5):413–418. https://doi.org/10.1038/nclimate2566

Zanotti C, Rotiroti M, Fumagalli L, Stefania GA, Canonaco F, Stefenelli G, Prévôt ASH, Leoni B, Bonomi T (2019a) Groundwater and surface water quality characterization through positive matrix factorization combined with GIS approach. Water Res 159:122–134. https://doi.org/https://doi.org/10.1016/j.watres.2019.04.058

Zanotti C, Rotiroti M, Sterlacchini S, Cappellini G, Fumagalli L, Stefania GA, Nannucci MS, Leoni B, Bonomi T (2019b) Choosing between linear and nonlinear models and avoiding overfitting for short and long term groundwater level forecasting in a linear system. J Hydrol 578:124015. https://doi.org/https://doi.org/10.1016/j.jhydrol.2019.124015

Zurada J, Karwowski W (2011) Knowledge discovery through experiential learning from business and other contemporary data sources: A review and reappraisal. Inf Syst Manag 28(3):258–274. https://doi.org/10.1080/10580530.2010.493846

Chapter 3: Study Area

The study area of this PhD project covers 440 km² within the Milan metropolitan area. Milan city is highly populated and urbanized, hosting 1.4 million people. Being located in the middle of the Po Plain, Milan has always been strategic and economically important for Northern Italy. Nowadays, an urban transformation is taking place, that is leading Milan to become an important European reality. Historically, the area has always been interested by an intense industrial and agricultural development (Bonomi et al. 2009; Pulighe and Lupia 2019). The northern and the central areas of the city are mostly urbanized, while agricultural activities are still conducted in the western and southern portions of the domain (Fig. 3.1). The Navigli canals (Naviglio Grande, Naviglio Pavese and Naviglio Martesana) have been exploited since the 12th century to provide water for these irrigation activities. In the past, these man-made structures were also used for commercial purposes. These surface water canals are part of a wide hydrographic network that characterizes the area. The Olona, Seveso and Lambro rivers, that originate from the Northern foothills, are part of this surface network. Except for Lambro River, Olona and Seveso rivers are partly culverted within Milan city.

The geological and hydrogeologic setting of this part of the Po Plain has been deeply studied both in the past (Regione Lombardia & ENI Divisione AGIP 2002) and recently (Regione Lombardia 2016). Three main hydrostructures can be identified: a shallow hydrostructure (ISS), an intermediate hydrostructure (ISI) and a deep hydrostructure (ISP). ISS has an average thickness of 50 meters, and it is mainly composed by sands and gravels. Moving deep towards the ISI, the lithological composition is characterized by the same materials, but with an increased presence of silty layers. A more uncertain lithological composition characterizes the ISP, due to an insufficient availability of geological information. Within the goals of this PhD project, the shallow aquifer of the ISS has always been the main focus of all the tasks.

The western and the south-western portions of the domain are interested by the presence of lowland springs: their occurrence is observed across the entire Po-Plain in a 20-km-wide belt. Changes from North to South in both the ground surface slope gradient and sediment permeability from coarse (i.e. gravel and sand) to fine (i.e. silt and clay) materials favour their formation, thus inducing GW to outflow (De Luca et al. 2014). As their flow rate is constant, these natural elements have been exploited in the past for irrigation purposes.

GW levels in the study area have consistently varied over time, mostly as a consequence of human activities. Industrialisation determined an extensive use of GW since the early 1960s; around 1975 this huge amount of withdrawals caused a general decrease of the water table. In the northern sector, a water level depth of more than 30 meters from the ground was measured. GW levels started to gradually recover from the end of the ’70s, triggered by intense precipitations, an economic crisis and the development of new industrial technologies (Bonomi 1999). Since the beginning of the ‘90s, the decommissioning of the industrial districts, mainly located in the northern sector of the town, led the water table to rise once again (i.e. with a maximum rise of about 10–15 meters in the northern area). The GW rebound caused flooding episodes for some underground structures (Cavallin and Bonomi 1997; Gattinoni and Scesi 2017; Colombo et al. 2018), including car parks and subway tunnels.

In recent years, the installation of low-enthalpy geothermal systems for heating and cooling of buildings has increased, to fulfil the goal of limiting greenhouse gases emissions. Two different kinds of geothermal systems can be adopted: ground-coupled heat pumps (GCHPs) and GW heat pumps (GWHPs). As regards Milan city, GWHPs are mostly installed especially in the downtown area. This choice is made as these installations are economically favoured only in presence of high thermal demands, as the costs of installation are compensated by the obtained thermal energy (Previati et al. 2022). Regional laws permit GW re-injection only in the shallow geological unit. However, for specific situations, GW is not discharged into the aquifer, but in surface water bodies: in this way, GW level rising can be locally controlled.

In the next future, a further subsurface development is expected, as already defined by urban planning policies (Plan of Government of the Territory, PGT, 2019). Thus, new UIs will be built. Consequently, the definition of an urban underground management plan figures as an important task to achieve, in order to properly handle all the underground resources, considering also the interaction between GW and the UIs.

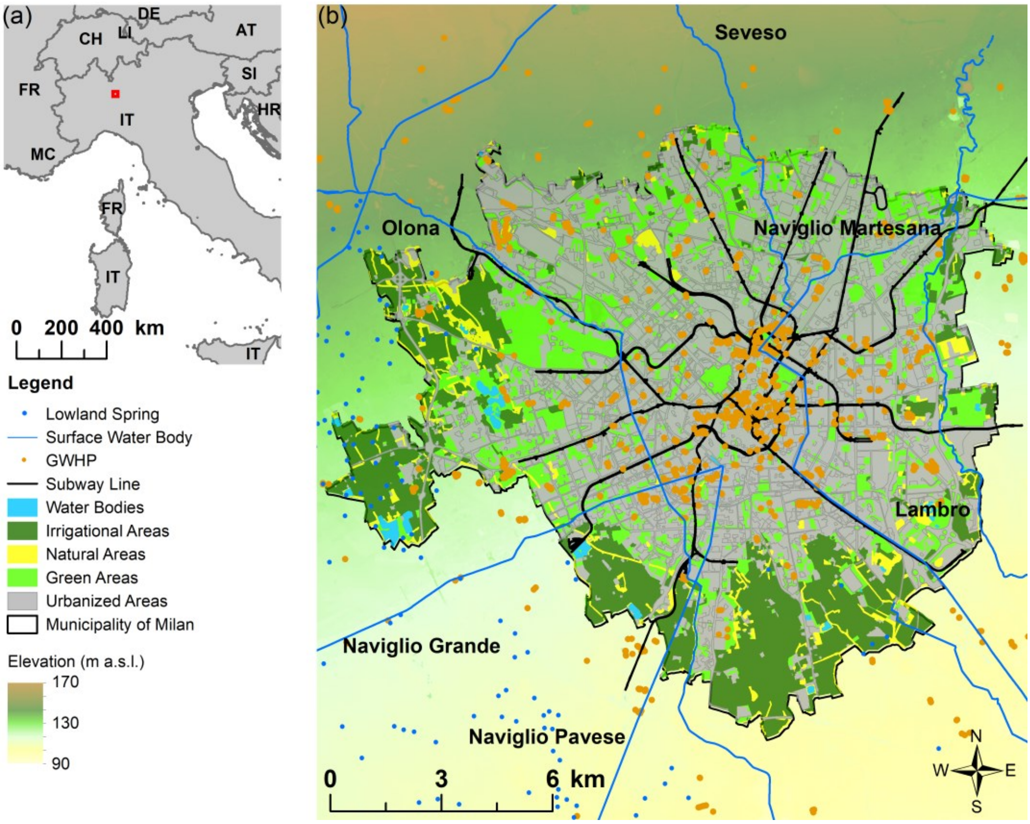

Fig. 3.1. a) Geographical setting of the study area; **b)** Main hydrographic (lowland springs and surface water network), anthropogenic elements (subway tunnels, GWHPs) and land use classes from Dusaf 6.0 (Regione Lombardia 2021). Information regarding the GWHPs is updated at July 2021 and has been obtained from Regione Lombardia 2021.

References

Bonomi T (1999) Groundwater level evolution in the Milan area: Natural and human issues. IAHS-AISH Publ (259):195–202

Bonomi T, Fumagalli L, Dotti N (2009) Fenomeno di inquinamento da solventi in acque sotterranee sfruttate ad uso potabile nel nord-ovest della provincia di Milano [Phenomenon of solvent pollution in groundwater exploited for drinking use in the north-west of Milan province]. Geol Appl 12:43–59

Cavallin A, Bonomi T (1997) Application of a hydrogeological model to analyze and manage groundwater processes in the urban environment: a case study in the Milan area, Italy

Colombo L, Gattinoni P, Scesi L (2018) Stochastic modelling of groundwater flow for hazard assessment along the underground infrastructures in Milan (northern Italy). Tunn Undergr Sp Technol 79(May):110–120. https://doi.org/10.1016/j.tust.2018.05.007

De Luca DA, Destefanis E, Forno MG, Lasagna M, Masciocco L (2014) The genesis and the hydrogeological features of the Turin Po Plain fontanili, typical lowland springs in Northern Italy. Bull Eng Geol Environ 73(2):409–427. https://doi.org/10.1007/s10064-013-0527-y

Gattinoni P, Scesi L (2017) The groundwater rise in the urban area of Milan (Italy) and its interactions with underground structures and infrastructures. Tunn Undergr Sp Technol 62:103–114. https://doi.org/10.1016/j.tust.2016.12.001

Previati A, Epting J, Crosta GB (2022) The subsurface urban heat island in Milan (Italy) - A modeling approach covering present and future thermal effects on groundwater regimes. Sci Total Environ 810:152119. https://doi.org/10.1016/j.scitotenv.2021.152119

Pulighe G, Lupia F (2019) Multitemporal geospatial evaluation of urban agriculture and (non)-sustainable food self-provisioning in Milan, Italy. Sustain 11(7). https://doi.org/10.3390/su11071846

Regione Lombardia (2016) Piano di Tutela ed Uso delle Acque (PTUA) [Water Protection and Use Plan (PTUA)]. Regione Lombardia, Milan, Italy

Regione Lombardia (2021) Geoportal of the Lombardy Region, Italy http://www.geoportale.regione.lombardia.it/ (Accessed on 1 December 2021)

Regione Lombardia & ENI Divisione AGIP (2002) Geologia degli acquiferi Padani della Regione Lombardia. [Geology of the Padan aquifers of the Lombardy Region].

Chapter 4: Thesis Structure

The PhD project has been organized in three sections:

- Section I: Implementation of a 3D Geodatabase (GDB) for urban underground infrastructures (UI);
- Section II: Hydrodynamic characterization of the shallow aquifer to support underground management;
- Section III: GW/UIs interactions.

I) Implementation of a 3D Geodatabase (GDB) for urban underground infrastructures (UIs)

This first section deals with the development of a methodology to create a detailed inventory of the UIs for the city of Milan.

To gather information on UIs, an Open Data municipal cartography was used as the primary source of information: the Topographic Database. In this way, the applied procedures, depending on data availability, could be replied also in other domains. In fact, the Topographic Database (DbT) is developed according to the European Standards defined by INSPIRE directive. The methodology has been developed through GIS tools and for some specific tasks required a manual digitization of some UIs elements.

The 3D GDB was subsequently adopted to reach other related purposes: through a piezometric reconstruction of different GW conditions, the areas showing a situation of submersion (i.e. UIs volumes lying below the water table) have been detected. The obtained results can provide a valid tool to the decision makers to manage the future underground development of the city, also considering GW/UIs interactions.

The results of this section have been summarized in the following published paper, that is presented in Chapter 5 of the PhD thesis:

A 3D Geodatabase for Urban Underground Infrastructures: Implementation and Application to Groundwater Management in Milan Metropolitan Area

Davide Sartirana [1] *, Marco Rotiroti [1], Chiara Zanotti [1], Tullia Bonomi [1], Letizia Fumagalli [1] and Mattia De Amicis [1]

[1]Department of Earth and Environmental Sciences, University of Milano-Bicocca, Piazza Della Scienza 1, 20126 Milan, Italy.

ISPRS Int. J. Geo-Inf. **2020**, *9*(10), 609; https://doi.org/10.3390/ijgi9100609

International Journal of
Geo-Information

Article

A 3D Geodatabase for Urban Underground Infrastructures: Implementation and Application to Groundwater Management in Milan Metropolitan Area

Davide Sartirana *, Marco Rotiroti, Chiara Zanotti, Tullia Bonomi, Letizia Fumagalli and Mattia De Amicis

Department of Earth and Environmental Sciences, University of Milano-Bicocca, Piazza Della Scienza 1, 20126 Milan, Italy; marco.rotiroti@unimib.it (M.R.); chiara.zanotti@unimib.it (C.Z.); tullia.bonomi@unimib.it (T.B.); letizia.fumagalli@unimib.it (L.F.); mattia.deamicis@unimib.it (M.D.A.)

* Correspondence: d.sartirana1@campus.unimib.it; Tel.: +39-02-6448-2882

Received: 16 September 2020; Accepted: 19 October 2020; Published: 21 October 2020

II) Hydrodynamic characterization of the shallow aquifer to support underground management

In this second part of the thesis, the main task was the application of data-driven methods to analyse GW time-series of 95 monitoring wells (MWs) of the shallow aquifer, covering the period 2005-2019. Different statistical techniques have been used to extract as much information as possible regarding the processes that influence the water table behaviour (i.e. geology, precipitations, withdrawals, and land use). Among the applied techniques, hierarchical cluster analysis was performed to group GW time-series depending on their piezometric trends. The application of clustering techniques for quantitative analysis has grown in recent years, while being mostly applied for qualitative investigations in the past. Results of the analysis carried out have been interpreted with a double aim: a) to identify different sectors of the domain having local hydrogeologic behaviours, to be possibly adopted in the future as GW management units; b) to elaborate targeted guidelines for the construction of new UIs within the territorial units identified. Through an improvement of the urban conceptual model, also this part of the study could provide valuable support to the stakeholders in the framework of urban underground management.

The results of this section have been summarized in the following published paper, that is presented in Chapter 6 of the PhD thesis:

Data-driven decision management of urban underground infrastructure through groundwater-level time-series cluster analysis: the case of Milan (Italy)

Davide Sartirana [1] *, Marco Rotiroti [1], Tullia Bonomi [1], Mattia De Amicis [1], Veronica Nava [1], Letizia Fumagalli [1] and Chiara Zanotti [1]

[1]Department of Earth and Environmental Sciences, University of Milano-Bicocca, Piazza Della Scienza 1, 20126 Milan, Italy.

Hydrogeol J **30**, 1157–1177 (2022). https://doi.org/10.1007/s10040-022-02494-5

Hydrogeology Journal
https://doi.org/10.1007/s10040-022-02494-5

PAPER

Check for updates

Data-driven decision management of urban underground infrastructure through groundwater-level time-series cluster analysis: the case of Milan (Italy)

Davide Sartirana[1] · Marco Rotiroti[1] · Tullia Bonomi[1] · Mattia De Amicis[1] · Veronica Nava[1] · Letizia Fumagalli[1] · Chiara Zanotti[1]

Received: 16 November 2021 / Accepted: 29 April 2022

III) GW/ UIs interactions:

The main task in this last part of the PhD project was the implementation of a local-scale urban numerical model for the western part of Milan city, aimed at identifying the interactions between GW and the UIs.

Particularly, the main goal of the model was to provide a preliminary estimate of GW infiltrations into UIs and the portions of the domain mostly affected by this issue. Flooding episodes have been documented in the past for different UIs. Through this approach, useful information could be provided to the stakeholders to design management solutions to face this issue. To do so, a steady-state GW flow model was realized using MODFLOW-USG as numerical code, modelling the UIs through a combination of two MODFLOW packages: HFB and DRN packages. Respectively, HFB was used to set the wall conductance depending on the presence of lining systems for a given UI, while the DRN package was set inside the HFB to simulate a possible water collector system, thus allowing to quantify the possible infiltrations. The numerical model was calibrated by means of a trial and error method against a maximum GW condition, thus reflecting a possible critical situation for UIs. A preliminary quantification of the possible infiltrations has been done by interpreting MODFLOW mass balance outputs.

The results of this section are discussed in the following published paper, that is presented in Chapter 7 of the PhD thesis:

Quantifying Groundwater Infiltrations into Subway Lines and Underground Car Parks Using MODFLOW-USG

Davide Sartirana [1] *, Chiara Zanotti [1], Marco Rotiroti [1], Mattia De Amicis [1], Mariachiara Caschetto [1], Agnese Redaelli [1], Letizia Fumagalli [1] and Tullia Bonomi [1]

[1]Department of Earth and Environmental Sciences, University of Milano-Bicocca, Piazza Della Scienza 1, 20126 Milan, Italy.

Water **2022**, 14(24), 4130; https://doi.org/10.3390/w14244130 water

Article

Quantifying Groundwater Infiltrations into Subway Lines and Underground Car Parks Using MODFLOW-USG

Davide Sartirana *, Chiara Zanotti, Marco Rotiroti, Mattia De Amicis, Mariachiara Caschetto, Agnese Redaelli, Letizia Fumagalli and Tullia Bonomi

Department of Earth and Environmental Sciences, University of Milano-Bicocca, Piazza della Scienza 1, 20126 Milan, Italy
* Correspondence: d.sartirana1@campus.unimib.it

Chapter 5: Implementation of a 3D Geodatabase (GDB) for urban underground infrastructures (UIs)

A 3D Geodatabase for Urban Underground Infrastructures: Implementation and Application to Groundwater Management in Milan Metropolitan Area

Davide Sartirana [1] *, Marco Rotiroti [1], Chiara Zanotti [1], Tullia Bonomi [1], Letizia Fumagalli [1] and Mattia De Amicis [1]

[1]Department of Earth and Environmental Sciences, University of Milano-Bicocca, Piazza Della Scienza 1, Milan, Italy; d.sartirana1@campus.unimib.it (D.S.); marco.rotiroti@unimib.it (M.R.); chiara.zanotti@unimib.it (C.Z.); tullia.bonomi@unimib.it (T.B.); letizia.fumagalli@unimib.it (L.F.); mattia.deamicis@unimib.it (M.D.A.)

*Correspondence: d.sartirana1@campus.unimib.it (D.S.); Tel.: +39-02-6448-2882

This chapter is largely based on the following paper: *ISPRS Int. J. Geo-Inf.* **2020**, *9*(10), 609; https://doi.org/10.3390/ijgi9100609

Keywords: Milan; underground structures and infrastructures; 3D geodatabase; geographic information systems; urban underground; groundwater management; groundwater modelling; Topographic Database

Abstract

The recent rapid increase in urbanization has led to the inclusion of underground spaces in urban planning policies. Among the main subsurface resources, a strong interaction between underground infrastructures and groundwater has emerged in many urban areas in the last few decades. Thus, listing the underground infrastructures is necessary to structure an urban conceptual model for groundwater management needs. Starting from a municipal cartography (Open Data), thus making the procedure replicable, a GIS methodology was proposed to gather all the underground infrastructures into an updatable 3D geodatabase (GDB) for the metropolitan city of Milan (Northern Italy). The underground volumes occupied by three categories of infrastructures were included in the GDB: a) private car parks, b) public car parks and c) subway lines and stations. The application of the GDB allowed estimating the volumes lying below the water table

in four periods, detected as groundwater minimums or maximums from the piezometric trend reconstructions. Due to groundwater rising or local hydrogeological conditions, the shallowest, non-waterproofed underground infrastructures were flooded in some periods considered. This was evaluated in a specific pilot area and qualitatively confirmed by local press and photographic documentation reviews. The methodology emerged as efficient for urban planning, particularly for urban conceptual models and groundwater management plans definition.

5.1. Introduction

Cities are intricate areas, where different elements interact. In the past, their expansion has generally occurred in the horizontal direction (urban sprawl) (Zhang 2016; Koziatek and Dragićević 2017; Guastella et al. 2019); despite this, underground urbanism was already conceived (Utudjian 1972; Barles and Guillerme 1995; Parriaux et al. 2006; Bélanger 2007; Sterling et al. 2012). According to previsions, 70% of the world's population is expected to live in cities by 2050 (Un-Habitat 2012). As a consequence of this rapid urbanization, space hunting is moving towards a three-dimensional trend (Li et al. 2013a; Li et al. 2013b): vertical urban development has thus been adopted to counteract urban sprawl (Koziatek and Dragićević 2017), thus increasing population density. This urban densification is leading to the building of deeper structures (Bobylev 2009; Bobylev 2016), which increases the tendency to "go underground" (Boisvert 2007; Nishioka et al. 2007; Rein 2009; Vähäaho 2014; Vähäaho 2016).

The increasing need for space in urban areas has recently enhanced urban underground consideration (Parriaux et al. 2007; Bobylev 2009; Sterling et al. 2012). Four subsurface resources are key to pursuing sustainable urban underground development: space for constructions, materials, water and energy (Parriaux et al. 2004; Parriaux et al. 2007; Li et al. 2013a; Hunt et al. 2016).

These resources interact with each other (Attard et al. 2017). In particular, a strong interaction between groundwater (GW) and underground infrastructures (UIs) has been observed (Parriaux et al. 2004; Blunier et al. 2007; Li 2011). In the last few decades, many cities around the world have faced a rising trend in GW levels, caused by the deindustrialization process. This produced some interferences between GW and UIs, such as subways, car parks and basements (Wilkinson 1985; George 1992; Hernández et al. 1997; Vázquez-Suñé et al. 1997; Mudd et al. 2004; Hayashi et al. 2009; Lamé 2013; Ducci and Sellerino 2015). The implementation of a geodatabase (GDB), including 3D locations and uses of the underground structures, could help to manage this issue (Attard et al. 2017). In this way, part of the large amount of data generally available in urban areas (Culshaw and Price 2011), but not stored in a systematic way (Vázquez-Suñé et al. 2016), could be gathered in a unique structure. The GDB will contribute to process data to be used for GW management, thus enabling the definition of an urban conceptual model, a necessary step for 3D numerical GW flow modelling. For this reason, these data need to be integrated with geological, hydrological, geomorphological and other required information. Furthermore, the increasing interest in open data for urban management and GW issues is a topic to be considered (Alawadhi et al. 2012; Fitch et al. 2016). Indeed, the opening of data entails several barriers, related both to providers (i.e. incomplete or obsolete information) and users (i.e. complexity of using and interpreting data); however, a large number of benefits are related to open-data: among them, the improvement of policy-making processes, the creation of new information combining existing data, and avoiding repetitively collecting the same information are included (Arzberger et al. 2004; Zurada and Karwowski 2011; Janssen et al. 2012).

The city of Milan experienced a strong water table rise in the last few decades (Beretta et al. 2004). As numerical GW flow modelling is the primary tool for evaluating the interactions between GW and UIs (Vázquez-Suñé et al. 2016), different 3D models have been realized for the urban area of Milan (Gattinoni and Scesi 2017; Colombo et al. 2018; De Caro et al. 2020). Among the UIs listed above, all these numerical models focused only on the subway lines: interactions between GW and car parks were not evaluated.

The aim of this work is to propose a methodology to estimate, on an urban scale, the volume of UIs lying below the water table. This is the basis for a further evaluation of the impacts of the interaction between GW and infrastructures, such as the perturbation of GW flow by infrastructures or the GW flooding of non-waterproofed infrastructures. Three categories of infrastructures were considered in this study: a) private car parks, b) public car parks and c) subway lines/stations and underground railway. To the best of the authors' knowledge, this is the first time that car parks were considered in evaluating GW/UIs interactions in the city of Milan. On the contrary, car parks have been considered in numerical models in other towns (Carneiro and Carvalho 2010; Attard et al. 2016a; Jurado and Feito 2017). The last part of this work is devoted to the evaluation, within a pilot area, of the impact of GW (i.e. flooding) on non-waterproofed public car parks and subway lines and stations. The comparison between the results of this evaluation and actual flooding events, identified by local press reviews and photographic documentation reviews, helped to validate, qualitatively, the whole methodology. The methodology here proposed is developed for the case study of Milan—however, it could be applied to other cities worldwide with similar characteristics (i.e. municipalities characterized by a subsurface infrastructure development).

5.2. Study Area

The study area (Fig. 5.1) covers 440 km^2 in the Milan metropolitan area, between longitudes 1,503,000 and 1,525,000 and latitudes 5,025,000 and 5,045,000 (Monte Mario Italy 1; ESPG: 3003). The city of Milan is inhabited by 1.4 million people (Istat 2011) and has had strong industrial and agricultural development (Bonomi 2009). It is located in the Po Plain, which hosts a sedimentary aquifer system whose hydrogeological structure has been previously investigated in detail (Regione Lombardia 2016). Three main hydrostructures can be identified: a shallow hydrostructure (ISS), an intermediate hydrostructure (ISI) and a deep hydrostructure (ISP). ISS and a portion of ISI are visible in Fig. 5.2. ISS is mainly composed of gravels and sands and hosts a phreatic aquifer. In the study area, it has a medium thickness of 50 meters and its bottom surface goes from 100 m a.s.l. (to the North) down to around 50 m a.s.l. (to the South). ISI hosts a semiconfined aquifer mainly composed of sand and gravels, with an increasing presence of silty and clayey layers compared to the upper hydrostructure. Its bottom surface goes from 70 m a.s.l. (to the North) down to −50 m a.s.l. (to the South) for the area of interest, with an increasing thickness moving from N to S along the cross section (Fig. 5.1b, Fig. 5.2). ISP hosts a confined aquifer, but its composition is mainly uncertain due to a reduced number of available data.

GW has been extensively exploited for industrial use since the early 1960s. The maximum water depletion (i.e. minimum GW levels) was reached in the years from the 1960s until the early 1990s, with a water table more than 30 meters deep in the northern sector. During this period, some UIs (car parks, subway lines) were built, sometimes with no waterproofing works (Cavallin and Bonomi 1997; Bonomi 1999; Beretta et al. 2004), neglecting the possibility of any future GW level rise. Since the early 1990s, because of the decommissioning of many industrial sites, GW levels have started to rise (i.e. with a maximum rise of about 10−15 meters in the northern area), generating many problems for UIs. Nowadays, the rising of GW is still causing severe problems, as occurs in other European urban areas, such as Paris, Barcelona and London (Wilkinson 1985; Vázquez-Suñé et al. 1997; Lamé 2013).

As an example of the infrastructure development of the subsurface, due to its widespread presence within the study area, the subway network (Fig. 5.1b) is described in detail below. Its construction began in the 1960s, focusing on the shallow portion of the unconfined aquifer. A top-down design mechanism was adopted, following a first-come-first-served basis approach (Bobylev 2006; Sterling 2007; Bobylev 2009). M1 and M2 lines were built at first, with a cut and cover method to avoid interrupting the traffic on the main roads (De Caro et al. 2020). Built during the GW drawdown phase, they were not designed with waterproofing systems (Colombo et al. 2018). M3 line and the underground railway were built in the 1990s: due to their greater depth, they were designed with waterproofing systems. Both these constraints and the diffusion of new excavation methods (Parriaux et al. 2004; De Caro et al. 2020) have led to the building of the most recent lines (M5 line completed in 2015; M4 line, still in construction) at greater depths; these lines have been designed to reach the most peripheral areas of the city.

Furthermore, Milan’s vertical development has increased in recent years, implying a deepest subsurface occupation from the UIs. At the beginning of 2019, the new Plan of Government of the Territory (PGT) (Milan Metropolitan City 2019a) was adopted. It aims at reducing soil consumption and developing new sections of subway lines. This will lead to a greater underground occupation, thus requiring a coordinated management of all the assets involved and reliable information on their location and properties.

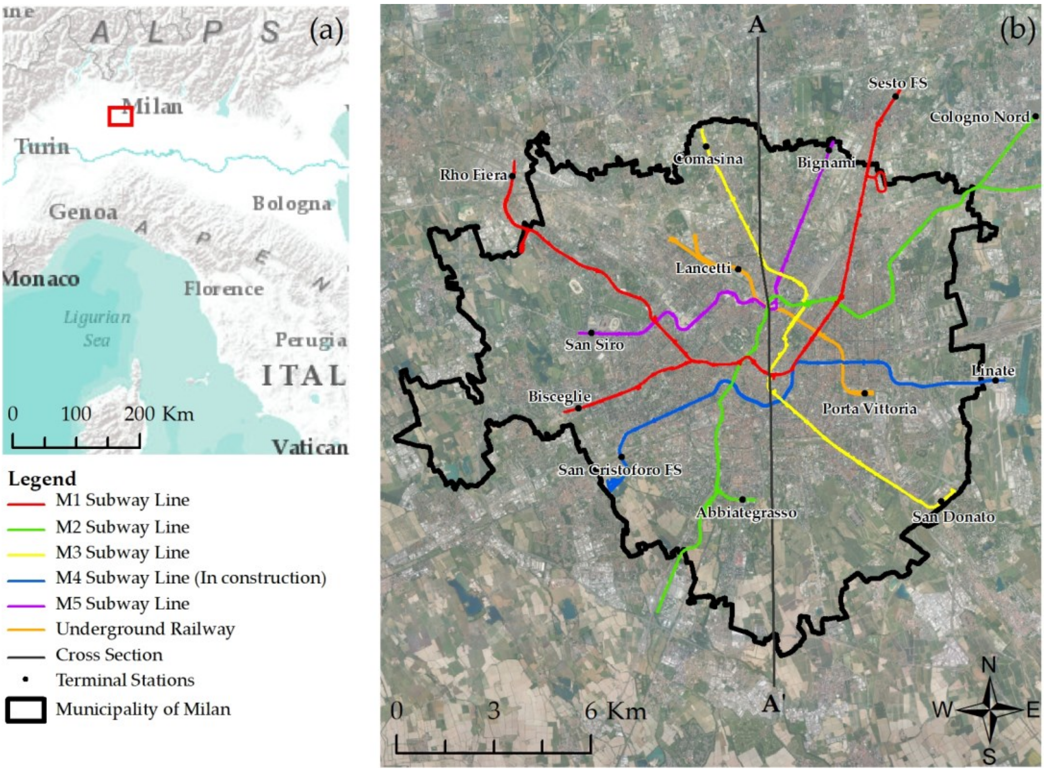

Fig. 5.1. a) Geographical setting of the study area; **b)** the subway network of Milan; the location of the terminal stations of each line is provided. Line AA’ points to the location of the cross section represented in Fig. 5.2. Satellite image Source: Geoportale Regione Lombardia.

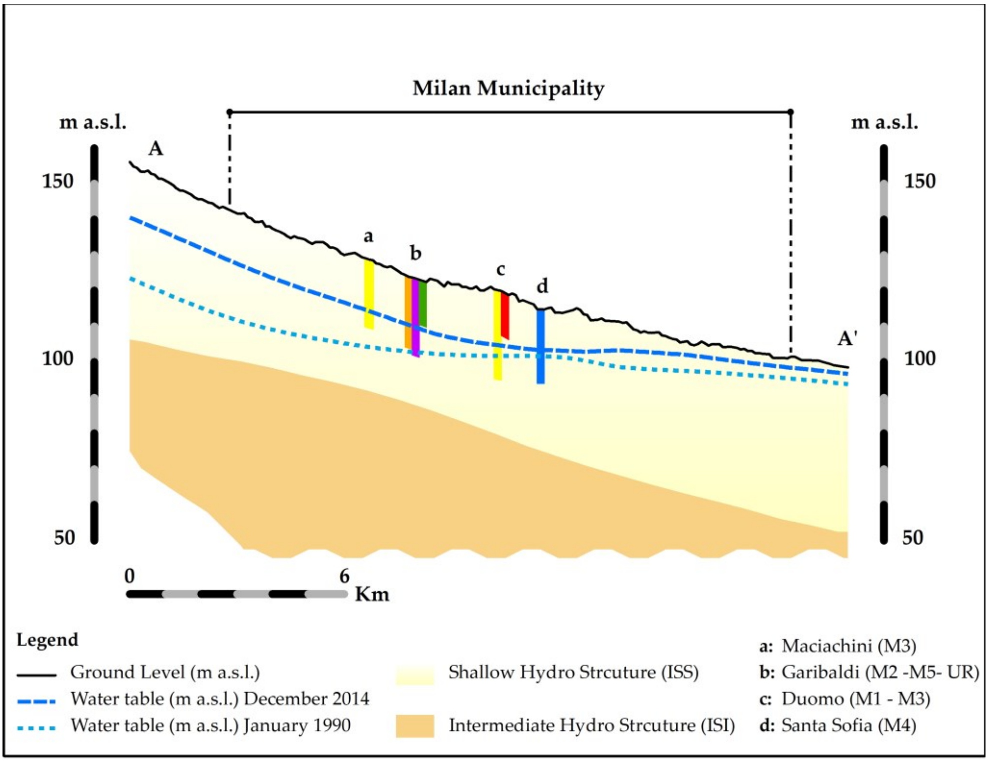

Fig. 5.2. Hydrogeological schematic N–S cross section of the study area, showing the location of some subway stations.

5.3. Materials and Methods

The methodology proposed in the present paper is composed of 4 steps: 1) implementation of a 3D GDB for UIs (3D GDB), including the calculation of the underground volume occupied by infrastructures, 2) water table reconstruction (GW), 3) calculation of infrastructure volumes (VOL) below the water table by combining the results of the previous steps, 4) evaluation of flooding of non-waterproofed infrastructures (FLOOD); the comparison between the results of this evaluation and actual flooding events, testified by local press news and photographic documentations, is used to qualitatively validate the whole methodology. A graphical representation of the methodology is given in Fig. 5.3.

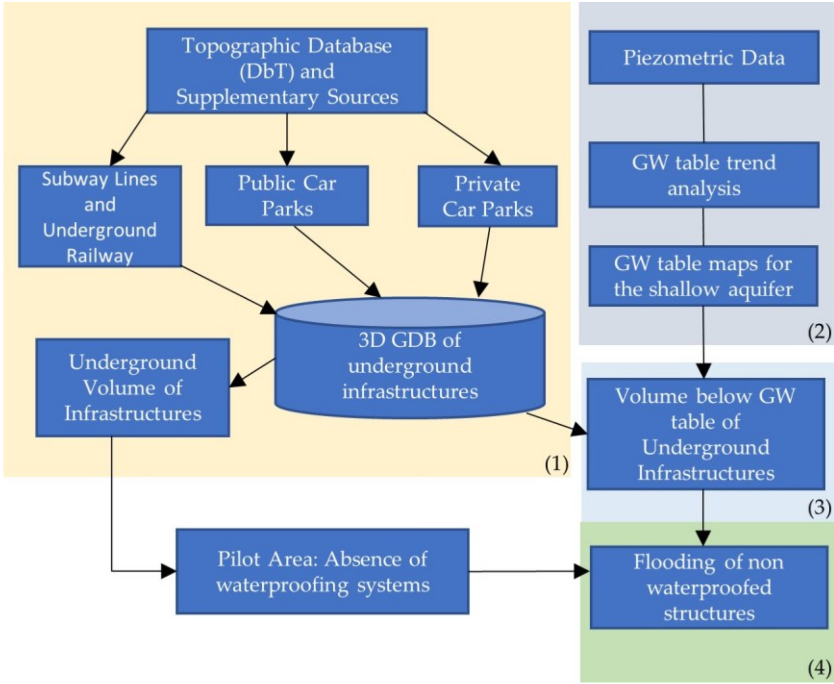

Fig. 5.3. Flowchart of the proposed methodology.

5.3.1. Implementation of a 3D Geodatabase for Underground Infrastructures

The Topographic Database (DbT, scale 1:2000), (Milan Metropolitan City 2019b) was used as the main source of information to build the 3D GDB. The DbT is an open-data basic cartographic tool owned by each municipality, used to represent the composition of the territory at the date of the air flight performed to build it. It reports the surface cartographic elements but not the underground volume occupied by infrastructures. This information resides in the urban Cadastre, a cartography which represents the inventory of the properties of the real estate units. In Italy, the Cadastre is property of the Revenue Agency: thus, it is a non-open data source. With the aim of generating a replicable procedure, thus only taking into account open-data sources of information, the Cadastre was not considered in this study. The DbT was shown to be useful but not sufficient in implementing the 3D GDB: thus, other supplementary sources were used to complete it. The list of public car parks is available as open data at the Municipality of Milan, while

Metropolitana Milanese S.p.a, the subway managing company, only provided for this study information on the tracks of the subway lines and the underground railway.

The main fields of the GDB, common to the three types of UIs, are: Name/ID; bottom reference (m a.s.l.); depth (m); area (m^2); volume (m^3). All the UIs were considered as polygon features.

Three supplementary fields were added both for public car parks and subway lines: period of construction, the number of underground floors and location for the former; period of construction, type of infrastructure (gallery or station) and waterproofing for the latter. Information on waterproofing was uploaded only for the subway lines since this was the only category of UIs having this information. For both private and public car parks it was difficult to obtain this information.

All the data collected were processed in GIS systems, with ArcMap 10.7 (ESRI 2013).

5.3.1.1. Private car parks

Within the specifications of the DbT, an information layer called "dressing lines" was included; these elements are mainly used for cartographic representation: among them, ramp lines are contained. Starting from the ramp lines, ramps were digitized as polygons through a neighborhood algorithm (i.e. buffer), to estimate their areal distribution.

Subsequently, an assumption was made: if an access ramp is present, then it leads to an underground volume. A spatial analysis procedure was therefore developed, to automatically identify all the buildings adjacent to the underground access ramps, listing them as elements having subsurface occupation (Fig. 5.4). Tests were carried out with different distances (3, 5 and 10 meters) to provide the definition of a suitable distance so that the closest building could be associated with a given ramp.

This methodology allowed us to identify the areal extension (with the same scale as the DbT) of the possible underground occupation, whose surface is comparable with the polygon of the building, but not the occupied volume, since the depth is not available. Therefore, given future GW management needs, a standard depth of 5 meters has so far been attributed to each element. This depth was considered exhaustive to satisfy the underground needs of each building, which were estimated as one floor. The bottom reference was calculated subtracting the attributed depth of 5 meters to the Digital Terrain Model value measured at the centroid of each infrastructure.

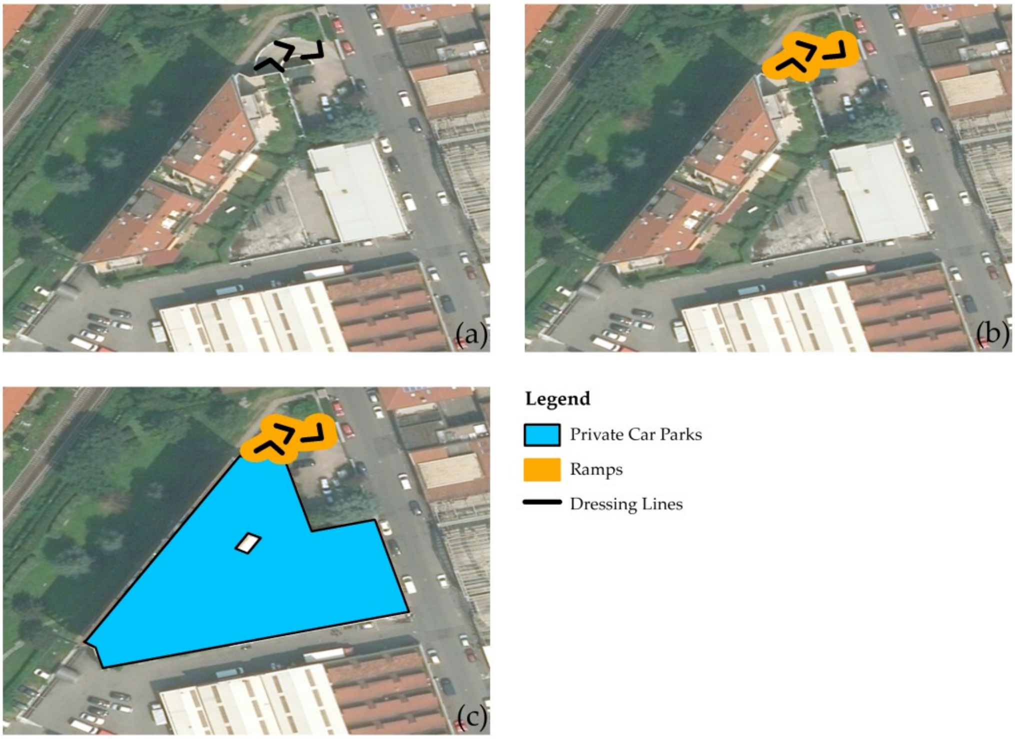

Fig. 5.4. Schematization of the procedure to calculate the underground volume occupied by private buildings. **a)** Identification of the dressing lines. **b)** Digitization of the ramp polygon associated to the dressing lines. **c)** Spatial analysis to associate the building with the ramp. Satellite image source: Geoportale Regione Lombardia.

5.3.1.2. Public car parks

The city of Milan has a list of 126 car parks classifiable as public (municipal-owned car parks, granted to private users). The perimeter of each public car park was manually digitized (time spent: three man-months) using the few elements present in the DbT (ventilation grilles, fire tanks, elevators lifts) as markers for the digitization, together with other documentary sources (press review, aerial images, public photographic archives). Thus, these elements were digitized with the same scale as the DbT. While for private car parks the subsurface occupation was estimated at one floor, these parks are characterized by a multi-story development: the number of underground floors depends on the parking needs of each area, with possible differences among different areas of the city. To estimate their volumetric impact on the subsurface, the existing number of underground floors was then considered. The total depth of each car park was assigned as follows: to the first floor, considering also the access ramp to the parking, a depth of 5 meters was assigned; to all the other floors, a depth of 3 meters was assigned (Pappa and Benardos 2007). The bottom reference of each public car park was calculated in the same way as for the private car parks.

5.3.1.3. Subway lines and underground railway

The subway lines and the underground railway are represented in the DbT as lines, but no information is available about the bottom elevation. Furthermore, since the DbT was updated to 2012, the M5 line, of more recent construction, does not appear.

The altimetric profiles of each subway line and of the underground railway, together with information on the average diameter of the tunnels of each track, were provided by Metropolitana Milanese S.p.a, the subway managing company. The digitization of points and of their altitude along the various sections of each line was carried out to define the lower limits of the infrastructures (bottom of the stations, intervention works and tunnels); from these limits, considering the average tunnel diameter of each line and since all the stations reach the ground level, reliable thicknesses and depths were considered. Thus, final polygons have a centimeter geometric accuracy. The M2 line and the underground railway are constituted both of superficial and underground stretches; the formers were not considered in the calculation.

5.3.2. Reconstruction of the Water Table

GW levels were provided by the local water authority (Metropolitana Milanese S.p.a); piezometric trends at each measured location were reconstructed to identify a global minimum, a local minimum, a global maximum, and a local maximum of the GW level time series. The period examined was between January 1990 and December 2019.

Potentiometric maps for the shallow aquifer were reconstructed for the identified periods. GW heads in wells were interpolated using universal kriging due to the presence of a piezometric trend (from NW to SE) (Bonomi et al. 1998; Beretta et al. 2004); (Isaaks and Srivastava 1989; Goovaerts 1997; Kitanidis 1997; Webster and Oliver 2001).

5.3.3. Calculation of Infrastructure Volumes Below the Water Table

Combining the results of the previous steps, volumes below the water table and their variation over time were quantified through a spatial analysis of the available data ("Polygon Volume" and "Surface Difference" tools available in ArcMap 10.7). The "Polygon Volume" tool was used to quantify the volumes lying below the water table for punctual infrastructures (i.e. private and public car parks), while the "Surface Difference" tool was used for subway lines; as these latter are continuous infrastructures, their bottom was considered as a surface, thus calculating the displacement between two surfaces (i.e. subway lines bottom and water table). The bottom of UIs was considered as the reference limit to quantify the volume of an infrastructure lying below the water table.

5.3.4. Evaluation of the Impact of Groundwater on Non-Waterproofed Infrastructures in a Pilot Area

Following the calculation of infrastructure volumes below the water table, a pilot area was identified, including the three categories of UIs, to evaluate the impact of GW on these infrastructures. If a lack of an appropriate waterproofed system emerged, these infrastructures were considered as vulnerable to infiltrations or flooding. Stretches of lines M1 and M2 fall within this area, as well as some of the oldest public car parks included in the GDB. The infrastructures identified as flooded were compared to available local press news and photographic documentations. Their matching can be considered as a qualitative validation of the whole methodology here proposed.

5.4. Results

5.4.1. 3D GDB Implementation and Analysis

The application of the methodology developed to identify private car parks led to the insertion into the GDB of 11,283 buildings out of 53,041 among those included in the DbT. This result was obtained using an association distance of a building with a given ramp of 5 meters, which emerged as the optimal distance for the study area. Their territorial distribution shows a higher concentration of underground occupation in areas urbanized after post-war reconstruction, in line with the development of the city urban fabric. An example of their features is provided in Table 5.1.

Table 5.1. Main features of selected private car parks (PrCP) located in the study area.

Name/ID	Bottom (m a.s.l.)	Depth (m)	Area × 10^3 (m^2)	Volume × 10^3 (m^3)
PrCP1	119.32	5	0.12	0.59
PrCP100	117.27	5	0.23	1.17
PrCP1000	112.99	5	1.37	6.87
PrCP10000	127.94	5	0.14	0.71
…	…	…	…	…
PrCP11283	127.52	5	0.48	2.39
Total Parks: 11,283				45,100.96

A brief example of the list and features of the 126 public car parks is provided in Table 5.2. The overall list is presented in Table S5.1 (Supplementary Materials). The highest density of underground car parks is in the city center, where the oldest (<1990) and the most recent (2007-2014) car parks were built. Furthermore, these parking lots present a higher depth with respect to the ones located in the most peripheral areas of the city, built mostly from the 1990-2002 period onward.

Table 5.2. Main features of some of the public car parks located in the study area. CP stands for construction period.

Name	Bottom (m a.s.l.)	Depth (m)	Area × 10^3 (m^2)	Volume × 10^3 (m^3)	CP	Floors	Location
Silla	131.3	5	5.82	29.1	2002-2007	1	North
Erculea	100.91	17	1.3	22.10	< 1990	5	Downtown
Risorgimento Nord	96.9	20	1.43	28.6	2007-2014	6	Downtown
Ciclamini/ Margherite	111.5	8	3	24	1990-2002	2	West
…	…	…	…	…	…	…	…
Cascina Bianca	106.2	5	7.88	39.4	2002-2007	1	South
Total Parks: 126				5,157			

An example of the main characteristics contained in the 3D GDB for the subway lines and the underground railway is provided in Table 5.3.

Table 5.3. Main features of some stretches of the subway lines and underground railway located in the study area. CP stands for construction period.

Name	**Bottom (m a.s.l.)**	**Depth (m)**	**Area × 10^3 (m^2)**	**Volume × 10^3 (m^3)**	**CP**	**Type**	**Waterproofed**
Duomo (M1)	107.64	12.47	5.56	69.33	<1990	Station	No
Sant'Agostino (M2)	99.12	17.35	1.37	23.77	<1990	Station	No
Duomo (M3)	95.7	25.05	4.59	114.98	1990-2002	Station	Yes
Linate (M4)	98.91	11.1	4.25	47.17	2021-2023	Station	Yes
…	…	…	…	…	…	…	…
Lotto (M5)	98.47	26.28	2.41	63.33	>2014	Station	Yes
Repubblica – P.ta Venezia (UR)	100.9	8.5	6.15	52.27	1990-2002	Gallery	Yes
Total elements: 388				13,702.67			

A map showing the location and volumes of all the underground infrastructural elements contained in the 3D GDB is provided in Fig. 5.5. Moreover, a more detailed visualization of the contents of the 3D GDB is made available through a WebGIS service (https://arcg.is/HHWDi0). Larger volumes for a single element reach up to more than 100×10^3 m^3 and refer to subway elements; smaller volumes are less than 10×10^3 m^3 and mainly refer to private car parks. However, total volume for each type of infrastructure reveals that private car parks occupy larger volumes (45×10^6 m^3) than railways (14×10^6 m^3), followed by public car parks (5×10^6 m^3).

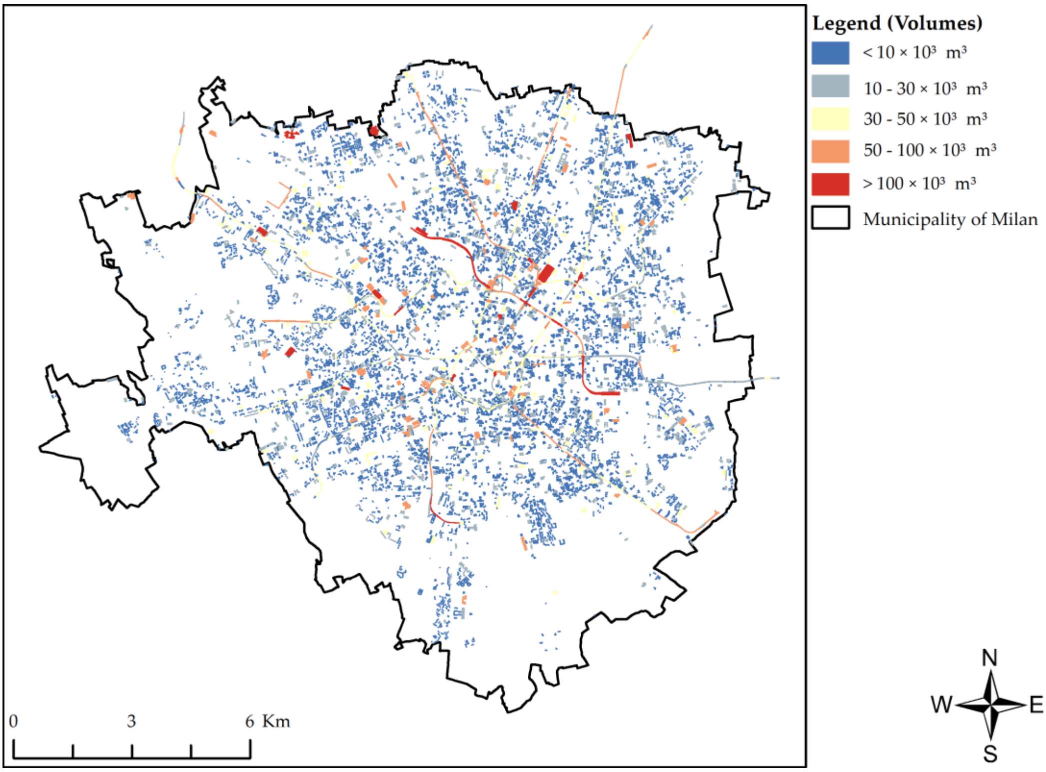

Fig. 5.5. Location and volumes of all the infrastructural elements contained in the 3D GDB (private and public car parks and subway lines).

5.4.2. GW Table

Ten monitoring wells (MW) (Fig. 5.6b), distributed across the domain, were selected to perform the piezometric trend reconstructions. As described in Section 5.3.2, four periods were identified: January 1990 (Jan90) as the global minimum of the whole considered GW level time series; December 2002 (Dec02) as a local maximum of the GW level time series; September 2007 (Sep07) as a local minimum; December 2014 (Dec14) as the global maximum. GW table maps for the shallow aquifer (ISS) for these four periods are provided in Supplementary Materials (Figs. S5.1, S5.2, S5.3 and S5.4). Jan90 could be identified as the overall starting point of the increasing trend consequent to the industrial decommissioning which began in the early 1990s (Beretta and Avanzini 1998; Bonomi et al. 1998). However, this is not the historical global minimum, which occurred at the end of the 1970s, determined by an intense industrial exploitation (Bonomi 1999). As visible in Fig. 5.6a, monitoring wells located in the northern part of the domain registered a wider oscillation of the water table than the southern ones. Reduced oscillations in the southern area are due to geological and hydrogeological reasons: changes in sediment permeability from coarse (i.e. gravel and sand) to fine (i.e. silt and clay) induce GW to outflow, forming numerous lowland springs (De Luca et al. 2014), and thus constraining GW oscillations.

A general rising trend is identifiable in the period considered, except for seasonal trends emerging in the local minimum and the global maximum periods.

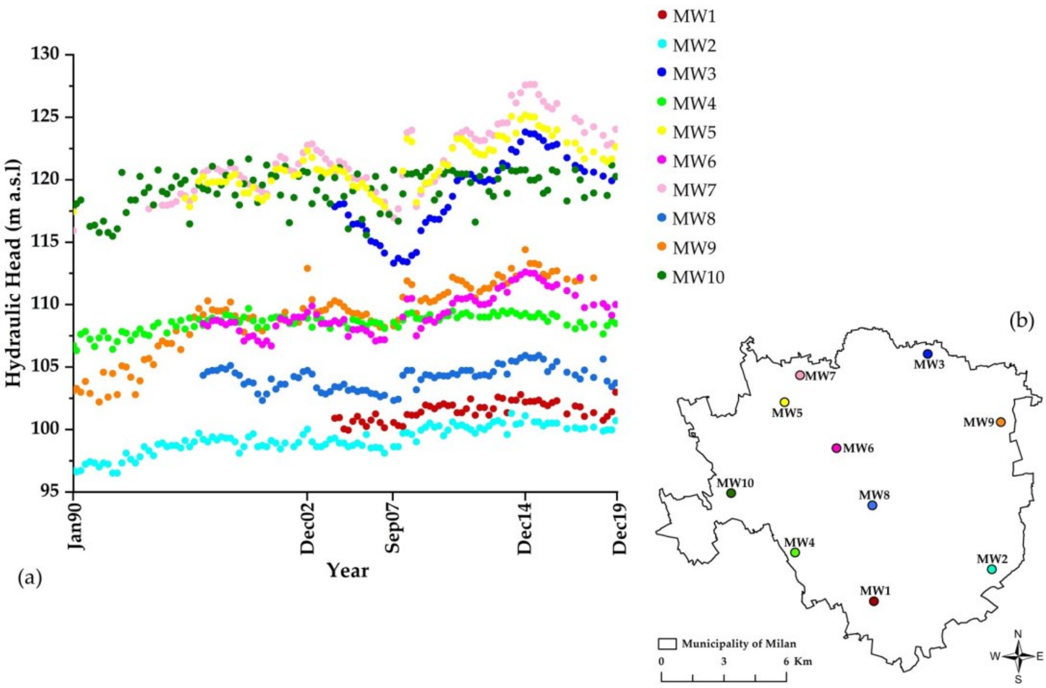

Fig. 5.6. a) Monitoring wells (MW) time series for the considered period (January 1990-December 2019). **b)** Location of the MWs in the study area.

5.4.3. Infrastructure Volumes Below the Water Table

The results in Fig. 5.7 are provided only for the local minimum (Sep07) and the global maximum condition (Dec14): the majority of UIs were built in these periods, thus facilitating the comparison of the results.

Volumes below the water table for private car parks were identified both in minimum and maximum GW level conditions (Fig. 5.7). In the minimum GW level period (Sep07), a few volumes were found to be below the water table (a total of 0.32×10^6 m^3), most of which were concentrated in the western part of the study area. In maximum GW level conditions (Dec14), the total amount of volumes below the water table increased, reaching 1.12×10^6 m^3, and their spatial distribution expanded toward the south-eastern portion of the area. Furthermore, a few volumes below the water table also emerged in the northern sector of the study area.

As regards public car parks, in the northern part of the area, the unsaturated zone of the aquifer is wider than in the southern part (Fig. 5.2); therefore, only deep volumes can actually be reached by the water table. Most of the public car parks in the northern part of the area are only developed on two underground floors, therefore they do not appear to be within the range of the water table oscillation. In contrast, in the southern part of the city, more car park volumes lie below the water table (Fig. 5.7). Particularly in the western part, where car park depth is limited to two underground floors, the analysis revealed that car park volumes are below the water table only during the maximum period. On the other hand, in the downtown, the car parks can have up to six floors. Because of this, the analysis identified several car parks with volumes below the water table also during the minimum period. In the southernmost part of the area, most of the car parks range between one and two floors, while only in a few cases do they reach three floors. In the latest case, the analysis showed volumes below the water table during both minimum and maximum conditions.

As regards the M1 subway line, its westmost stretch, close to Bisceglie station (M1-a, Fig. 5.7), was frequently below the water table. Apart from Jan90, when this section was still under construction, some portions of this stretch always revealed an interaction with the water table. Volumes below the water table were also identified in the most recent northern stretch of this line, including Rho Fiera and Pero stations (completed in 2005) for both Sep07 and Dec14 periods (M1-b, Fig. 5.7). Furthermore, during the maximum GW level periods, some similar situations emerged in different areas: in particular, in the northern stretches of the line, from Bonola to Uruguay stations (M1-c, Fig. 5.7b), and in the stretch between QT8 and Lotto stations (M1-d, Fig. 5.7b). In the downtown areas, a few volumes below the water table emerged in the maximum periods between Palestro and Porta Venezia (M1-e, Fig. 5.7b), Porta Venezia and Lima (M1-f, Fig. 5.7b) and between Loreto and Pasteur stations (M1-g, Fig. 5.7b).

For the M2 line, the section around Sant'Agostino station (M2-a, Fig. 5.7) emerged as the stretch that most frequently reveals volumes below the water table, during all the considered periods. From Dec02 onward, the section between Loreto and Udine stations (M2-b, Fig. 5.7b), particularly between Piola and Lambrate stations (M2-c, Fig. 5.7), showed some volumes below the water table. During the maximum GW levels periods, volumes below the water table also emerged in the downtown areas between Lanza and Moscova (M2-d, Fig. 5.7b), and between Garibaldi and Gioia stations (M2-e, Fig. 5.7b).

The M3 line was inaugurated around the middle of 1990, so Jan90 was not evaluated in the analysis. Except for Centrale and Repubblica stations (M3-a, Fig. 5.7b), located in the downtown area, the central part of the line was always below the water table. A similar situation was for the southern stretch of the line.

The underground railway was inaugurated in 1997. As for the M3 line, volumes below the water table were identified along most of the line.

The analysis of the volumes below the water table was not performed for M4 and M5 lines. The M4 line is under construction, and its completion is expected to be between 2021 and 2023. The M5 line was inaugurated in 2015, so after the identified GW local and global periods.

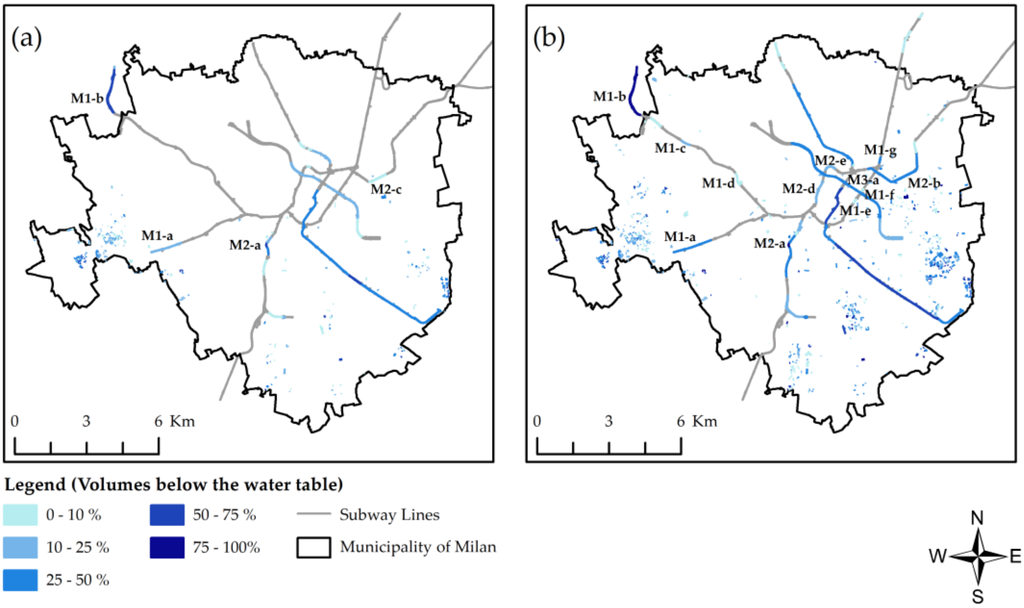

Fig. 5.7. Volumes lying below the water table for the local minimum of Sep07 **a)** and for the global maximum of Dec14 **b)**. Color coding indicates percentages of the volumes below the water table.

The results that emerged in this study for the subway lines and the underground railway are consistent with what was discussed by Colombo (Colombo 1999), who identified the M1-a, M1-c to M1-g, M2-a and M2-c to M2-e areas as the most critical concerning GW/UIs interactions.

The evolution of the volumes lying below the water table over time is reported in Fig. 5.8 as percentages of the total volume for each type of infrastructure for the four periods considered. A general increasing trend of the volumes below the water table has been observed, connected to the GW rising trend visible in Fig. 5.6a, with marked seasonal oscillations for the local minimum of Sep07 and the global maximum of Dec14. Percentages are minimal for private car parks, due to their reduced depth, while an increase is visible for public car parks and subway lines. For these latter cases, the increase is related to their period of construction, with the more recent lines showing a higher percentage of volumes below the water table.

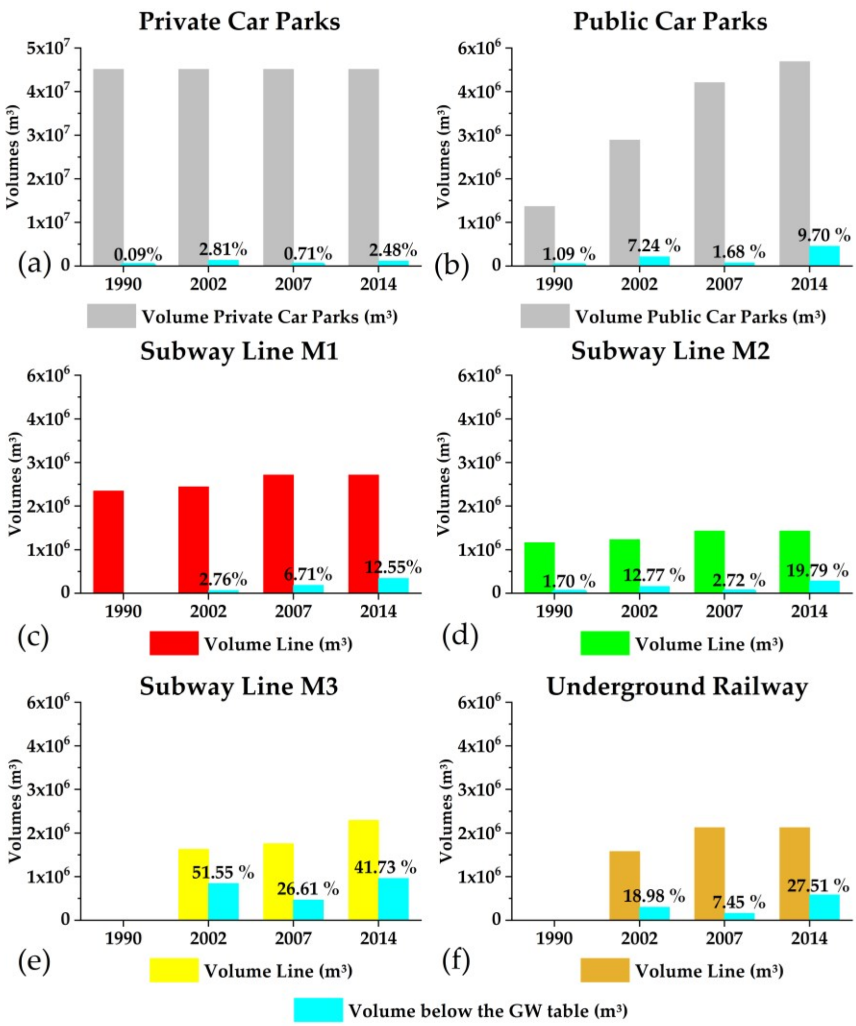

Fig. 5.8. Volumes and portions below the water table (cyan expressed as percentages of the total volume) over time for: **a)** Private Car Parks, **b)** Public Car Parks, **c)** Subway Line M1, **d)** Subway Line M2, **e)** Subway Line M3, **f)** Underground Railway. *Y*-axis scale is the same for all the categories, except for Private Car Parks, where 10^7 has been kept as an order of magnitude.

5.4.4. Impact of Groundwater on Non-Waterproofed Infrastructures in a Pilot Area

The impact of GW on non-waterproofed infrastructures was evaluated for a pilot area of 2.56 km^2 (Fig. 5.9), located in the downtown area, including five public car parks, six stations and eight stretches of the subway lines M1 and M2. Except for Sant'Ambrogio car park, which was inaugurated in 2014, the other public car parks were theorized as non-waterproofed. In this area, volumes lying below the GW table were not identified for private car parks.

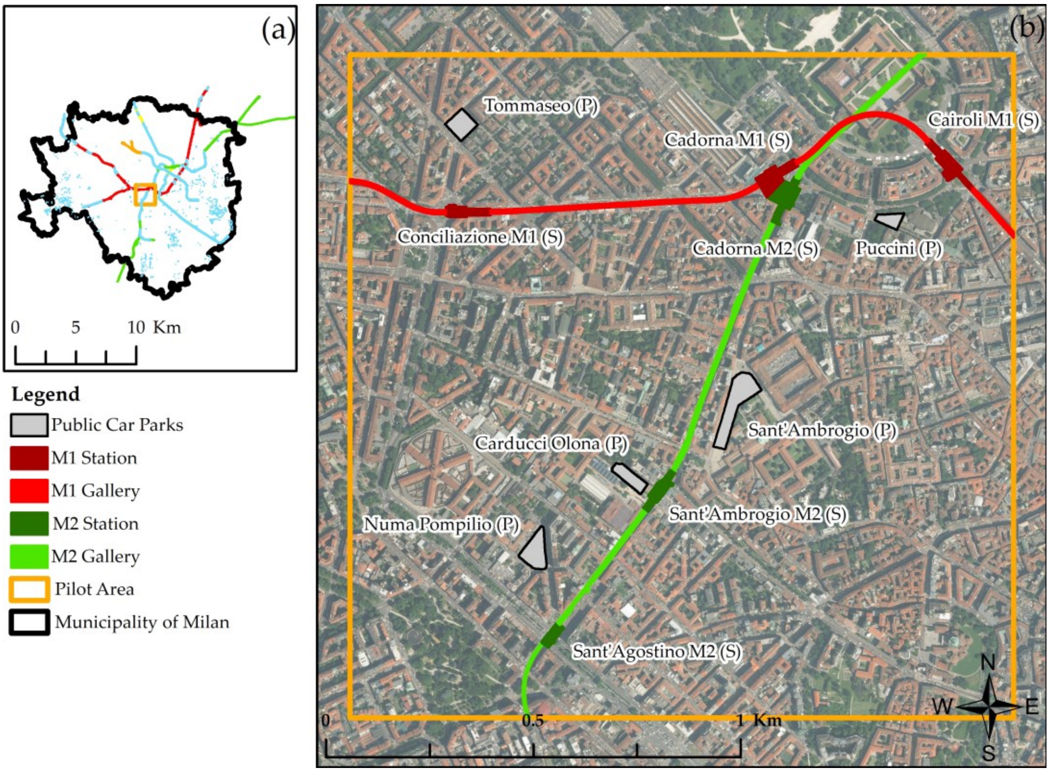

Fig. 5.9. a) Geographical setting of the pilot area. Locations of volumes lying below the GW table for the maximum GW level condition of Dec14 are shown. **b)** UIs within the pilot area. (P) means public car park; (S) means station. Satellite image Source: Geoportale Regione Lombardia.

A graphical representation of the volumes lying below the water table for all the periods considered is provided in Fig. 5.10, providing information on the possible risk of flooding due to non-waterproofing. In this work, the quantification of flooding was not examined; thus, flooding is intended just as a qualitative validation (i.e. infrastructures which can present infiltrations or flooding).

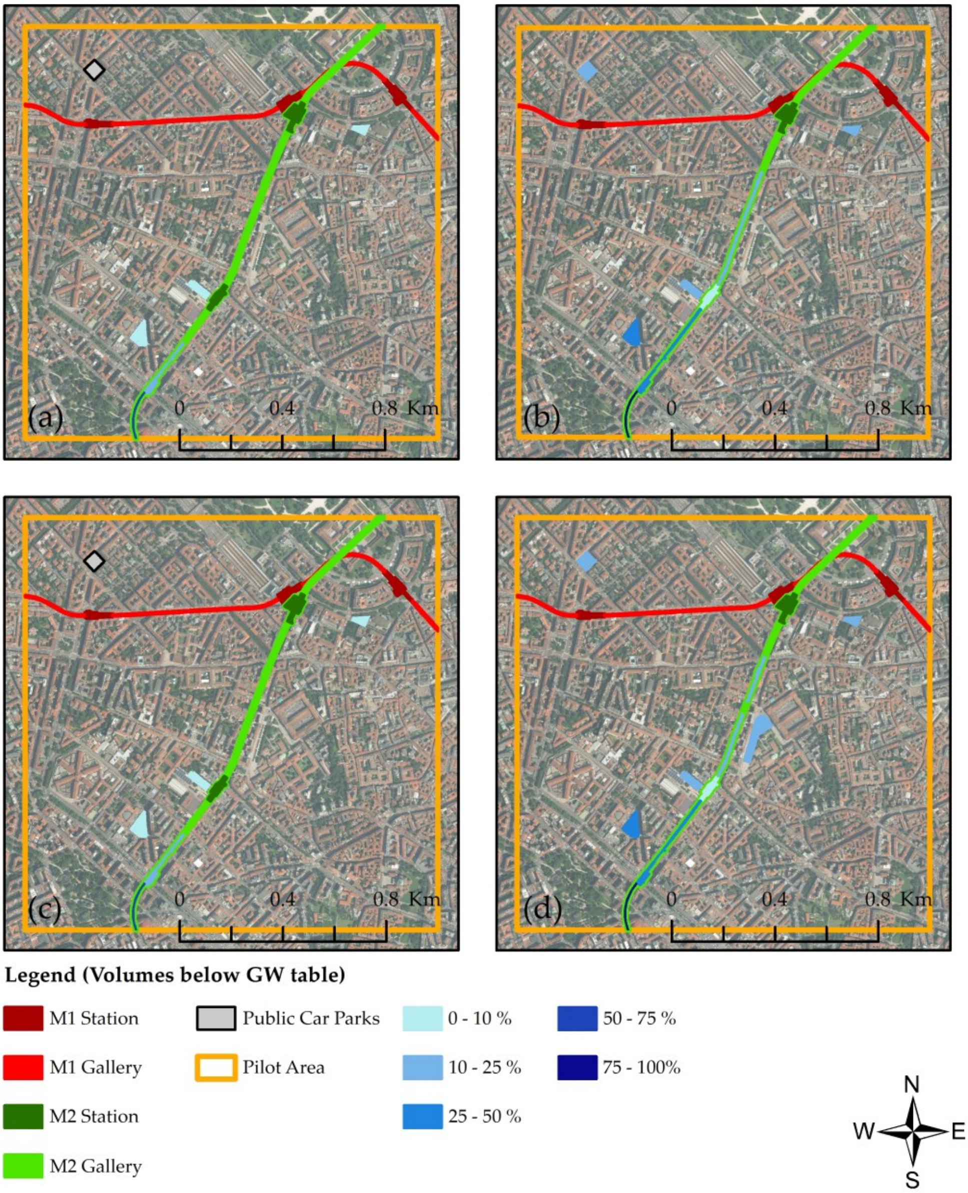

Fig. 5.10. Volumes lying below the GW table in **a)** Jan90, **b)** Dec02, **c)** Sep07, **d)** Dec14. Colour coding indicates percentages of the volumes below the water table. Satellite image Source: Geoportale Regione Lombardia.

The results for all the infrastructural elements considered are summarized in Table 5.4. Concerning subway stations, Sant'Agostino (line M2) was the most affected, followed by Sant'Ambrogio (line M2), which was only slightly affected. Accordingly, the M2 line stretches to/from and between these stations were estimated to be flooded. On the contrary, line M1 stretches and stations, located in the northern portion of the pilot area, did not reveal volumes below the water table in each of the periods considered (Fig. 5.10), as occurred also for the considered northern portion of the M2 line (Fig. 5.10), due to their shallower depth.

An additional 3D reconstruction of the historical evolution of the most affected Sant'Agostino M2 station was realized (Fig. 5.11). During GW maximums (Figs. 5.11c and 5.11e), the gallery stretches to and from the station was completely submerged by the water table, and thus flooded. Moreover, the flooding of the station and galleries is estimated, with a lower extent, also for GW minimum periods. Thus, Sant'Agostino station can be considered as being constantly impacted by flooding. This assumption is confirmed by actual flooding events that frequently happened in the last 10 years, as documented by local press and photographic documentations (Fig. 5.12).

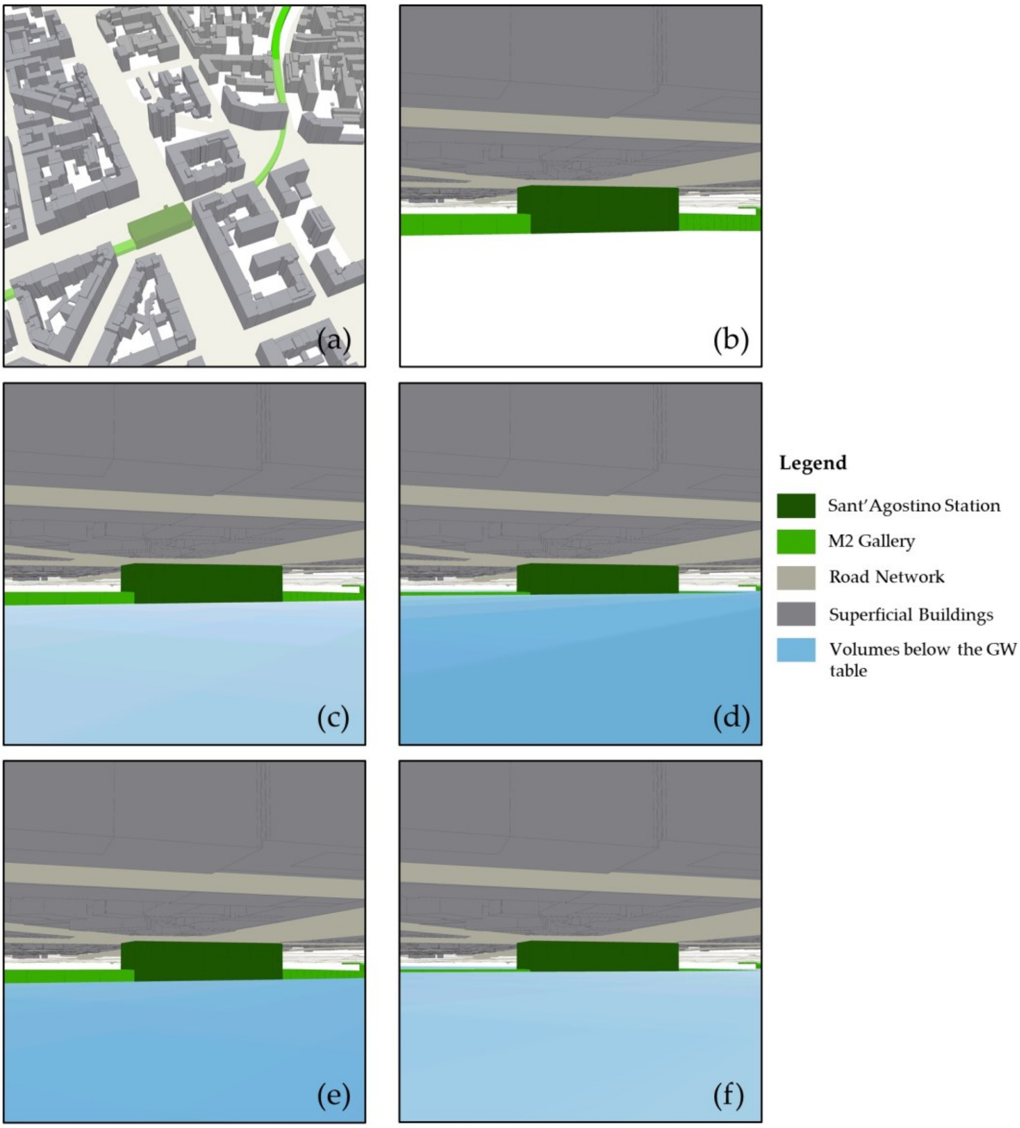

Fig. 5.11. a) Three-dimensional surface reconstruction close to Sant'Agostino station. Sant'Agostino station is visible below the road network. **b)** Three-dimensional underground reconstruction of Sant'Agostino station. Volumes below the GW table of Sant'Agostino station in **c)** Jan90, **d)** Dec02, **e)** Sep07, **f)** Dec14. Images were realized with ArcGIS Pro.

Concerning public car parks, due to their deeper structures, volumes below the water table have been identified in all the considered periods, apart from Tommaseo, which is above the water table under minimum-level conditions (Fig. 5.10). As regards Numa

Pompilio, as for Sant'Agostino station, the identified flooding is confirmed by photographic documentation (Fig. 5.12c). Some waterproofing works have been carried out in the last decade to counteract this situation (Fig. 5.12d). On the contrary, flooding episodes have not been documented for Sant'Ambrogio car park, which, being more recent, was designed as being waterproof. This approach should also be applied in the other areas that emerged as critical from this work.

Table 5.4. Features and volumes below the GW table of the underground structures within the pilot area. V Jan90 (%), V Dec02 (%), V Sep07 (%) and V Dec14 (%) refers to the percentage volume below the water table of the UIs for each of the periods considered. (V) means volume; (G) means gallery; (P) means underground car park; (S) means station. Sant'Ambrogio car park was considered only in the final period because it was completed in 2014. CP stands for construction period.

Type	**Name**	**Depth (m)**	**Area × 10^3 (m^2)**	**Volume × 10^3 (m^3)**	**CP**	**V Jan90 (%)**	**V Dec02 (%)**	**V Sep07 (%)**	**V Dec14 (%)**
S	Cadorna M1	10.65	3.53	37.59	< 1990	0	0	0	0
S	Cairoli M1	10.16	3.40	34.54	< 1990	0	0	0	0
S	Concilia zione M1	9.5	2.22	21.09	< 1990	0	0	0	0
S	Cadorna M2	10.31	4.06	41.86	< 1990	0	0	0	0
S	Sant'Ag ostino M2	17.35	1.37	23.77	< 1990	16.47	35.79	16.50	34.85
S	Sant'A mbrogio M2	12.77	2.41	30.77	< 1990	0	3.46	0	9.79

Type	**Name**	**Depth (m)**	**Area × 10^3 (m^2)**	**Volume × 10^3 (m^3)**	**CP**	**V Jan90 (%)**	**V Dec02 (%)**	**V Sep07 (%)**	**V Dec14 (%)**
G	Pagano – Conciliazione M1	6.5	2.34	15.21	< 1990	0	0	0	0
G	Conciliazione – Cadorna M1	6.5	6.18	40.17	< 1990	0	0	0	0
G	Cadorna – Cairoli M1	6.5	3.55	23.07	< 1990	0	0	0	0
G	Cairoli – Cordusio M1	6.5	1.4	9.1	< 1990	0	0	0	0
G	Porta Genova – Sant'Agostino M2	7	1.08	7.56	< 1990	63.76	113.88	65.68	106.66
G	Sant'Agostino – Sant'Ambogio M2	7	3	21	< 1990	12.62	42.77	12.40	49.88
G	Sant'Ambrogio –	7	6.4	44.8	< 1990	0	13.76	0	20.65

Type	Name	Depth (m)	Area × 10^3 (m^2)	Volume × 10^3 (m^3)	CP	V Jan90 (%)	V Dec02 (%)	V Sep07 (%)	V Dec14 (%)
	Cadorna M2								
G	Cadorna – Lanza M2	7	3.98	27.86	< 1990	0	0	0	0
P	Carducci Olona	17	3.42	58.14	< 1990	4.26	17.63	3.75	20.79
P	Numa Pompilio	17	4.07	69.27	< 1990	8.65	27.72	8.28	28.18
P	Puccini	20	1.68	33.65	< 1990	3.56	19.27	2.84	22.69
P	Sant'Ambrogio	17	7.41	125.93	2007-2014	---	---	---	22.40
P	Tommaseo	17	3.15	53.60	< 1990	0	13.29	0	19.85

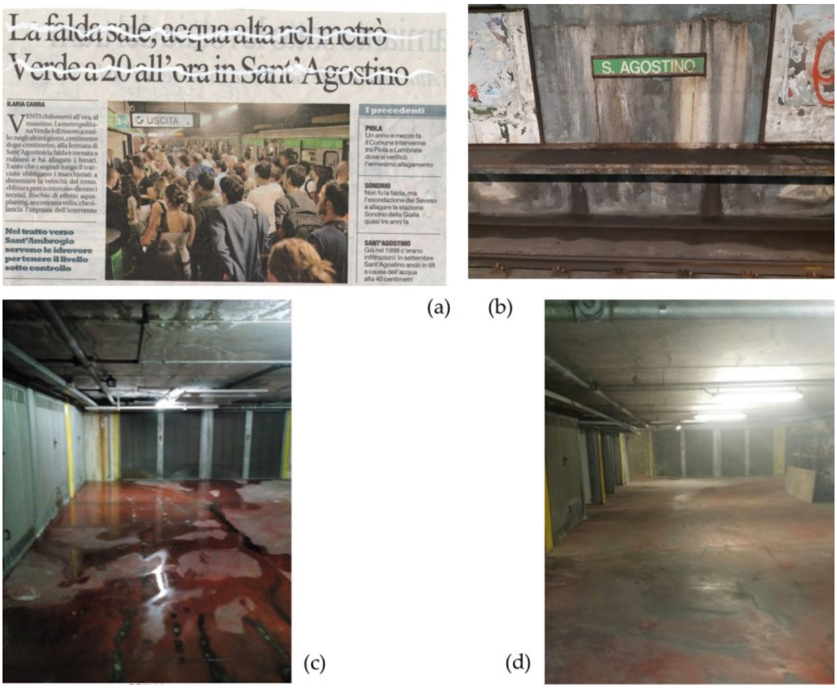

La falda sale, acqua alta nel metrò Verde a 20 all'ora in Sant'Agostino

ILARIA CARRA

VENTI chilometri all'ora, al massimo. La metropolitana Verde è di nuovo a mollo: negli ultimi giorni, centimetro dopo centimetro, alla fermata di Sant'Agostino la falda è tornata a rialzarsi e ha allagato i binari. Tanto che i segnali lungo il tracciato obbligano i macchinisti a dimezzare la velocità del treno. «Misura precauzionale» dicono i tecnici. Rischio di effetto aquaplaning, ancora una volta, che rilancia l'urgenza dell'intervento

Nel tratto verso Sant'Ambrogio servono le idrovore per tenere il livello sotto controllo

I precedenti

PIOLA
Un anno e mezzo fa il Comune intervenne tra Piola e Lambrate dove si verificò l'ennesimo allagamento

SONDRIO
Non fu la falda, ma l'esondazione del Seveso a allagare la stazione Sondrio della Gialla quasi tre anni fa

SANT'AGOSTINO
Già nel 1998 c'erano infiltrazioni: in settembre Sant'Agostino andò in tilt a causa dell'acqua alta 40 centimetri

Fig. 5.12. a) Newspaper article of "La Repubblica" (2nd July 2013), dealing with flooding episodes in Sant'Agostino station. **b)** Flooding evidence in Sant'Agostino station (8th September 2020). (Image credits to the authors). **c)** Flooding evidence in Numa Pompilio public car park. **d)** Absence of flooding evidence after waterproofing works in Numa Pompilio public car park. **c)** and **d)**: images were provided by Rete Irene.

5.5. Discussion

An urban transformation, which also involves the underground aspects, is taking place for the city of Milan. A detailed inventory of all the UIs is thus required.

The GDB has allowed to gather part of the wide array of urban data, usually coming from different sources (institutions, stakeholders, public and private owners) (Culshaw and Price 2011; Li 2011), standardizing dissimilarities among data to properly settle them for GW management needs. Due to the database's simple and updatable structure, data that with time could become available in the future will in fact be rapidly integrated with the already existing information. Its realization has been aided by Geographic Information Systems (GIS): their capacity for storing, analyzing and managing all types of geographical data (de Rienzo et al. 2009; Delmastro et al. 2016) has allowed to easily collect information coming from different sources in a single structure; moreover, the UIs were accurately reconstructed according to their real depths and volumes.

The methodology applied to define the underground occupation of private buildings (private car parks) is, to the best of the authors' knowledge, an element of novelty; it attempts to fill a lack of information through a spatial analysis procedure, exploiting all the cartographic content available in the DbT. However, it still requires a phase of refinement. Indeed, in some cases, the underground volumes may be overestimated, as for those ramps that have a superficial development but do not lead to underground car parks (instead leading into buildings, i.e. supermarkets). In other cases, the underground volumes may be underestimated: the methodology fails to highlight those access ramps that fall within the perimeter of the building and therefore are not visible in the creation phase of the DbT; however, this latter case is not a very common building typology for the study area considered. Future developments will concern both a further detailed validation of the obtained results (i.e. looking for coherence with respect to known situations) and the consequent elimination of the overestimated elements.

The application of the methodology for the city of Milan was possible due to the availability of the DbT data distributed by the "Decimetro" geoportal (Milan Metropolitan City 2019b). The DbT is developed according to the European Standards (INSPIRE) (Directive 2007): this contributes to the replicability of the procedure in other study areas. Other factors are needed to strengthen the application of this methodology elsewhere: the availability of the same typology of data, a strict collaboration among institutions, the presence of a policy aimed at stimulating the use of open-data, and the expertise of using and extracting valuable information from data (Janssen et al. 2012). The association distance between the ramp and the building adopted for the city of Milan may not be suitable for other urban realities, thus making a previous site-specific calibration necessary.

The integration of the DbT with other supplementary sources brings out a lack of collaboration among institutions, typical of urban data management (Culshaw and Price

2011; Li 2011); a closer cooperation among institutions would contribute to easily managing data both for urban underground planning and GW management aspects.

The GDB application has thus allowed to evaluate how the subsurface volumes lying below the water table have changed among time.

In general, in the northern part of the study area, considering an assigned depth of five meters, and a higher depth of the water table, private car parks do not present volumes below the water table. However, in a few cases, volumes lying below the water table were also identified in the northern sector during maximum GW levels. This was associated with problems related to the Digital Terrain Model, which can be not fully representative of the ground level at a given point. This can be considered as a limit of the methodology: however, this problem emerged only in a few isolated situations.

The congestion of public car parks in the downtown Milan area is related to a high demand for infrastructure (Bobylev 2009), due to socio-economic needs: the majority of the economic activities is located in the city center (Istat 2011; Milan Metropolitan City 2019a). The volumes of the deepest infrastructures were shown to lie below the water table: therefore, future infrastructures in this area should be planned with adequate waterproofing techniques. The reduced subsurface volume in the peripheral areas is related to a decreased socio-economic demand: despite this, as for the private car parks, volumes lying below the water table were identified, in particular when the hydraulic head was higher. This is due to hydrogeological reasons: in the southern portion of the study area, the water table has always been historically close to the ground level due to the presence of fine deposits (i.e. silt and clay) with low values of hydraulic conductivity (Beretta et al. 1985; Airoldi and Casati 1989; Francani et al. 1994; Airoldi et al. 1997; Beretta et al. 2004), which force GW to reach the ground level; in the western area, the presence of clay lenses determines the existence of a perched aquifer located around 6-8 meters below ground level, with strong seasonal oscillations (Bonomi et al. 2009). An overall reduced presence of subsurface volumes (Fig. 5.5) in these peripheral areas, compared to the downtown, is also amenable to these reasons.

The majority of the subsurface volumes lying below the water table for the subway line M1 is in the northern stretch, between Rho Fiera and Pero stations (M1-b): their construction method differs from that used for the rest of the line; these two stations were built at greater depths. For the same reason, Sant'Agostino station was revealed as the most recurring area below GW level for M2 line: its two rails were built as overlapping pipes, thus determining a major depth of subsurface occupation. As determined by the focus on the pilot area, in Dec02 and Dec14, the considered stretch of gallery from Porta Genova to Sant'Agostino (M2-a) was completely submerged, with the GW level above the top of the gallery. The stretch between Loreto and Udine stations (M2-b) was revealed as another critical area. In particular, the section between Piola and Lambrate stations (M2-c) was subjected to waterproofing works during the summer of 2019 to overcome flooding problems. Since these lines were built without any impermeabilization, the increase in stretches lying below the water table due to GW rising, both for the M1 and M2 lines, should be monitored by the subway managing company. Due to their depth, M3 line and the underground railway revealed a high percentage of subsurface volumes below the GW level: to overcome this problem, they were designed with waterproofing systems; M3 interaction with GW in the southern sector of the domain is amenable both to a deeper development of the line and a closer elevation of the water table to the ground level.

As reported in Section 5.4.3, the methodology allowed to verify what was already described in a previous work (Colombo 1999), where M1-a, M1-c to M1-g, M2-a and M2-c to M2-e areas were already pointed out as the most critical concerning GW/UIs interactions. At the same time, as reported in Section 5.4.4, flooding evidence, also reported by local press reviews, occurred where the oldest UIs, showing volumes below the water table, were designed without waterproofing techniques. This acts as a qualitative validation both of the methodology used to implement the GDB and its usefulness in GW management. In the future, citizen science approaches (Bhattacharjee 2005; Bonney et al. 2009; Bonney et al. 2014; Bonney et al. 2016) or social media (i.e. tweets of metro passengers) could be exploited to validate the methodology, thus enlisting the public in organized scientific research. Both the city administrations and private companies could benefit from the implementation of this methodology, identifying the main critical areas of interaction, thus properly planning future underground development or adopting remediation strategies if necessary, especially focusing on the oldest non-waterproofed infrastructures. The GDB has in fact allowed to analyze the interaction between GW and UIs both at a city scale and at a more detailed level.

The integration of the GDB with numerical GW flow models will make it possible to define future scenarios of interaction according to the trend of the piezometric levels. As a further step, it should be interesting to evaluate if a different degree of interaction with the water table (i.e. UIs partially or completely submerged by the water table) could lead to a different flooding risk for the subsurface elements. The infrastructural elements have both an active and passive effect on GW (Dassargues 1997; Bonomi and Bellini 2003; Ricci et al. 2007; Pujades et al. 2012; Attard et al. 2015; Velasco et al. 2015; Attard et al. 2016b; Gattinoni and Scesi 2017; Colombo et al. 2018; De Caro et al. 2020). This contributes to characterizing urban modelling as a specific branch of hydrogeology, with its own time, scales, and dynamics of the hydrogeological processes (Vázquez-Suñé et al. 2005). Thus, this information needs to be analyzed and combined together with the large set of geological, hydrological, geomorphological and other features (Kresic and Mikszewski 2012) necessary to detail a complete urban conceptual model for the domain: this is an important step, as the conceptual model is the basis of an appropriate GW management plan. Using a standardized 3D GDB, the urban conceptual model would not need to be frequently revised, a both time- and cost-consuming activity (Vázquez-Suñé et al. 2005).

The implementation of a 3D vision of the volumes below the water table over time (Fig. 5.11) was revealed to be a comprehensible tool to evaluate this phenomenon: an increased use of these instruments will both guarantee a complete 3D vision of the subsurface and a proper 3D urban planning. The use of the GDB in a wider coupled 3D GIS–GW model (such as MODFLOW (McDonald and Harbaugh 1988) or FEFLOW (Diersch 2013)) system will be thus efficient to plan sustainable and integrated GW management, helping local stakeholders and regulators to manage not only GW, but all the underground resources in a more efficient and sustainable way. To this aim, the use of tools as WebGIS services could guarantee an effective way of spreading the existing information.

Moreover, an easy identification of the main UIs will help to overcome the lack of coordination, lack of planning and lack of understanding of the other domains among the different stakeholders (Parriaux et al. 2007; Goel et al. 2012; Besner 2016), thus avoiding jeopardizing the potential of the resources below the city (Parriaux et al. 2007). Considering the urban development declared in the Plan of Government of the Territory, the GDB would contribute to maintaining the underground potential, guaranteeing a long-term management of the urban underground space.

5.6. Conclusions

This work dealt with the proposal of a methodology to quantify volumes of UIs lying below the water table for Milan metropolitan area, which has been affected by an interaction between GW and UIs in the last few decades. This study has allowed us to:

1. Create a detailed inventory of the UIs through a standardized 3D GDB, to manage the existing data and incorporate new information in an efficient and easy way. This was realized using open data as the main source of information.
2. Identify the main areas where infrastructural volumes lie below the water table, and to evaluate how this situation has varied among time according to GW trends, with attention to non-waterproofed infrastructures. This, to the best of our knowledge, has been done for the first time both for private and public car parks.
3. Provide to the decision makers and stakeholders a useful tool to properly plan and manage the future urban underground development of Milan metropolitan area, in relation also to GW aspects.

An integration of this approach with GW numerical models will contribute to improving urban GW management. Through the analysis of the piezometric trends, different GW level scenarios will be tested, thus evaluating the effects of climate change or of possible variations in the pumping rates. Future perspectives will also consider the creation of a script to automatize the calculation both of GW levels and underground volumes; in this way, the urban conceptual model could be managed as a dynamic construct, always including in the analysis new hydrogeological and infrastructural elements. In the end, empowering the use of tools as 3D GIS and WebGIS services could be a way to make the information effectively available to the stakeholders, thus contributing to proper urban planning. Furthermore, the methodology used here could be applied in other similar case studies worldwide.

Supplementary Materials: The following are available online at http://www.mdpi.com/2220-9964/9/10/0609/s1, Table S5.1: Complete list and features of the underground car parks located in the study area, Fig. S5.1: GW table map for Jan90, Fig. S5.2: GW table map for Dec02, Fig. S5.3: GW table map for Sep07, Fig. S5.4: GW table map for Dec14, link to the WebGIS service.

Funding: This research received no external funding.

Acknowledgments: The authors are grateful to Metropolitana Milanese S.p.a for the providing of both the altimetric profiles of the subway lines and the underground railway and the piezometric data for trend reconstructions. The authors thank the four anonymous reviewers for their comments, which helped to improve this article.

Conflicts of Interest: The authors declare no conflict of interests.

References

Airoldi R, Casati P (1989) Le falde idriche del sottosuolo di Milano. Comune di Milano

Airoldi R, Peterlongo G, Casati P, De Amicis M (1997) Oscillazioni del livello della falda idrica sotterranea milanese nel periodo 1990-1995. Acque Sotter - Ital J Groundw, 53, 41–49.

Alawadhi S, Aldama-Nalda A, Chourabi H, Gil-Garcia JR, Leung S, Mellouli S, Nam T, Pardo TA, Scholl HJ, Walker S (2012) Building understanding of smart city initiatives. Lect Notes Comput Sci (including Subser Lect Notes Artif Intell Lect Notes Bioinformatics) 7443 LNCS:40–53. https://doi.org/10.1007/978-3-642-33489-4_4

Arzberger P, Schroeder P, Beaulieu A, Bowker G, Casey K, Laaksonen L, Moorman D, Uhlir P, Wouters P (2004) Policy forum. 303(March):1777–1779

Attard G, Cuvillier L, Eisenlohr L, Rossier Y, Winiarski T (2016a) Deterministic modelling of the cumulative impacts of underground structures on urban groundwater flow and the definition of a potential state of urban groundwater flow: example of Lyon, France. Hydrogeol J 24(5):1213–1229. https://doi.org/10.1007/s10040-016-1385-z

Attard G, Rossier Y, Winiarski T, Eisenlohr L (2016b) Deterministic modeling of the impact of underground structures on urban groundwater temperature. Sci Total Environ 572:986–994. https://doi.org/10.1016/j.scitotenv.2016.07.229

Attard G, Rossier Y, Winiarski T, Eisenlohr L (2017) Urban underground development confronted by the challenges of groundwater resources: Guidelines dedicated to the construction of underground structures in urban aquifers. Land use policy 64:461–469. https://doi.org/10.1016/j.landusepol.2017.03.015

Attard G, Winiarski T, Rossier Y, Eisenlohr L (2015) Review: Impact of underground structures on the flow of urban groundwater. Hydrogeol J 24(1):5–19. https://doi.org/10.1007/s10040-015-1317-3

Barles S, Guillerme A (1995) L'urbanisme souterrain. FeniXX: Paris, France, 1995; ISBN 2705916261.

Bélanger P (2007) Underground landscape: The urbanism and infrastructure of Toronto's downtown pedestrian network. Tunn Undergr Sp Technol 22(3):272–292. https://doi.org/10.1016/j.tust.2006.07.005

Beretta GP, Cavallin A, Francani V, Mazzarella S, Pagotto A (1985) Primo bilancio idrogeologico della Pianura Milanese; Consorzio per l'Acqua Potabile ai Comuni della Provincia di Milano: Milano, Italy.

Beretta GP, Avanzini M (1998) La gestione sostenibile del sollevamento della falda a Milano ed hinterland. L'Acqua; Rivista bimestrale dell'Associazione Idrotecnica Italiana: Roma, Italy.

Beretta GP, Avanzini M, Pagotto A (2004) Managing groundwater rise: Experimental results and modelling of water pumping from a quarry lake in Milan urban area (Italy). Environ Geol 45(5):600–608. https://doi.org/10.1007/s00254-003-0918-7

Besner J (2016) Underground space needs an interdisciplinary approach. Tunn Undergr Sp Technol 55(February 1985):224–228. https://doi.org/10.1016/j.tust.2015.10.025

Bhattacharjee Y (2005) Citizen scientists supplement work of Cornell researchers: a half-century of interaction with bird watchers has evolved into a robust and growing collaboration between volunteers and a leading ornithology lab. Science (80-) 308(5727):1402–1404

Blunier P, Tacher L, Parriaux A (2007) Systemic approach of urban underground resources exploitation. 11th ACUUS Int Conf - Undergr Sp Expand Front :43–48

Bobylev N (2006) Strategic environmental assessment of urban underground infrastructure development policies. Tunn Undergr Sp Technol 21(3–4)

Bobylev N (2009) Mainstreaming sustainable development into a city's Master plan: A case of Urban Underground Space use. Land use policy 26(4):1128–1137.

https://doi.org/10.1016/j.landusepol.2009.02.003

Bobylev N (2016) Transitions to a High Density Urban Underground Space. Procedia Eng 165:184–192. https://doi.org/10.1016/j.proeng.2016.11.750

Boisvert M (2007) Extensions of Indoor walkways into the public domain - A partnership experiment. 11th ACUUS Int Conf - Undergr Sp Expand Front :519–525

Bonney R, Cooper CB, Dickinson J, Kelling S, Phillips T, Rosenberg KV, Shirk J (2009) Citizen science: A developing tool for expanding science knowledge and scientific literacy. Bioscience 59(11):977–984. https://doi.org/10.1525/bio.2009.59.11.9

Bonney R, Phillips TB, Ballard HL, Enck JW (2016) Can citizen science enhance public understanding of science? Public Underst Sci 25(1):2–16. https://doi.org/10.1177/0963662515607406

Bonney R, Shirk JL, Phillips TB, Wiggins A, Ballard HL, Miller-Rushing AJ, Parrish JK (2014) Next steps for citizen science. Science (80-) 343(6178):1436–1437. https://doi.org/10.1126/science.1251554

Bonomi T (1999) Groundwater level evolution in the Milan area: Natural and human issues. IAHS-AISH Publ (259):195–202

Bonomi T (2009) Database development and 3D modeling of textural variations in heterogeneous, unconsolidated aquifer media: Application to the Milan plain. Comput Geosci 35(1):134–145. https://doi.org/10.1016/j.cageo.2007.09.006

Bonomi T, Bellini R (2003) The tunnel impact on the groundwater level in an urban area: a modelling approach to forecast it. RMZ - Materials and Geoenvironment 50(1):45–48

Bonomi T, Cavallin A, De Amicis M, Rizzi S, Tizzone R, Trefiletti P (1998) Evoluzione della dinamica piezometrica nell'area milanese in funzione di alcuni aspetti socio-economici. In: Atti della Giornata Mondiale dell'Acqua" Acque Sotterranee: Risorsa Invisibile". pp 9–17

Bonomi T, Fumagalli L, Dotti N (2009) Fenomeno di inquinamento da solventi in acque sotterranee sfruttate ad uso potabile nel nord-ovest della provincia di Milano. G. Geol. Appl 12:43–59

Carneiro J, Carvalho JM (2010) Groundwater modelling as an urban planning tool: Issues raised by a small-scale model. Q J Eng Geol Hydrogeol 43(2):157–170. https://doi.org/10.1144/1470-9236/08-028

Cavallin A, Bonomi T (1997) Application of a hydrogeological model to analyze and manage groundwater processes in the urban environment: a case study in the Milan area, Italy. Groundwater in the Urban Environment; Balkema: Rotterdam, The Netherlands; pp. 91–96.

Colombo A (1999) Milano e l'innalzamento della falda. Cave e Cantieri 2:26–36

Colombo L, Gattinoni P, Scesi L (2018) Stochastic modelling of groundwater flow for hazard assessment along the underground infrastructures in Milan (northern Italy). Tunn Undergr Sp Technol 79(May):110–120. https://doi.org/10.1016/j.tust.2018.05.007

Culshaw MG, Price SJ (2011) The 2010 Hans Cloos lecture. Bull Eng Geol Environ 70(3):333–376. https://doi.org/10.1007/s10064-011-0377-4

Dassargues A (1997) Groundwater modelling to predict the impact of tunnel on the behavior of water table aquifer in urban condition. Groundw. Urban Enviroment, Process. Manag. Chitt. et.al. 225–230

De Caro M, Crosta GB, Previati A (2020) Modelling the interference of underground structures with groundwater flow and remedial solutions in Milan. Eng Geol 272(May):105652. https://doi.org/10.1016/j.enggeo.2020.105652

De Luca DA, Destefanis E, Forno MG, Lasagna M, Masciocco L (2014) The genesis and the hydrogeological features of the Turin Po Plain fontanili, typical lowland springs in Northern Italy. Bull Eng Geol Environ 73(2):409–427. https://doi.org/10.1007/s10064-013-0527-y de Rienzo F, Oreste P, Pelizza S (2009) 3D GIS supporting underground urbanisation in the City of Turin (Italy). Geotech Geol Eng 27(4):539–547. https://doi.org/10.1007/s10706-009-9255-2

Delmastro C, Lavagno E, Schranz L (2016) Underground urbanism: Master Plans and Sectorial Plans. Tunn Undergr Sp Technol 55:103–111. https://doi.org/10.1016/j.tust.2016.01.001

Diersch HJG (2013) FEFLOW: finite element modeling of flow, mass and heat transport in porous and fractured media. Springer Science & Business Media: Berlin, Germany; ISBN 364238739X.

Directive I (2007) Directive 2007/2/EC of the European Parliament and of the Council of 14 March 2007 establishing an Infrastructure for Spatial Information in the European Community (INSPIRE). Publ Off J 25th April

Ducci D, Sellerino M (2015) Groundwater Mass Balance in Urbanized Areas Estimated by a Groundwater Flow Model Based on a 3D Hydrostratigraphical Model: the Case Study of the Eastern Plain of Naples (Italy). Water Resour Manag 29(12):4319–4333. https://doi.org/10.1007/s11269-015-1062-3

ESRI (2013) ArcMAP Desktop, Release 10.5. 1. ESRI: Redlands, CA, USA, 2013.

Fitch P, Brodaric B, Stenson M, Booth N (2016) Integrated groundwater data management. In: Integrated groundwater management. Springer, Cham, pp 667–692

Francani V, Beretta GP, Avanzini M, Nespoli M (1994) Indagine preliminare sull'uso sostenibile delle falde profonde nella Provincia di Milano. Available online: http: //hdl.handle.net/11311/505392 (Accessed on 15 June 2020).

Gattinoni P, Scesi L (2017) The groundwater rise in the urban area of Milan (Italy) and its interactions with underground structures and infrastructures. Tunn Undergr Sp Technol 62:103–114. https://doi.org/10.1016/j.tust.2016.12.001

George DJ (1992) Rising groundwater: a problem of development in some urban areas of the Middle East. In: Geohazards. Springer, pp 171–182

Goel RK, Singh B, Zhao J (2012) Underground infrastructures: planning, design, and construction. Butterworth-Heinemann: Oxford, UK; ISBN 0123971683.

Goovaerts P (1997) Geostatistics for natural resources evaluation. Oxford University Press on Demand; ISBN 0123971683.

Guastella G, Oueslati W, Pareglio S (2019) Patterns of urban spatial expansion in European Cities. Sustain 11(8):1–15. https://doi.org/10.3390/su11082247

Hayashi T, Tokunaga T, Aichi M, Shimada J, Taniguchi M (2009) Effects of human activities and urbanization on groundwater environments: An example from the aquifer system of Tokyo and the surrounding area. Sci Total Environ 407(9):3165–3172. https://doi.org/10.1016/j.scitotenv.2008.07.012

Hernández MA, González N, Chilton J (1997) Impact of rising piezometric levels on Greater Buenos Aires due to partial changing of water services infrastructure. In Groundwater in the Urban Environment, Proceedings of the XXVII IAH Congress on Groundwater in the Urban Environment, Nottingham, UK, 21–27 September 1997; Balkema: Rotterdam, The Netherlands; Brookfield, VT, USA, 1997.

Hunt DVL, Makana LO, Jefferson I, Rogers CDF (2016) Liveable cities and urban underground space. Tunn Undergr Sp Technol 55:8–20. https://doi.org/10.1016/j.tust.2015.11.015

Isaaks EH, Srivastava RM (1989) An introduction to applied geostatistics. Oxford Univ Press New York

Istat (2011) L'italia del censimento. Struttura demografica e processo di rilevazione, Lombardia [Italy in the census. Demographic structure and survey process, Lombardy]

Janssen M, Charalabidis Y, Zuiderwijk A (2012) Benefits, Adoption Barriers and Myths of Open Data and Open Government. Inf Syst Manag 29(4):258–268. https://doi.org/10.1080/10580530.2012.716740

Jurado JM, Feito LOFR (2017) 3D GIS based on WebGL for the management of underground utilities. Hydrogeol J :2–5. https://doi.org/10.2312/ceig.20171209

Kitanidis PK (1997) Introduction to geostatistics: applications in hydrogeology. Cambridge university press; ISBN 0521587476.

Koziatek O, Dragićević S (2017) iCity 3D: A geosimualtion method and tool for three-dimensional modeling of vertical urban development. Landsc Urban Plan 167(June):356–367. https://doi.org/10.1016/j.landurbplan.2017.06.021

Kresic N, Mikszewski A (2012) Hydrogeological conceptual site models: data analysis and visualization. CRC press; ISBN 1439852286.

Lamé A (2013) Modélisation hydrogéologique des aquifères de Paris et impacts des aménagements du sous-sol sur les écoulements souterrains [Hydrogeological modeling of the Paris aquifers and impacts of subsoil development on underground flows]

Li HQ (2011) Sustainable 3D Urban Governance: Creating a " Deep City " for Our Modern City. Swiss Fed Inst Technol Lausanne (EPFL), Switz :1–14

Li HQ, Parriaux A, Thalmann P, Li XZ (2013a) An integrated planning concept for the emerging underground urbanism: Deep City Method Part 1 concept, process and application. Tunn Undergr Sp Technol 38:559–568. https://doi.org/10.1016/j.tust.2013.04.010

Li HQ, Li X, Parriaux A, Thalmann P (2013b) An integrated planning concept for the emerging underground urbanism: Deep City Method Part 2 case study for resource supply and project valuation. Tunn Undergr Sp Technol 38:569–580. https://doi.org/10.1016/j.tust.2013.04.009

McDonald MG, Harbaugh AW (1988) A modular three-dimensional finite-difference ground-water flow model. US Geological Survey: Preston, WV, USA, 1988.

Milan Metropolitan City (2019a) Documento di piano Milano 2030 Visione, Costruzione, Strategie, Spazi [Milan 2030 plan document Vision, Construction, Strategies, Spaces]

Milan Metropolitan City (2019b) Decimetro: Sistema Decisionale Città Metropolitana di Milano. https://www.cittametropolitana.mi.it/DeCiMetro/DBT/index.html (Accessed on 15 June 2020).

Mudd GM, Deletic A, Fletcher TD, Wendelborn A (2004) A review of urban groundwater in Melbourne: Considerations for WSUD. In: WSUD 2004: Cities as Catchments; International Conference on Water Sensitive Urban Design, Proceedings of. Engineers Australia, p 428

Nishioka S, Tannaka Y, Minemura T (2007) Deep underground usage for effective executing of city facility construction. 11th ACUUS Int Conf - Undergr Sp Expand Front :291–295

Pappa M, Benardos A (2007) Comparative evaluation of alternative methods for the construction of underground car parks. 11th ACUUS Int Conf - Undergr Sp Expand Front :487–492

Parriaux A, Blunier P, Maire P, Tacher L (2007) The DEEP CITY Project: A Global Concept for a Sustainable Urban Underground Management. 11th ACUUS Int Conf Sp Expand Front Athens, Greece :255–260

Parriaux A, Tacher L, Joliquin P (2004) The hidden side of cities - Towards three-dimensional land planning. Energy Build 36(4):335–341. https://doi.org/10.1016/j.enbuild.2004.01.026

Parriaux A, Tacher L, Kaufmann V, Blunier P (2006) Underground resources and sustainable development in urban areas

Pujades E, López A, Carrera J, Vázquez-Suñé E, Jurado A (2012) Barrier effect of underground structures on aquifers. Eng Geol 144–145:41–49. https://doi.org/10.1016/j.enggeo.2012.07.004

Regione Lombardia (2016) Piano di Tutela ed Uso delle Acque (PTUA) [Water Protection and Use Plan (PTUA)].

Rein J (2009) AMFORA Amsterdam_alternative multifunctional subterranean development Amsterdam. In: 45th ISOCARP Congress

Ricci G, Enrione R, Eusebio A, Crova R (2007) Numerical modelling of the interference between underground structures and aquifers in urban environment. The Turin subway - Line 1. "Proceedings 33rd ITA-AITES World Tunn Congr - Undergr Sp - 4th Dimens Metropolises" 2(December 2019):1323–1329

Sterling R, Admiraal H, Bobylev N, Parker H, Godard JP, Vähäaho I, Rogers CDF, Shi X, Hanamura T (2012) Sustainability issues for underground space in urban areas. Proc Inst Civ Eng Des Plan 165(4):241–254

Sterling RL (2007) Urban underground space use planning: a growing dilemma. Urban Plan Int 6(004)

Un-Habitat (2012) State of the World's Cities 2008/9: Harmonious Cities. Routledge

Utudjian E (1972) L'urbanisme souterrain. Presses universitaires de France

Vähäaho I (2014) Underground space planning in Helsinki. J Rock Mech Geotech Eng 6(5):387–398. https://doi.org/10.1016/j.jrmge.2014.05.005

Vähäaho I (2016) An introduction to the development for urban underground space in Helsinki. Tunn Undergr Sp Technol 55:324–328. https://doi.org/10.1016/j.tust.2015.10.001

Vázquez-Suñé E, Marazuela MÁ, Velasco V, Diviu M, Pérez-Estaún A, Álvarez-Marrón J (2016) A geological model for the management of subsurface data in the urban environment of Barcelona and surrounding area. Solid Earth 7(5):1317–1329. https://doi.org/10.5194/se-7-1317-2016

Vázquez-Suñé E, Sánchez-Vila X, Carrera J (2005) Introductory review of specific factors influencing urban groundwater, an emerging branch of hydrogeology, with reference to Barcelona, Spain. Hydrogeol J 13(3):522–533. https://doi.org/10.1007/s10040-004-0360-2

Vázquez-Suñé E, Sánchez-Vila X, Carrera J, Marizza M, Arandes R (1997) Rising groundwater levels in Barcelona: evolution and effects on urban structures. In: Groundwater in the Urban Environment. pp 267–271

Velasco V, Montfort D, Vàzquez-Suñé E, Font-Capo J, Carrera J, Pujades E (2015) Assessment of the barrier effect caused by underground constructions on porous aquifers with low hydraulic gradient: A case study of the metro construction in Barcelona, Spain. Eng Geol 196:238–250. https://doi.org/10.1016/j.enggeo.2015.07.006

Webster R, Oliver MA (2001) Cross-correlation, co-regionalization, and co-kriging. Geostatistics Environ Sci Chichester, UK, John Wiley Sons

Wilkinson W (1985) Rising groundwater levels in London and possible effects on engineering structures. Proc 18th Congr Int Assoc Hydrogeol Cambridge :145–157

Zhang XQ (2016) The trends, promises and challenges of urbanisation in the world. Habitat Int 54(13):241–252. https://doi.org/10.1016/j.habitatint.2015.11.018

Zurada J, Karwowski W (2011) Knowledge discovery through experiential learning from business and other contemporary data sources: A review and reappraisal. Inf Syst Manag 28(3):258–274. https://doi.org/10.1080/10580530.2010.493846

Electronic Supplementary Material

A 3D Geodatabase for Urban Underground Infrastructures: Implementation and Application to Groundwater Management in Milan Metropolitan Area.

Davide Sartirana [1] *, Marco Rotiroti [1], Chiara Zanotti [1], Tullia Bonomi [1], Letizia Fumagalli [1] and Mattia De Amicis [1]

[1]Department of Earth and Environmental Sciences, University of Milano-Bicocca, Piazza Della Scienza 1, Milan, Italy; d.sartirana1@campus.unimib.it (D.S.); marco.rotiroti@unimib.it (M.R.); chiara.zanotti@unimib.it (C.Z.); tullia.bonomi@unimib.it (T.B.); letizia.fumagalli@unimib.it (L.F.); mattia.deamicis@unimib.it (M.D.A.)

*Correspondence: d.sartirana1@campus.unimib.it (D.S.); Tel.: +39-02-6448-2882

Table S5.1. Complete list and main features of the underground car parks located in the study area. CP stands for construction period.

Name	Bottom (m a.s.l.)	Depth (m)	Area × 10^3 (m^2)	Volume × 10^3 (m^3)	CP	Floors	Location
Arduino	112.9	11	5.67	62.37	< 1990	3	Downtown
Benedetto Marcello	106.53	14	3.05	42.7	< 1990	4	Downtown
Carducci Olona	101.2	17	3.42	58.14	< 1990	5	Downtown
Cesariano	111.5	11	4.54	49.94	< 1990	3	Downtown
Conca del Naviglio	101.92	14	2.43	34.02	< 1990	4	Downtown
Emo	116.23	11	2.76	30.36	< 1990	3	North
Erculea	100.91	17	1.3	22.1	< 1990	5	Downtown

Name	Bottom (m a.s.l.)	Depth (m)	Area × 10^3 (m^2)	Volume × 10^3 (m^3)	CP	Floors	Location
Fratelli Bandiera	103.5	14	2.81	39.34	< 1990	4	Downtown
Giotto	107.05	14	4.49	62.86	< 1990	4	Downtown
Giulio Cesare	109.2	14	4.42	61.88	< 1990	4	Downtown
Gramsci	110.2	14	4.3	60.2	< 1990	4	Downtown
Majno	101.86	17	2.05	34.85	< 1990	5	Downtown
Manusardi	100.25	14	2.12	29.68	< 1990	4	Downtown
Mascagni	102.2	14	4.63	64.82	< 1990	4	Downtown
Numa Pompilio	100.7	17	4.07	69.19	< 1990	5	Downtown
Ozanam	105.63	14	4.6	64.4	< 1990	4	Downtown
Pavia	99.84	14	3.38	47.32	< 1990	4	Downtown
Piazza Diaz	108.5	11	2.4	26.4	< 1990	3	Downtown
Puccini	101.33	20	1.68	33.6	< 1990	6	Downtown
Rio de Janeiro	105.7	11	2.27	24.97	< 1990	3	Downtown
Rio de Janeiro/Andrea del Sarto	105.7	11	2.64	29.04	< 1990	3	Downtown
Rossetti	115.2	8	2.88	23.04	< 1990	2	Downtown
San Barnaba	105.4	11	7.45	81.95	< 1990	3	Downtown
Solera Mantegazza	107.85	14	2.92	40.88	< 1990	4	Downtown

Name	Bottom (m a.s.l.)	Depth (m)	Area × 10³ (m²)	Volume × 10³ (m³)	CP	Floors	Location
Toce/Boltraffio	115.33	11	4.55	50.05	< 1990	3	Downtown
Tommaseo	103.89	17	3.15	53.55	< 1990	5	Downtown
Veglia/Caserta	120.9	8	22.28	178.24	< 1990	2	North
Vittor Pisani	107.58	14	8.78	122.92	< 1990	4	Downtown
Alghero	122.72	5	2.12	10.6	1990-2002	1	North
Ampere/Compagni	104.5	14	2	28	1990-2002	4	Downtown
Aretusa Nord	110.75	11	4.39	48.29	1990-2002	3	Downtown
Bacchiglione/Scheiwiller	99.9	11	3.35	36.85	1990-2002	3	South
Balilla/Zamenhof	105.66	8	2.4	19.2	1990-2002	2	Downtown
Bellosio/Facchinetti	102.46	8	3.71	29.68	1990-2002	2	Downtown
Bicocca P7	122.1	11	5.67	62.37	1990-2002	3	North
Bicocca P8	125.5	8	6.67	53.36	1990-2002	2	North
Capecelatro/Pessano	116.35	8	5.05	40.4	1990-2002	2	Downtown
Cardinal Ferrari	101.53	14	2.24	31.36	1990-2002	4	Downtown
Caterina da Forlì	108.97	11	10.35	113.85	1990-2002	3	Downtown
Cechov	122.54	8	2.92	23.36	1990-2002	2	North
Cervi/Assietta	130.11	8	8.05	64.4	1990-2002	2	North

Name	**Bottom (m a.s.l.)**	**Depth (m)**	**Area × 10^3 (m^2)**	**Volume × 10^3 (m^3)**	**CP**	**Floors**	**Location**
Ciceri Visconti	101.47	11	4.16	45.76	1990-2002	3	Downtown
Ciclamini/Margherite	111.5	8	3	24	1990-2002	2	West
Cilea 100	126.83	8	4.37	34.96	1990-2002	2	North
Costa/Loreto	106.9	14	1.97	27.58	1990-2002	4	Downtown
Dateo Sud	102.8	14	2.11	29.54	1990-2002	4	Downtown
Don Calabria	116.85	8	6.4	51.2	1990-2002	2	North
Donati/Redaelli	110.01	8	9.53	76.24	1990-2002	2	Downtown
Etiopia	111.66	8	0.5	4	1990-2002	2	Downtown
Feltrinelli	101.83	5	8.3	41.5	1990-2002	1	South
Grado	118.77	8	1.68	13.44	1990-2002	2	North
Graf/De Pisis Ovest	128.9	8	5.94	47.52	1990-2002	2	North
Isimbardi	102.9	8	2.64	21.12	1990-2002	2	South
Lampugnano	119.85	8	3.78	30.24	1990-2002	2	North
Leone XIII	115.35	8	7.4	59.2	1990-2002	2	Downtown
Menotti Serrati	98.94	5	7.5	37.5	1990-2002	1	South
Moisè Loria/Stromboli	101.5	17	3	51	1990-2002	5	Downtown
Monte Popera/Piana	101.12	5	2.8	14	1990-2002	1	South

Name	Bottom (m a.s.l.)	Depth (m)	Area × 10^3 (m^2)	Volume × 10^3 (m^3)	CP	Floors	Location
Moscova	107	14	7.32	102.48	1990-2002	4	Downtown
Nikolajevka	113.4	8	4.64	37.12	1990-2002	2	West
Ojetti	124.16	8	7.03	56.24	1990-2002	2	North
Po	105.2	14	6.87	96.18	1990-2002	4	Downtown
Risorgimento Sud	102.8	14	2.11	29.54	1990-2002	4	Downtown
Sarca/Nota	123.99	8	4.4	35.2	1990-2002	2	North
Spaventa/Meda	104.44	8	5.46	43.68	1990-2002	2	South
Suzzani	129.85	8	3.56	28.48	1990-2002	2	North
Trechi	132.14	8	3.97	31.76	1990-2002	2	North
Viganò	110.61	14	2.19	30.66	1990-2002	4	Downtown
Volontari	108.8	14	1.3	18.2	1990-2002	4	Downtown
Accursio	115.6	14	4.55	63.7	2002-2007	4	North
Adda	102	20	0.81	16.2	2002-2007	6	Downtown
Avezzana	98.07	11	2.04	22.44	2002-2007	3	South
Balla	125.58	8	2.65	21.2	2002-2007	2	North
Bazzini	102.2	17	1.49	25.33	2002-2007	5	Downtown
Betti	123.7	8	5.69	45.52	2002-2007	2	North

Name	Bottom (m a.s.l.)	Depth (m)	Area × 10^3 (m^2)	Volume × 10^3 (m^3)	CP	Floors	Location
Betulle Est	118.01	5	4.6	23	2002-2007	1	West
Betulle Ovest	118.2	5	2.49	12.45	2002-2007	1	West
Bibbiena/Centro Civico	105.65	8	3.86	30.88	2002-2007	2	Downtown
Bordighera/Alzaia Naviglio Pavese	102.56	11	3.32	36.52	2002-2007	3	South
Broggini	119.07	5	2.17	10.85	2002-2007	1	West
Carafa/Conte Verde	120.2	11	3.3	36.3	2002-2007	3	North
Caroli/Ricordo	121.53	8	3.77	30.16	2002-2007	2	North
Cascina Bianca	106.2	5	7.88	39.4	2002-2007	1	South
Dalmazia	101.75	8	2.09	16.72	2002-2007	2	Downtown
De Lemene	120.6	8	2.29	18.32	2002-2007	2	North
De Nicola/San Vigilio	106.46	5	4.78	23.9	2002-2007	1	South
De Pretis/San Vigilio	106.4	5	4.52	22.6	2002-2007	1	South
De Pretis/Voltri	106.89	5	4.73	23.65	2002-2007	1	South
Gandhi/Perlasca	128.2	8	4.31	34.48	2002-2007	2	North
Giulio Romano	96.45	17	2.48	42.16	2002-2007	5	Downtown
Govone	110.19	17	1.6	27.2	2002-2007	5	Downtown
Leoncavallo	108	14	2.54	35.56	2002-2007	4	Downtown

Name	**Bottom (m a.s.l.)**	**Depth (m)**	**Area × 10³ (m²)**	**Volume × 10³ (m³)**	**CP**	**Floors**	**Location**
Lucerna	113.39	8	4	32	2002-2007	2	West
Maffei	100.9	14	3.41	47.74	2002-2007	4	Downtown
Marmolada	124.4	11	3.36	36.96	2002-2007	3	North
Monte Baldo	117.22	8	3.1	24.8	2002-2007	2	Downtown
Monte Velino/Cadibona	102.83	8	7.05	56.4	2002-2007	2	Downtown
Montemartini/Fabio Massimo	101.38	8	7.16	57.28	2002-2007	2	South
Murani	101.6	14	3.38	47.32	2002-2007	4	Downtown
Muttoni/Quarenghi	124.8	8	3.99	31.92	2002-2007	2	North
Novelli	103.2	14	1.17	16.38	2002-2007	4	Downtown
Populonia/Valassina	117.68	11	8.68	95.48	2002-2007	3	North
Prinetti/Vida	114.2	11	3.25	35.75	2002-2007	3	North
Riccione	120.95	11	1.91	21.01	2002-2007	3	North
Romagnoli/Bertieri	107.34	11	2.11	23.21	2002-2007	3	Downtown
Salmoiraghi/Stuparich	115.37	11	1.76	19.36	2002-2007	3	Downtown
Sammartini/Lunigiana	112.3	11	3.49	38.39	2002-2007	3	Downtown
San Giusto/Val Poschiavina	116.7	8	5.56	44.48	2002-2007	2	Downtown
Silla	131.3	5	5.82	29.1	2002-2007	1	North

Name	Bottom (m a.s.l.)	Depth (m)	Area × 10^3 (m^2)	Volume × 10^3 (m^3)	CP	Floors	Location
Trani/Malipiero/Mecenate	100.1	8	5.92	47.36	2002-2007	2	Downtown
Valsesia Est	116.45	5	3.42	17.1	2002-2007	1	West
Valsesia Ovest	116.6	5	1.96	9.8	2002-2007	1	West
Washington/Piemonte	100.35	20	3.02	60.4	2002-2007	6	Downtown
Correggio Est	107.81	14	1.03	14.42	2007-2014	4	Downtown
Correggio Ovest	106.95	14	2.75	38.5	2007-2014	4	Downtown
Dateo Nord	99.8	17	1.94	32.98	2007-2014	5	Downtown
Manuzio	103.56	17	2.27	38.59	2007-2014	5	Downtown
Meda	102.85	17	2.1	35.7	2007-2014	5	Downtown
Osculati/Camerino	125.14	11	0.45	4.95	2007-2014	3	North
Quinto Alpini	106.47	14	1.66	23.24	2007-2014	4	Downtown
Risorgimento nord	96.9	20	1.43	28.6	2007-2014	6	Downtown
Sabotino	96.91	17	2.47	41.99	2007-2014	5	Downtown
Sant'Ambrogio	102	17	7.41	125.97	2007-2014	5	Downtown
Savona Tolstoj	110.67	5	1.08	5.4	2007-2014	1	Downtown
Vittadini	99.23	14	3.63	50.82	2007-2014	4	Downtown
XXV Aprile	105.2	17	5.07	86.19	2007-2014	5	Downtown

Name	Bottom (m a.s.l.)	Depth (m)	Area × 10³ (m²)	Volume × 10³ (m³)	CP	Floors	Location
Total parks: 126				5,157			

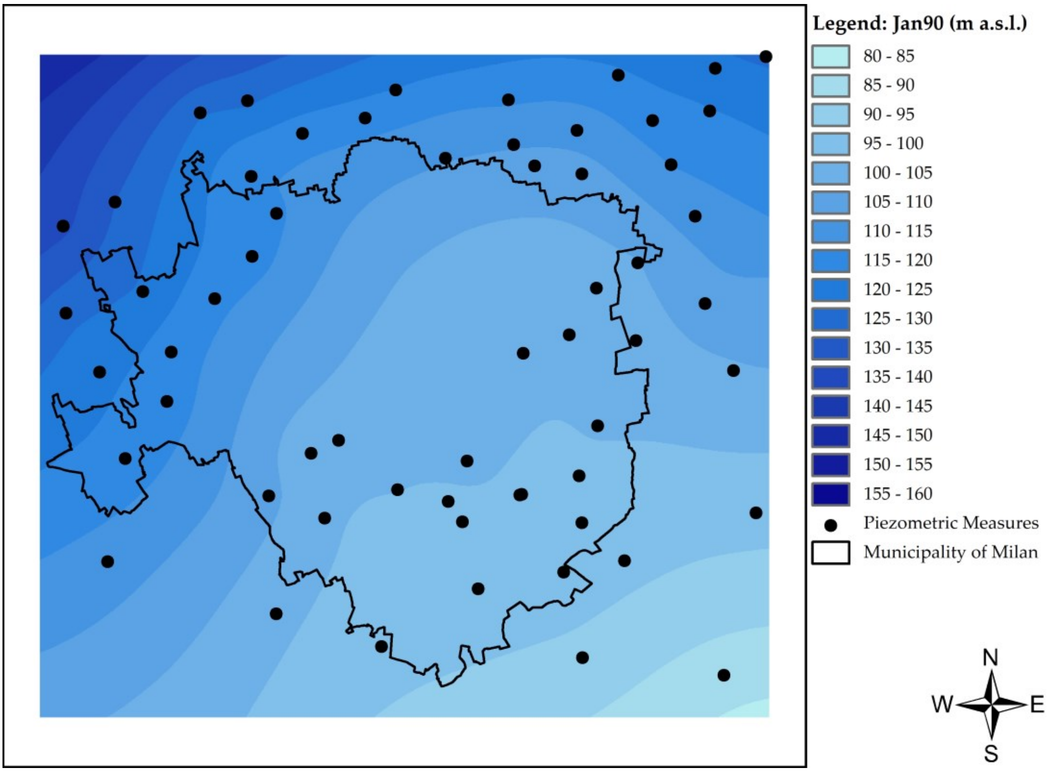

Fig. S5.1. GW table map for Jan90.

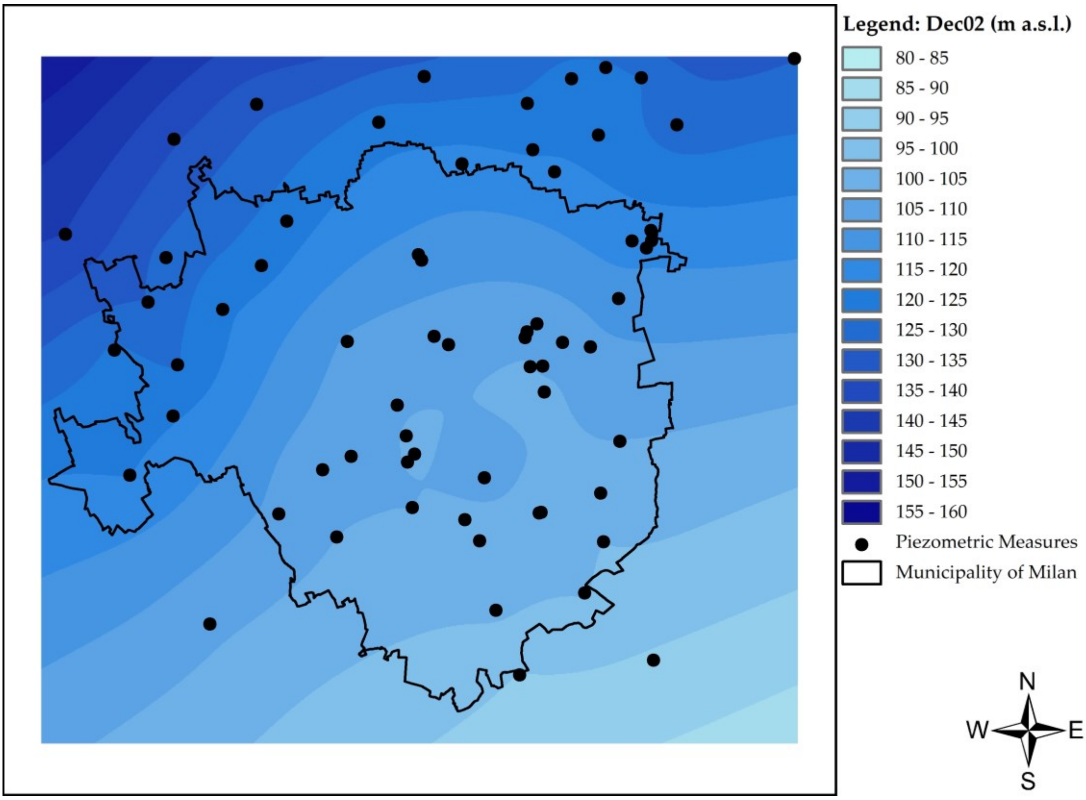

Fig. S5.2. GW table map for Dec02.

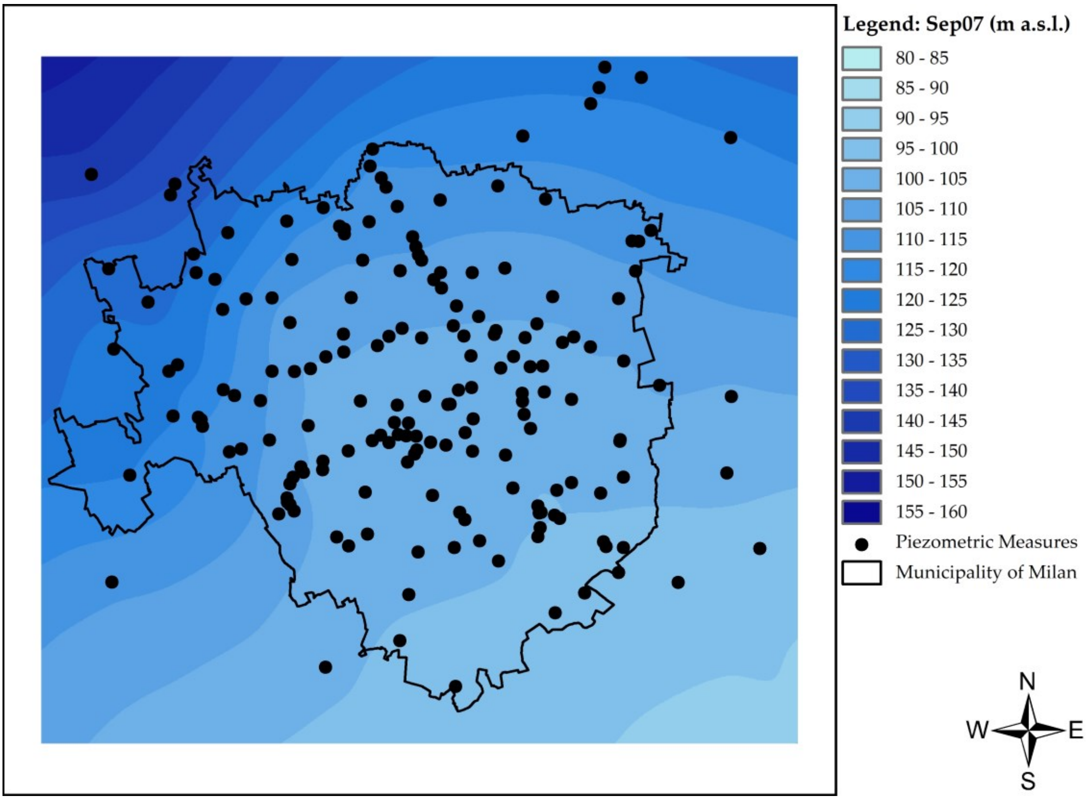

Fig. S5.3. GW table map for Sep07.

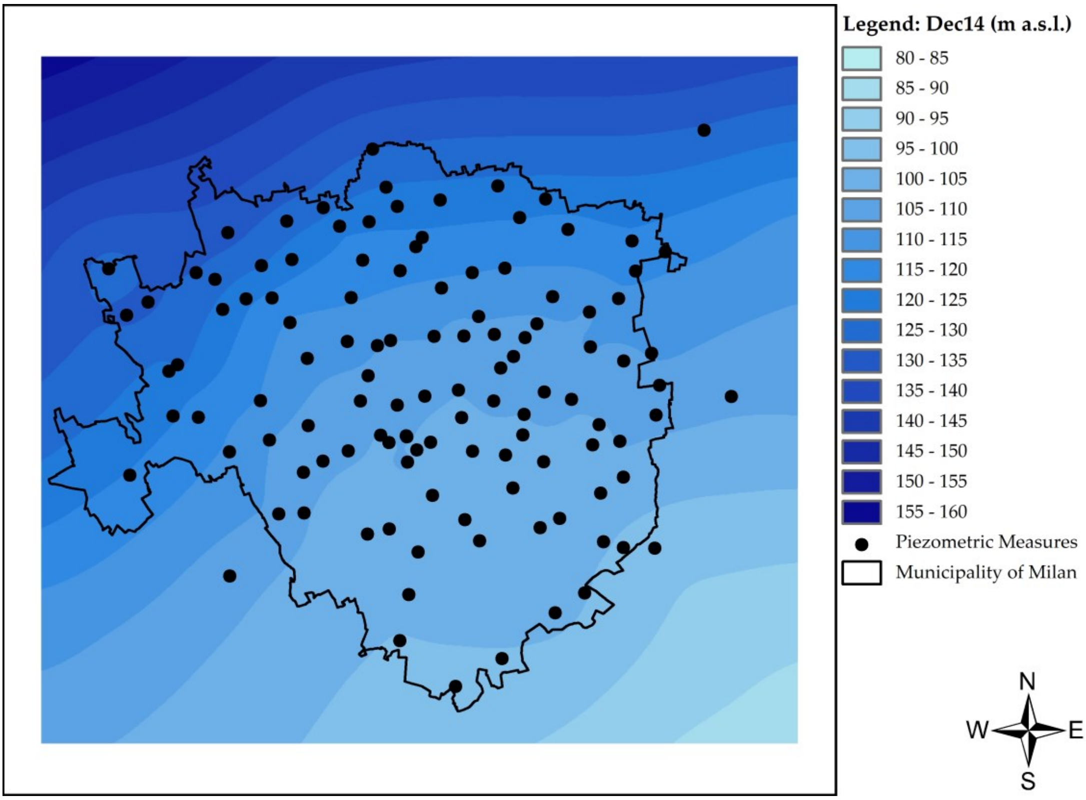

Fig. S5.4. GW table map for Dec14.

Link to the WebGIS service: https://arcg.is/HHWDi0. This allows a more detailed visualization of the contents of the 3D GDB.

Chapter 6: Hydrodynamic characterization of the shallow aquifer to support underground management

Data-driven decision management of urban underground infrastructure through groundwater-level time-series cluster analysis: the case of Milan (Italy)

Davide Sartirana[1]*, Marco Rotiroti[1], Tullia Bonomi[1], Mattia De Amicis[1], Veronica Nava[1], Letizia Fumagalli[1] and Chiara Zanotti[1]

[1]Department of Earth and Environmental Sciences, University of Milano-Bicocca, Piazza Della Scienza 1, 20126 Milan, Italy

*corresponding author: d.sartirana1@campus.unimib.it

This chapter is largely based on the following paper: *Hydrogeol J* **30**, 1157–1177 (2022). https://doi.org/10.1007/s10040-022-02494-5

Keywords: urban groundwater; rising groundwater levels; shallow aquifer; public car parks; Italy

Abstract

The significant increase in urbanization has resulted in greater use of the subsurface in urban planning and, therefore, increased interaction between groundwater and underground infrastructure. Numerical models are the primary tool adopted to manage the resulting problems; however, their construction is time- and cost-consuming. Groundwater-level time-series analysis can be a complementary method, as this data-driven approach does not require an extensive understanding of the geological and boundary conditions, even if providing insights into the hydrogeologic behaviour. Thus, a data-driven approach was adopted to analyse groundwater time-series of the shallow aquifer, occupied by several underground structures, beneath Milan city (Northern Italy). Statistical (Mann-Kendall and Sen's slope estimator, autocorrelation and cross-correlation, hierarchical cluster analysis) and geospatial techniques were used to detect the potential variables influencing the groundwater levels of 95 monitoring wells, covering the period 2005-2019. A general rising trend of the water table was identified, with local hydrogeologic differences in the western and southernmost areas. Based on time-series analysis results, four management areas have been identified. These areas

could act as future geographic units with specific groundwater management strategies. In particular, subsurface public car parks can be classified with respect to groundwater flooding as a) not submerged, b) possibly critical, or c) submerged at different groundwater conditions. According to these outcomes, targeted guidelines for constructing new car parks have been elaborated for each management area. The methodology proved to be efficient in improving the urban conceptual model and helping stakeholders design the planned underground development, considering groundwater aspects.

6.1. Introduction

Groundwater (GW) represents the most valuable source of freshwater on a global scale (Li et al. 2013a), as it is used for drinking, agricultural and industrial purposes (Filimonau and Barth 2016). As the world population is projected to grow in the next decades, increasing demand for this resource is expected, and this may provoke stress both in terms of GW quality and quantity (Pollicino et al. 2021); in particular, GW demand is gradually increasing in urban areas, where 70% of the world population is expected to be living by 2050 (Un-Habitat 2012). To limit urban sprawl, the tendency to look for new building spaces in the vertical direction has increased (Li et al. 2013b; Li et al. 2013c; Koziatek and Dragićević 2017), leading to enhanced use of urban underground (Parriaux et al. 2007; Sterling et al. 2012; Bobylev 2016; Vähäaho 2016). In the last few decades, as a result of the deindustrialization process, several cities worldwide have faced rising GW levels, which has generated some interference between underground infrastructures (UIs) (i.e. basements, car parks and subway lines) and GW (Wilkinson 1985; George 1992; Hernández et al. 1997; Vázquez-Suñé et al. 1997; Mudd et al. 2004; Hayashi et al. 2009; Lamé 2013; Ducci and Sellerino 2015). The GW/UIs interaction needs to be properly managed to ensure a sustainable use of urban underground spaces. Numerical GW flow modelling can be used for evaluating the interference between GW and underground structures (Vázquez-Suñé et al. 2005; García-Gil et al. 2015) and for identifying possible management strategies. A variety of three-dimensional (3D) numerical models has been realized worldwide (Attard et al.

2015). However, the construction of a 3D numerical model is generally a multi-step procedure requiring detailed knowledge of the aquifer system, both from the geological and hydrological features and, thus, such models take a considerable amount of time to develop. As the information is sometimes lacking or scattered among different sources, the conceptual model also needs to be frequently revised: this could be considered costly and time-consuming (Vázquez-Suñé et al. 2005). Within this scope, data-driven techniques can constitute a valid complementary approach, providing preliminary insights into the main drivers affecting the aquifer behaviour (Chae et al. 2010; Obergfell et al. 2013), without requiring an extensive approximation of subsurface parameters and boundary conditions. Generally, adopting data-driven methods is faster and more easy-applicable than numerical models (Bakker and Schaars 2019) and could represent a reasonable compromise between model complexity and costs (Stevenazzi et al. 2017). However, time-series analysis is indispensable to support GW model calibration (Bakker and Schaars 2019). In particular, time-series analysis of GW levels allows one to detect trends (Patle et al. 2015), and thereby identify the causes of water level variations, through the investigation of input-output connections (Obergfell et al. 2013); for these reasons, this approach can be adopted to plan effective GW management strategies, thus bringing valuable information to planners and decision makers (Best et al. 2021). Also, as modelling should make maximum use of existing data, by assimilating its information content (Lotti et al. 2021), data-driven methods could support the construction of a 3D numerical model.

Different time-series analysis techniques have been applied to interpret GW systems processes. Statistical tests such as the Mann-Kendall test and Sen's slope estimator have been widely applied to detect long-term trends from GW level series, for evaluating their significance and magnitude (Tabari et al. 2012; Singh et al. 2015; Meggiorin et al. 2021). Furthermore, statistical tests have been sometimes combined with geospatial approaches in a geographical information system (GIS) environment to identify those areas of GW-level rise or drawdown, determined by the existence of a trend (Chaudhuri and Ale 2014; de Brito Neto et al. 2016; Anand et al. 2020). On the other hand, clustering techniques have been mainly adopted for GW quality, but recently different studies have applied these techniques to GW level time-series (Pathak and Dodamani 2019; Rinderer et al. 2019; Naranjo-Fernández et al. 2020; Sottani et al. 2020).

The present study aimed at proposing, for the city of Milan (Lombardy, Northern Italy), a data-driven approach to support decision making for urban UIs in relation to GW aspects. In this way, the stakeholders could properly manage the future underground development of the city in a more targeted way, also considering hydrogeologic features. To the best of the authors' knowledge, this is the first time that GW/UIs interactions have been managed through the support of data-driven methods. A set of statistical techniques has been applied to GW-level time-series of the shallow aquifer in Milan, with two main purposes: a) to identify different spatial zones with local hydrogeologic peculiarities, possibly acting as future GW management territorial units, and to investigate the potential features influencing GW levels (i.e. geology, precipitation, withdrawals, land use) and b) to elaborate targeted guidelines for UIs management, mainly focusing on the constructions of new public car parks. Underground car parks have been mainly considered, as their interference with the GW has been only partially investigated. Nonetheless, this procedure could be applied to every category of UIs.

The data-driven analysis proposed in this study has been fine-tuned for the Milan metropolitan area – notwithstanding, it could be applied to other urban areas worldwide that have subsurface infrastructure development and a complex shallow aquifer system that requires an integrated urban GW management strategy.

6.2. Hydrogeological conceptual model of the study area

The study area (182 km^2) is the city of Milan (Fig. 6.1). It hosts 1.4 million people (Istat 2011) and it is characterized by intense industrial and agricultural development (Bonomi 2009). The land use in the western and southern areas is still mainly agricultural, while the remaining areas of the city are mainly urbanized. A wide hydrographic network characterizes the area (Fig. 6.1b): among the main rivers, Olona and Seveso are culverted within the city, while the Naviglio Grande and Naviglio Pavese are man-made surface channels mainly used for irrigation. Milan is located in the middle of the Po Plain (Fig.

1a), in proximity to the lowland springs belt and lies on a sedimentary aquifer system whose hydrogeologic structure has been deeply studied in past years (Regione Lombardia & ENI 2002). A recent classification (Regione Lombardia 2016) has identified three main hydrostructures: a shallow hydrostructure (ISS), an intermediate hydrostructure (ISI) and a deep hydrostructure (ISP). In the study area, ISS has a medium thickness of 50 meters with a bottom surface ranging from 100 m above sea level (a.s.l.) (to the North) down to around 50 m a.s.l. (to the South). It hosts a shallow aquifer (Fig. 6.2) (Fig. S6.1 of the electronic supplementary material (ESM)), not exploited for drinking needs. This shallow aquifer is the focus of this study. It is mainly composed of sands and gravels. The same lithology, but with an increasing presence of silty and clayey layers, characterizes the ISI. Finally, because of a limited amount of data, the ISP has an uncertain lithological composition.

GW has been extensively exploited for industrial use since the early 1960s; around 1975 there was a water table depth of more than 30 meters in the northern sector. Subsequently, since the early 1990s, the dismantling of the biggest factories, mainly located in the northern sector of the town, led the water table to rise once again (i.e. with a maximum rise of about 10-15 meters in the northern area): this caused flooding episodes for some non-waterproofed underground structures (Cavallin and Bonomi 1997; Beretta et al. 2004; Gattinoni and Scesi 2017; Colombo et al. 2018), including car parks and the oldest, shallower subway lines (Fig. 6.1b). Thus, the most recent subway lines (Fig. 6.1b), also due to their greater depth, were designed with waterproof systems. Public car parks were built in sequential phases starting from the middle of the 1980s. Now, 126 underground public car parks are listed in the territory (Fig. 6.1b) (Table S6.1 of the ESM). The information (i.e. bottom elevation (m a.s.l.), period of construction, location) on subway lines, and public and private car parks is stored in a 3D GDB (Sartirana et al. 2020), allowing for proper management of the UIs in the framework of GW management (Fig. 6.2).

Moreover, the number of low-enthalpy geothermal systems in the shallow aquifer increased in the last decades due to regional laws in the scope of European goals to reduce greenhouse gas emissions. Particularly, open-loop GW heat pumps (GWHPs) serve large building systems, mainly in the downtown area (Previati and Crosta 2021a) (Fig. 6.1b). The average depth of GWHP filters ranges between 17 and 34 meters (Regione Lombardia 2021a). In some cases, GWHPs discharge exploited water to surface water bodies to limit the GW rise.

The adoption of the Plan of Government for the Territory (PGT) (Milan Metropolitan City 2019) in 2019 will favour further subsurface occupation by developing new subway line sections and reducing soil consumption with consequent changes in the subsurface. Hence, the need for coordinated management among the stakeholders arises, supported by evidence from shallow-aquifer studies.

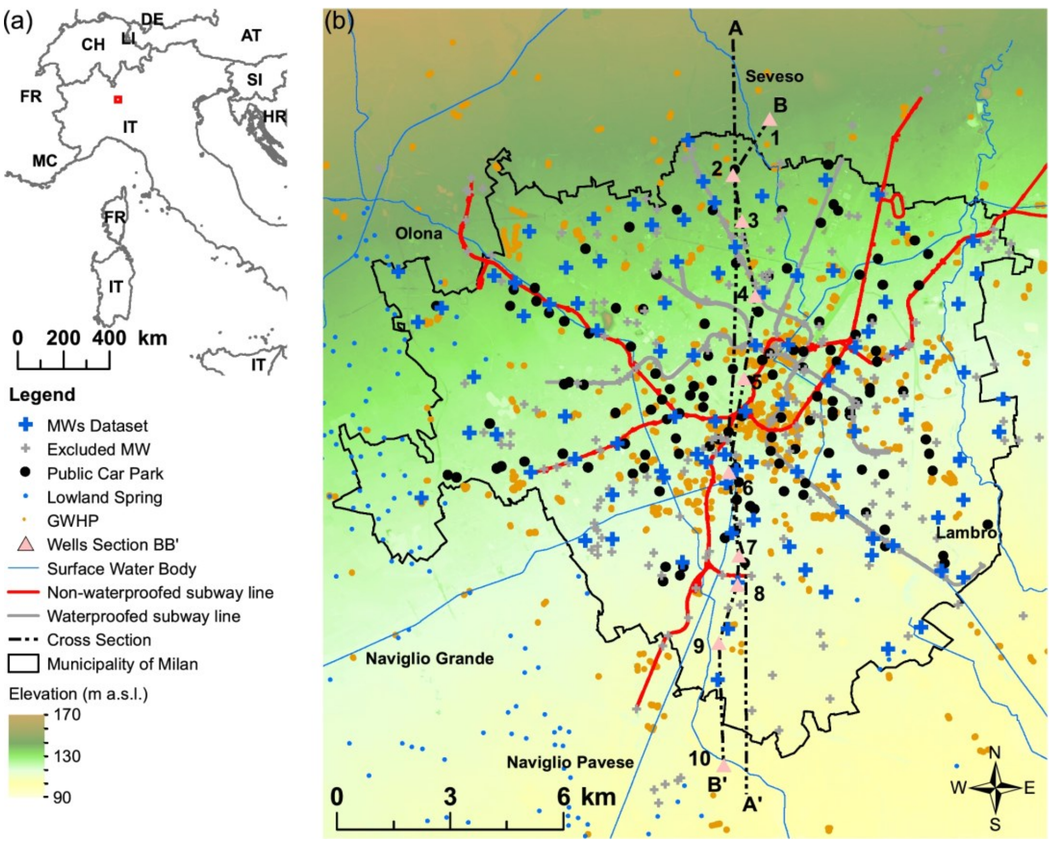

Fig. 6.1. a) Geographical setting of the study area; **b)** Main hydrogeologic features (lowland springs and surface water bodies), non-waterproofed and waterproofed subway lines, public car parks, GW heat pumps (GWHPs) and wells crossed by section BB’; line AA’ points to the location of the cross section that is visible in Fig. 6.2; line BB’ points to the location of the

geological profile that is shown in Fig. S6.1 of the ESM. To obtain a clear representation, public car parks have been represented as points instead of polygons.

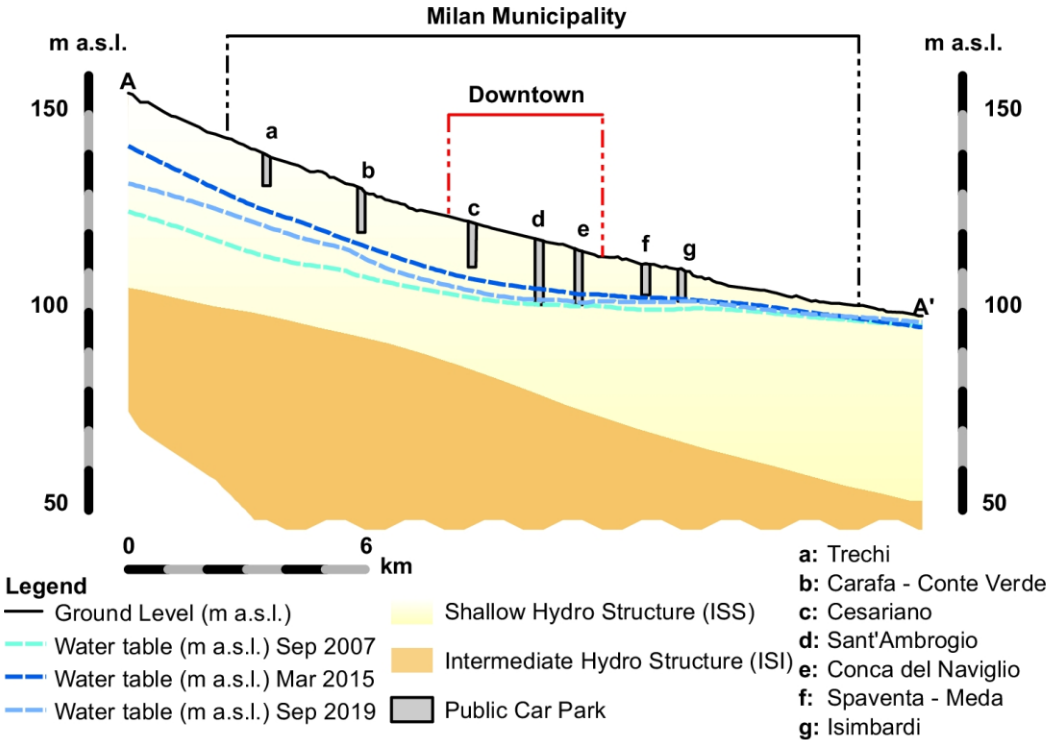

Fig. 6.2. Hydrogeologic schematic N–S cross section AA' of the study area, showing the location of some public car parks. The water table elevations of three different GW conditions are also reported. For its location see Fig. 6.1b.

6.3. Materials and Methods

The methodology proposed in this study is composed of 7 steps: 1) Dataset pre-processing, 2) GW time-series trend analysis, including the Mann-Kendall test, Sen's slope estimator and a time-series reversal points assessment, 3) Correlation analysis, through autocorrelation function (ACF) and cross-correlation function (CCF) with precipitation data; 4) GW time-series clustering, applying hierarchical cluster analysis (HCA); 5) Water table reconstruction and GW volume calculation under specific GW conditions identified at point 2; based on the outcomes of points 1-5, the subsequent steps were: 6) Identification of GW management areas (MAs); 7) Definition of guidelines for UIs management. A graphical representation of the adopted workflow is given in Fig. 6.3.

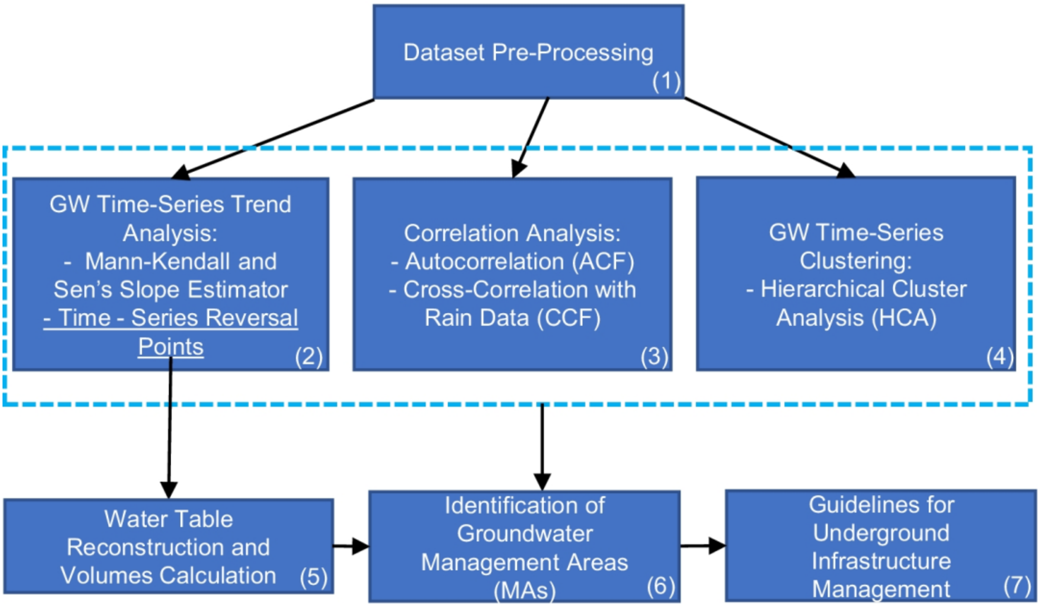

Fig. 6.3. Adopted workflow.

6.3.1. Data-driven time-series analysis

6.3.1.1. Available data and Pre-processing

GW level data were provided by Metropolitana Milanese Spa, the local water supplier. The original dataset spans from 1950 to 2019, but data are scattered over ca. 300 monitoring wells (MWs) changing over time due to the monitoring network evolution (Fig. 6.1b). Excluding MWs not having a useful data resolution, a subset of the most consistent time-series was identified for the time-series analysis, consisting of 95 MWs (Fig. 6.1b) monitored over the 2005-2019 time's span.

Two measures per year are available (March and September; with 30 observations in total). Once the final dataset had been defined, it was checked for possible errors or outliers (Azzellino et al. 2019). Outlier analysis was performed through the non-parametric interquartile range test, since the Shapiro-Wilk test highlighted that the data distribution was not normal. Errors were corrected manually only if clearly identifiable in the original data (i.e. ground level values), after verifying that they could offer insights into some hydrogeologic process that should not be neglected (Peterson et al. 2018).

As for precipitation, the data of Paderno Dugnano rain gauge (located just northward of the city of Milan) were considered, monitored by the regional environmental protection agency (ARPA Lombardia 2021).

6.3.1.2. Mann-Kendall test and Sen's slope estimator

The Mann-Kendall test (Mann 1945; Kendall 1948) is a rank-based, non-parametric test widely used for trend detection (i.e. upward or downward trend) in hydrological variables since it is non-parametric and robust to extreme data (Singh et al. 2015; Anand et al. 2020; Meggiorin et al. 2021). The null hypothesis (H_0) is the absence of a trend, while the alternative hypothesis (H_1) is the presence of a significant trend. A confidence level of 95% was used as the threshold value.

The Sen's slope estimator (Sen 1968) was applied to estimate the magnitude of the analysed trend. It is a non-parametric unbiased estimator of trends, more robust to outliers than a linear regression estimator (Hirsch et al. 1982). A positive value of Sen's slope indicates an increasing trend, whereas a negative one indicates a decreasing trend.

6.3.1.3. Time-series reversal points

The reversal points analysis for the time-series aimed at identifying when an upward (or downward) trend has been reversed. This could be useful in GW management, as it allows one to precisely comprehend the dynamics of the water table in a given period.

The Pettitt test (Pettitt 1979) is a widely applied statistical tool to detect an abrupt change in a dataset. Despite its common use, it seems not so adaptable when trying to identify a pure reversal point (i.e. a shift from an upward trend to a downward trend), at least in small datasets (Frollini et al. 2021).

Therefore, reversal points were identified here as the time-series point determining a change in the sign of the difference between successive couples of data, previously smoothed through a loess function to avoid noise effect. This analysis was performed in the R environment, using the imputeTS package (Moritz and Bartz-Beielstein 2017), ts function (Becker et al. 1988) and stl function (Cleveland et al. 1990).

In this way, only the most recurrent GW-level minimum and maximum conditions among the different MWs have been investigated.

An additional description of their subsequent application is given at Section “Water table reconstruction and GW volumes calculation”. Further details on the adopted approach and the R script are available in the ESM.

6.3.1.4. Autocorrelation and cross-correlation

Autocorrelation is the correlation of a time-series with itself at different time lags. It indicates whether the past values of a time-series influence the current state. Here, autocorrelation analysis was performed for all the MWs through the R Package statistics (R Core Team 2021) to investigate at the study scale the “memory effect” of the GW system, which can be considered as the requested amount of time to get rid of the dependency from a previous condition (Tamburini and Menichetti 2020).

The cross-correlation is a measure of similarity between two time-series as a function of the displacement of one with respect to the other. To evaluate a possible delayed dependency at different time lags of GW levels (output series) on rainfall data (input series), a cross-correlation analysis between these variables was conducted. Thus, rainfall data were aggregated at a six-month time step (cumulative rainfall periods: October-March / April-September) to keep equal data length while correlating the two variables and to avoid spurious conclusions that would arise from not using equal data records (Kumar et al. 2009).

6.3.1.5. Groundwater Time-Series Clustering

Hierarchical cluster analysis (HCA) was performed, considering GW level measurements at different times as different variables, using the Ward hierarchical method (Ward Jr 1963).

The squared Euclidean distance was adopted as a measure of similarity between samples (Triki et al. 2014; Bloomfield et al. 2015) to compare the GW levels of different MWs at individual seasons, without associating the GW levels of different seasons, which could have happened when applying other distances typical of the time-series analysis.

In order to analyse both spatial and temporal patterns over a time-series, not only the initial GW measurements, but also seasonal differences between couples of successive observations have been considered. In both cases, to guarantee an equal weight for each considered variable in the calculation of the Euclidean distance matrix, HCA was carried out on standardized data (i.e. autoscaling; mean = 0 and variance = 1; (Judd 1980)). The HCA dataset, therefore, resulted in 95 rows (i.e. monitoring wells) and 59 variables (columns, i.e. GW level measures for March-September from 2005 to 2019 and seasonal variations between successive GW measures).

The HCA requires continuous data and no missing values. Therefore, missing data were filled considering trend similarity among neighbouring MWs. First, a GIS analysis was carried out to identify the MWs nearest to those containing missing values. Missing values were then filled by calculating the average difference between the time-series containing missing values and the most similar neighbouring MW; this average was calculated over the previous and the following observations surrounding the missing values, and then applying (summing/subtracting) it to the date of the missing value. In this way, possible relevant peaks in the GW time-series were conserved, avoiding any smoothing effect that could result from the time-series interpolation or other filling methods.

6.3.1.6. Water Table Reconstruction and Groundwater Volumes Calculation

Potentiometric maps for the shallow aquifer have been reconstructed, for the identified global minimum and maximum conditions (Section: Groundwater minimum and maximum), and for the last measure of the time-series (September 2019, Sep19). Further piezometric levels, available for each specific period both inside and outside the study area (i.e. control points), have been employed to properly reconstruct the potentiometric maps.

As in the study area the presence of a spatial piezometric trend (NW- SE) has been detected (Bonomi et al. 1998; Beretta et al. 2004), GW heads in MWs have been interpolated using universal kriging (Isaaks and Srivastava 1989; Goovaerts 1997; Kitanidis 1997; Webster and Oliver 2001). Subsequently, the volume of water in the shallow aquifer, determined from the difference between the potentiometric heads in maps of the different GW conditions, has been calculated and the content of mobile water contained in that portion of the subsurface has been estimated considering the effective porosity (n_{e}). Reckoning the quantities of both occupied volumes and mobile water could in fact be deemed as a proper way of assessing the impact of GW on different resources, including manmade ones (Bonomi et al. 2010). To do so, geological information on the subsurface was required. The parametrisation of the hydrogeologic properties, such as hydraulic conductivity, has been readapted from a previous work of the research group on the same study area (Bonomi et al. 2010). Classes of effective porosity have been then extracted from the hydraulic conductivity values of the subsurface volumes derived from comparison of the water tables. This step was performed through the use of conversion conductivity–effective porosity tables, previously entered in a reference database (Bonomi et al. 2010; Bonomi et al. 2014).

6.3.2. Decision management

On the basis of the results that emerged in previous steps, different spatial units (management areas, MAs) have been aggregated as a result of their hydrogeologic features (Chaudhuri and Ale 2013) in the context of a more targeted GW management strategy. Moreover, a deeper analysis associated with UIs, with a focus on public car parks, was elaborated through a GIS methodology previously applied by Sartirana et al. 2020, to evaluate the interaction between public car parks and the water table. This analysis was carried out on the identified GW-level minimum and maximum conditions and for Sep19. Based on these results, public car parks have been grouped into three categories with respect to GW flooding for each period: not submerged, possibly critical, submerged. A public car park was defined as “not submerged” or “submerged” if the water table was respectively below or above the bottom of the car park structure. The category “possibly critical” included all the public car parks showing a difference between the reference plan and the water table of less than one meter. Engineering aspects, such as the possible uplift risks generated by buoyancy as a result of the aquifer pressure, are beyond the aims of this work. The identified possibility of submersion for each car park, therefore, facilitated a list of targeted management proposals, including suggested guidelines for the construction of new public car parks, based on the detected hydrogeologic evidence.

6.4. Results

6.4.1. Data-driven time-series analysis

6.4.1.1. Mann-Kendall test and Sen’s slope estimator

Trend analysis through the Mann-Kendall test and Sen’s slope estimator showed a general increasing trend in the GW levels. Results are visible in Fig. 6.4. Particularly, at 95% confidence level, 86 out of 95 MWs showed an increasing trend throughout the considered period, with a medium slope ranging from 0.20 to 0.60 in the northern sector, from 0.10 to 0.20 in the central portion of the domain, and from 0.00 to 0.10 in the southern area. Only 9 out of 95 MWs did not show significant trends, all located in the westernmost portion of the study area, except for one in the southernmost.

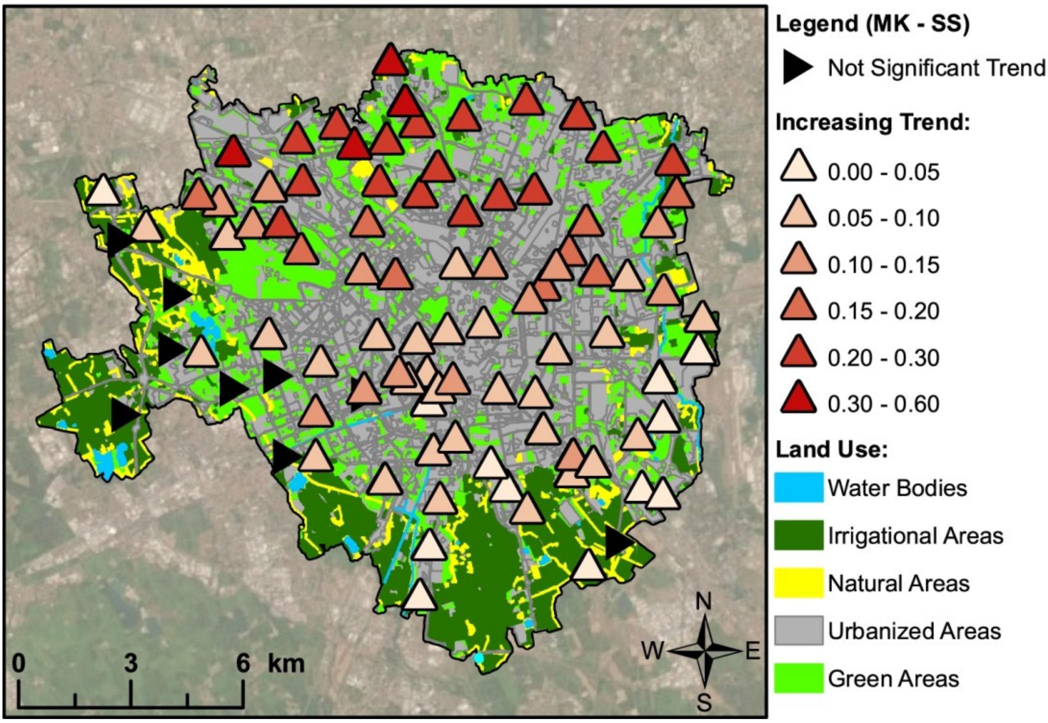

Fig. 6.4. Statistically significant or not significant trends of the GW-level time-series for the analysed period. Colour coding indicates the magnitude of the trend, estimated by Sen's slope estimator. Land use classes have been represented from the geographic database Dusaf 6.0 (Regione Lombardia 2021). Service Layer Credits: Esri, Maxar, GeoEye, Earthstar Geographics, CNES/Airbus DS, United States Department of Agriculture (USDA), US Geological Survey (USGS), AeroGRID, IGN (University of Copenhagen) and the GIS User Community.

6.4.1.2. Groundwater minimum and maximum

Through the adopted approach developed in R, the global GW minimum and maximum conditions have been identified. Results are visible in Fig. 6.5. Moreover, for a subset of selected MWs, the identified reversal points are visible, together with their GW trends in Fig. 6.6. The complete list of the identified reversal points for all the MWs is available at Table S6.2 of the ESM. As observable in Fig. 6.5, among the considered GW level time-series, September 2007 (Sep07) has been mainly identified as the global minimum condition; however, Sep07 is not identifiable as the historical global minimum, which took place at the end of the 1970s, as a consequence of intense industrial exploitation of

GW (Bonomi 1999). Instead, March 2015 (Mar15) has been detected as the global maximum. As a general description for the study area, Sep07 comes at the end of a decreasing phase that began in December 2002, as described in a previous work about the same area (Sartirana et al. 2020). A rising phase, steeper in the northern sector, as confirmed by the Sen's slope estimator (Fig. 6.4), has been detected from Sep07 up to Mar15, while a subsequent declining phase took place from Mar15 up to Sep19 (final measurement of the dataset). Some MWs, mostly located in the peripheral areas, showed their GW minimum condition earlier than Sep07 (i.e. Mar07); in contrast, in the northernmost areas, the GW minimum was sometimes detected later than Sep07 (i.e. Mar08). Moreover, a higher number of reversal points has been identified for the MWs located in the peripheral sectors (eastern and western sides) and in the southern areas, with respect to the MWs placed in the northern and central parts of the domain (Fig. 6.6). Local minimum and maximum conditions have been also identified (Table S6.2 of the ESM): respectively, September 2012 and September 2011. However, these local situations have not been further investigated, thus reconstructing the piezometric surfaces of the water table only for the Sep07, Mar15, and for Sep19.

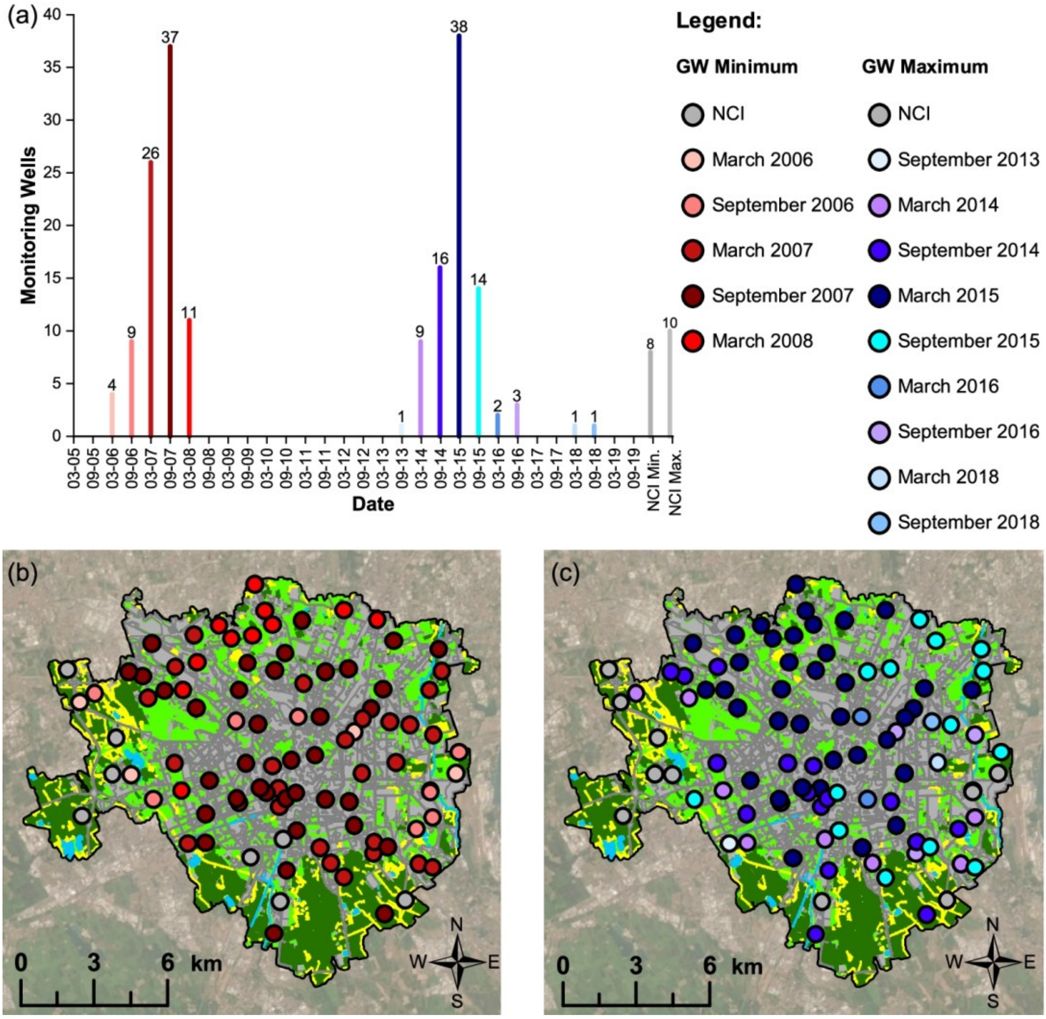

Fig. 6.5. a) Identified reversal points for GW level minimum and maximum conditions. Dates on the X-axis are provided according to format mm-yy. Spatial and temporal distribution of the identified reversal points for **b)** GW minimum **c)** GW maximum. NCI stands for 'not clearly identifiable'.

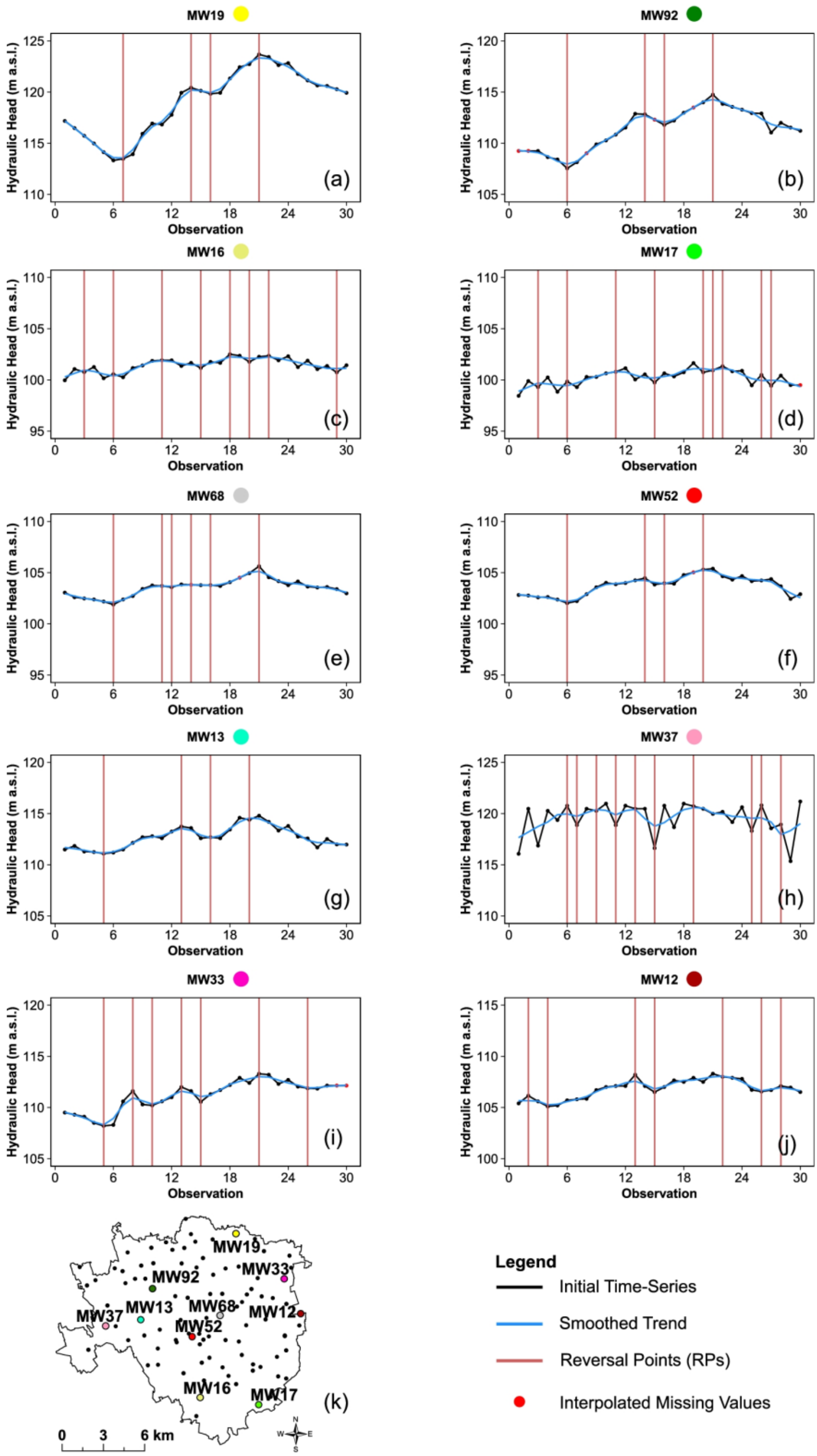
MW19
MW92
MW16
MW17
MW68
MW52
MW13
MW37
MW33
MW12
Hydraulic Head (m a.s.l.)
Observation
(a)
(b)
(c)
(d)
(e)
(f)
(g)
(h)
(i)
(j)
(k)
0 3 6 km
Legend
Initial Time-Series
Smoothed Trend
Reversal Points (RPs)
Interpolated Missing Values

Fig. 6.6. GW-level time-series and reversal points for the selected monitoring wells (MWs). **a), b)** MWs time-series located in the North. **c), d)** MWs time-series located in the South. **e), f)** MWs time-series located downtown. **g), h)** MWs time-series located in the West. **i), j)** MWs time-series located in the East. **k)** Location of selected MWs time-series. To better compare the time-series, the X-axis scale has been set with intervals of six observations (i.e. three years); the Y-axis scale has been kept the same for all the time-series graphics (15 meters).

6.4.1.3. Autocorrelation and Cross-correlation with rain data

Autocorrelation analysis was performed on the MWs considering 10 lags. For each MW, the number of significantly autocorrelated lags was determined and this is represented in Fig. 6.7. Results (Fig. 6.7a) show that autocorrelation can be significant for up to 6 lags in the northern sector, which correspond to a three-year time span. In the central part of the area, significant autocorrelation was detected for a maximum of 4 lags (i.e. 2 years), while a more heterogeneous situation is visible in the southernmost part. A westernmost group of MWs shows no degree of correlation.

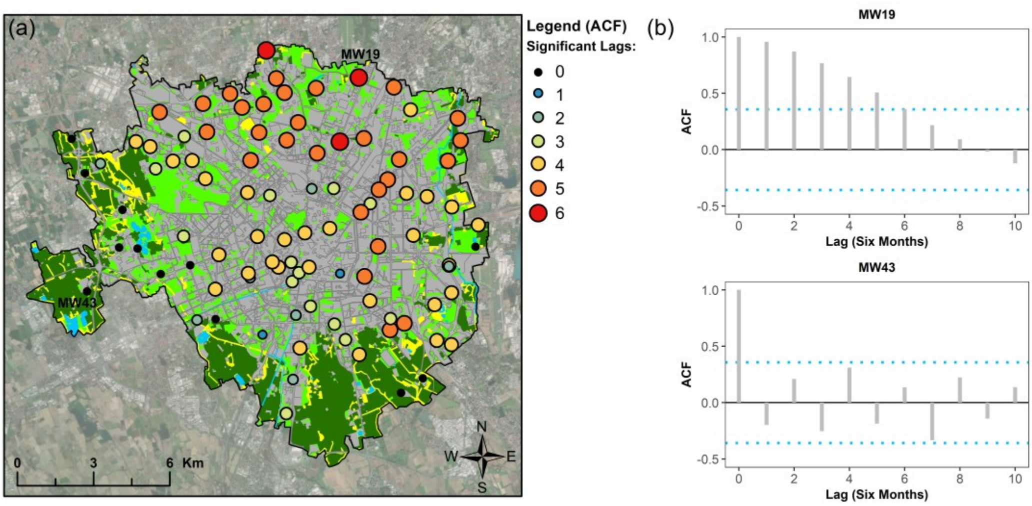

Fig. 6.7. a) Significant number of lags for each GW-level time-series; colour coding and dot sizes represent the number of significant lags. **b)** Autocorrelation plots for two selected MWs: the horizontal light blue dashed line indicates the significant level of autocorrelation (ACF) based on the record length (Bloomfield et al. 2015). The 95% significance level in both cases is ±0.3578. For the legend of land use classes, refer to Fig. 6.4.

Correlation of GW time-series with rain data has been evaluated up to Lag −2 (possible response time: one year), as these lags have been considered as the most environmentally significant; results are shown in Fig. 6.8.

At Lag 0 (i.e. no temporal shift), the MWs located in the most peripheral areas showed a significant correlation with rain data, indicating a direct and fast response of piezometric level to precipitation (Fig. 6.8a) mainly in the western and the southernmost sectors, which showed a shorter autocorrelation and therefore a lower memory of the GW system. A significant but lower correlation was detected in the eastern sector of the domain. Thus, in these areas, GW levels respond rapidly to local precipitation events. At Lag −1 (response time: six months) a more pronounced correlation between rain data and GW levels has been noticed in the northern and the central sectors of the domain (Fig. 6.8b), thus indicating a less rapid response of GW levels to rainfall; whereas, a reduced significant correlation has been identified in the western and southern sectors, that showed a significant correlation at Lag 0. Finally, at Lag −2 (response time: one year), a significant correlation with rain data was identified for 74 out of 95 MWs (Fig. 6.8c), thus showing a widespread dependency of GW-level time-series on rain data.

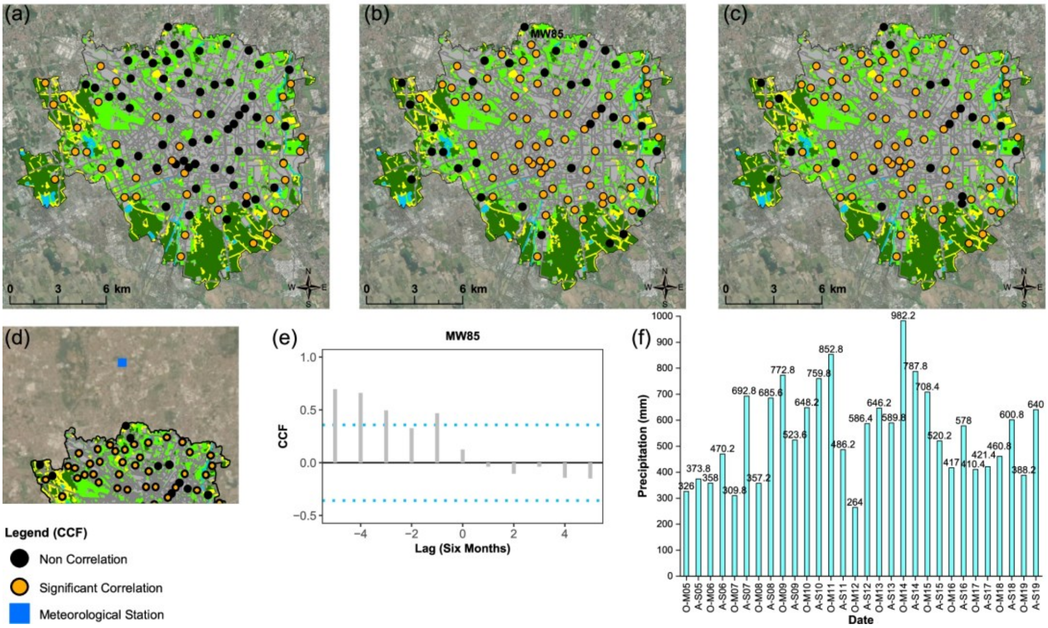

Fig. 6.8. Cross-correlation function with rainfall data at **a)** Lag 0 **b)** Lag −1 **c)** Lag −2. **d)** Location of Paderno Dugnano rain gauge station. **e)** Cross-correlation plot for one selected MW: the horizontal light blue dashed line indicates the significant level of cross-correlation (CCF) based on the record length (Bloomfield et al. 2015). The 95% significance level in both cases is ±0.3578. **f)** Time-series of meteorological data for Paderno Dugnano rain gauge. O-M stands for October–March; A-S stands for April–September. For the legend of land use classes, refer to Fig. 6.4.

6.4.1.4. Hierarchical Cluster analysis

According to the dendrogram in Fig. 6.9c, the possible solutions are at *k*=2, 3, 4 and 8, where *k* is the number of clusters. MWs have been grouped into 8 clusters (C1-C8; Figs. 6.9a and 6.9c), as this allowed a more detailed exploration and interpretation of the study area's environmental variability (Rinderer et al. 2019). Two clusters (C1 and C4) contain most of the MWs (23 out of 95 are contained in C1, while 34 out of 95 are included in C4); two clusters (C2 and C3) both contain 12 MWs, while the remaining four clusters (C5-C8) contain at most four MWs, thus describing more specific situations. The MWs of C1 are mainly located in the southern sector, while a few are close to the downtown area. These MWs are characterized by a relatively stable GW level, with hydraulic head variations of two-three meters. This characteristic is due to the local geology for the southern MWs, showing GW heads close to the ground level, with a constrained possibility of oscillation; close to the downtown area, the non-consumptive employment of GW exerted by GWHPs could contribute to maintaining GW levels as relatively stable. Cluster C2 includes 12 MWs located in a transition belt between the northern and the central sector. As illustrated in Fig. 6.9b, the main differences between C3 and C4 are the average GW level of the cluster and the range of hydraulic head variations (i.e. within ~ 5 m), while the cluster trends are rather similar. Despite this similarity, MWs in C3 are characterized by a steeper rising (around 8-10 meters) phase in the period between Sep07 and Mar15 (GW minimum and maximum conditions respectively). C4 contains 34 MWs, distributed in the central portion of the domain: the average trend of this group is similar to C1, even if a less oscillating declining phase has been observed between Mar05 and Sep07; also for this cluster, stable GW levels could depend on the use of GWHPs. Three MWs located in the northern part of the domain are included in C5: a GW level peak for Sep08 was the main driver determining a medium GW level trend that differs from C3 and C8, whose MWs are similarly sited northward. C6 and C7 contain four and three MWs respectively: both these clusters group MWs located in the westernmost part of the study area; the average GW level of these clusters shows a high fluctuating trend, with no evident rising or declining phases. This may prove a rapid response of the water table to local conditions, as identified also from the results of the autocorrelation and cross-correlation functions. Four MWs, located in the northernmost area of the domain, are grouped in C8: the average trend of this cluster is comparable in its first part to the trend of C3, while the declining period from Mar15 is more oscillating than the linear declining phase of C3; thus, this second part of the trend is more comparable to C5 trend. The average hydraulic head variation is around 7-8 meters.

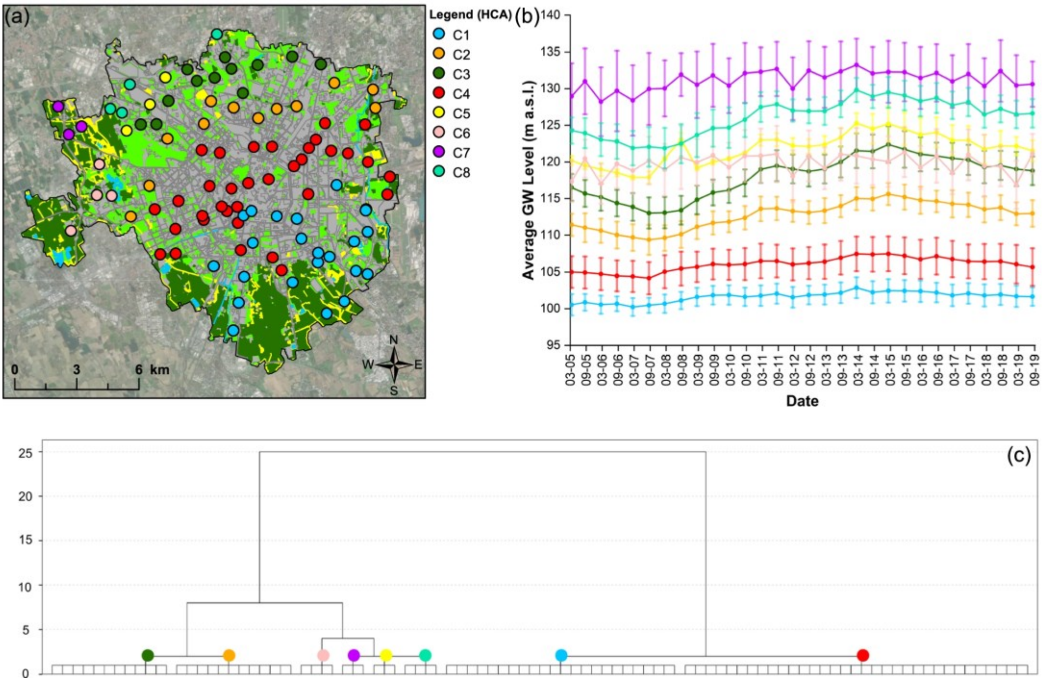

Fig. 6.9. a) Spatial distribution of the resulting clusters; **b)** Average GW level of the resulting clusters; error bars are sized according to standard deviation. **c)** Cluster analysis dendrogram of the 95 MWs. For the legend of land use classes, refer to Fig. 6.4.

6.4.1.5. Water Table and Groundwater Volumes calculation

GW potentiometric maps of the shallow aquifer for the identified GW level minimum and maximum conditions (Sep07, Mar15) and for Sep19 are shown in Figs. 6.10a and 6.10c. Their raster differences are displayed in Fig. 6.10d and Fig. 6.10e. As observable from Fig. 6.10d, in the northern portion of the domain, characterized by a steeper rising trend (Fig. 6.4) and a wide unsaturated zone (Fig. 6.2), hydraulic heads (m a.s.l.) differed by more than ten meters between the minimum and maximum conditions. In the NW this difference was limited to around four meters. Moving South, the difference values oscillated between three and five meters close to the downtown area; in the South and West, the differences in hydraulic heads were between zero and two meters, confirming a reduced/not significant rising trend. In these areas, despite Sep07 being identified as the GW level minimum, in a few spot locations the hydraulic head of Sep07 was higher than Mar15. This could be due to the irrigation activities generating a GW maximum at the end of the summer season. Moreover, as the unsaturated zone of the southern part of the shallow aquifer is thinner than in the northern part (Fig. 6.2), GW level oscillations are limited, and the GW minimum and maximum conditions are less evident. On the other hand, the eastern side of the domain shows different behaviour, with a global GW maximum higher than the global minimum. As regards the Mar15-Sep19 investigation (Fig. 6.10e), hydraulic head differences appeared limited with respect to the Mar15-Sep07 analysis (Fig. 6.10d). In the North, the hydraulic head differences did not exceed six meters, with three meters as the maximum difference observable near the downtown area, while a similarly limited oscillation was detected for the southern sector, if compared to the Mar15-Sep07 analysis. With respect to the western portion, hydraulic heads of Sep19 were general higher than in Mar15, despite Sep19 coming at the end of a declining trend period. In terms of subsurface volumes impacted by these GW oscillations, the rising trend between Sep07 and Mar15 determined an occupation of 704.94 × 10^6 m^3. In contrast, the declining phase that took place from Mar15 onward determined a reduction of 289.62 × 10^6 m^3 of GW in the shallow aquifer. As for the mobile water included in these volumes, eight classes of effective porosity have been introduced for the calculation, deriving their values from the hydraulic conductivity values of the lithologies in these subsurface portions. A detailed description of these classes (n_e) has been provided in Table 6.1.

Table 6.1. Classes of effective porosity and conversion of hydraulic conductivity into effective porosity values.

Class of effective porosity	Hydraulic conductivity (m/d)	Effective porosity value
1	<42	0.18
2	42-70	0.19
3	71-100	0.20
4	101-130	0.21
5	131-160	0.22
6	161-190	0.23

Class of effective porosity	Hydraulic conductivity (m/d)	Effective porosity value
7	191-220	0.24
8	>221	0.25

Effective porosity values ranging from 0.18-0.19 have been attributed to fine grain-size materials (hydraulic conductivity (*K*) ranging from 38 to 70 m/s), while higher values have been assigned respectively to medium-grain (0.20-0.22, with *K* from 71 to 160 m/s) and coarse materials (0.23-0.25, with *K* from 161 to 262 m/s).

Based on this classification, for the Sep07-Mar15 period there has been an estimated increase of 149.53 × 10^6 m^3 of mobile water, while for the Mar15-Sep19 period, a decrease of 62.69 × 10^6 m^3.

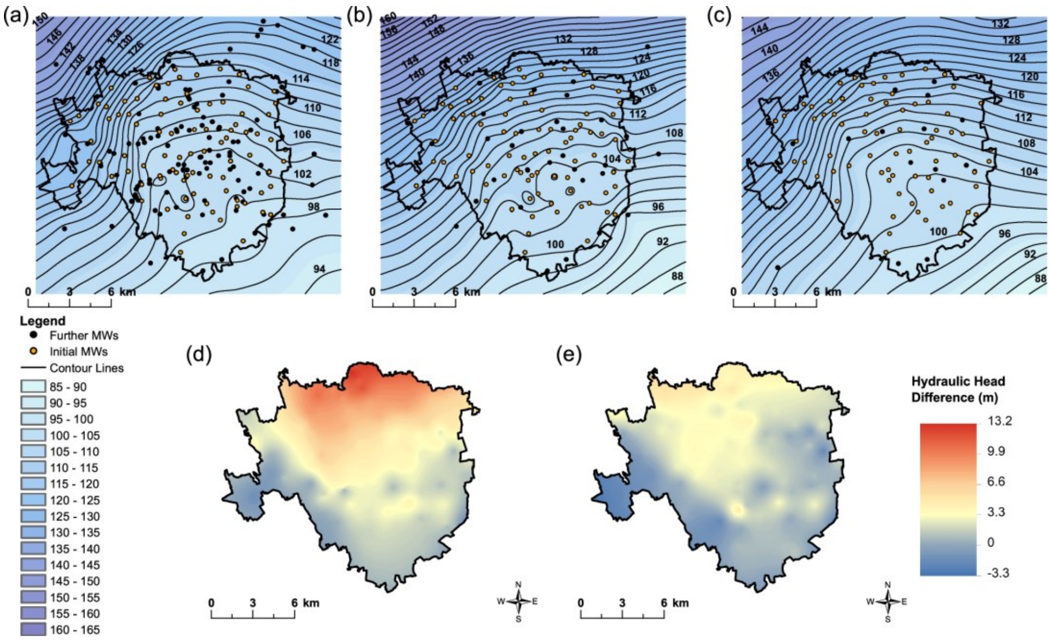

Fig. 6.10. GW potentiometric maps for **a)** Sep07 **b)** Mar15 **c)** Sep19; **d)** Hydraulic head difference between the maximum (Mar15) and minimum condition (Sep07); **e)** Hydraulic head difference between the maximum (Mar15) and final GW condition (Sep19).

6.5. Discussion

As planned by the local authorities (Milan Metropolitan City 2019), in the framework of a general urban transformation, urban underground development is occurring for the city of Milan. This implies an integrated management scheme, taking GW aspects into account. Thus, a data-driven methodology was adopted in this study to identify GW management areas (MAs) and elaborate management proposals for the UIs. In particular, greater attention has been paid to public car parks. To do so, a set of statistical and geospatial techniques, which are scientifically appropriate, has been adopted to assess spatial-temporal patterns of GW levels (Chaudhuri and Ale 2014).

6.5.1. Improved conceptual model

The obtained results showed a general spatial agreement, identifying different hydrogeologic features among various domain sectors.

The northern sector showed the highest trend magnitude (Fig. 6.4): in this area, the greater unsaturated thickness (Fig. 6.2) allows the water table to oscillate widely. This hydrogeologic condition facilitated the GW rebound that started at the beginning of the 1990s, triggered by both the industrial decommissioning and a gradual decrease in resident population (Bonomi 1999; De Caro et al. 2020). In the same sector, the autocorrelation coefficient turned out to be significant at up to six lags, implying a long-term memory of the system and a significant dependency from previous measures (Dinpashoh et al. 2014; Neto et al. 2016). The downtown sector showed a lower trend magnitude than the northern sector. This lower trend can depend on a possible anthropogenic influence associated with extensive use of GWHPs and a significant presence of UIs controlling GW levels. These areas showed a delayed response to precipitation events, with a significant correlation at Lag −1 (response time: six months): this could be due to a) the greatest depth of the water table (Fig. 6.2), mainly in the North, which determines a delayed GW response, and b) a reduced infiltration rate dependent on an urbanized land use, visible for both sectors (Fig. 6.4). These factors contributed also to a delayed identification of reversal points, as occurred for the GW minimum: in the North this condition was in part identified in Mar08 (Fig. 6.5b), and not in Sep07 as for the majority of the time-series (Fig. 6.5a).

In the South, depending on its hydraulic gradient, the water table is close to the ground level (Fig. 6.2), which limits the rising trend. Moreover, as for the western sector, a decrease in grain size from coarse (i.e. gravel and sand) to fine sediments (i.e. silt and clay), moving from N to S, determines a change in the aquifer transmissivity: this leads to the formation of the lowland springs, forcing GW both close to the ground level and to outflow, thus constraining water table oscillations (De Luca et al. 2014). As well, in the West, the presence of clay lenses determines the formation of local perched aquifers, with a medium depth ranging from six to eight meters below the ground level (Bonomi et al. 2009). Western time-series are also marked by the presence of seasonal fluctuations (Fig. 6.9b), with a GW level minimum in March and a maximum in September. Land use could influence this cyclical condition. This area is mainly agricultural (Fig. 6.4), with maize and rice as primary cultures (Bernini et al. 2019; Pulighe and Lupia 2019): as the irrigation period goes from April to September, a GW level maximum is expected at the end of this season, with a water table response generally delayed by less than one month compared to the beginning of the flooding activities (Lasagna et al. 2020). All these factors could explain the reduced significant autocorrelation in the South and the almost complete absence of autocorrelation in the West, highlighting a lack of system memory in these areas and a rapid response to external drivers. The significant cross-correlation with rain data at Lag 0, providing insights into a rapid aquifer recharge by rainfall (Lasagna et al. 2020), is in line with these outcomes. This aspect also appeared from reversal points analysis, as in these areas the identified GW level minimum and maximum condition partly occurred in advance from Sep07 (GW minimum) and Mar15 (GW maximum) (Fig. 6.5).

The widespread correlation at Lag −2 (response time: one year) could be attributed, in particular for these peripheral sectors of the domain, to a sort of periodicity of GW time-series, mainly attributable to the agricultural activities that led to a cyclical hydraulic maximum at the end of the summer season.

In contrast, different hydrogeologic settings could explain the discrepancy in correlation results between western and eastern sectors (Fig. 6.7a), as land use distribution is mostly similar. In the East, the paleochannel of the Lambro River (Fig. 6.1), with coarse materials and a higher transmissivity, determines a difference from the geological system of the lowland springs and the local perched aquifers previously described for the western sector, influencing correlation results.

These findings highlighted that the degree of autocorrelation influences the slope magnitude of GW level trends. In addition, the thickness of the unsaturated zone revealed to be a contributory factor on MWs autocorrelation (Bloomfield and Marchant 2013). As regards cross-correlation with rain data, results pinpointed that lag times between the GW level responses to precipitation events are related to the lithological conditions and the thickness of the unsaturated zone (Kotchoni et al. 2019). Moreover, land use distribution could be considered as an additional factor influencing the infiltration rate (Scanlon et al. 2005).

The final grouping of GW time-series in 8 clusters is consistent with the results previously described. Northern time-series are grouped into C3, C5 and C8: these time-series both show the highest trend magnitude and the highest degree of autocorrelation; moreover, their correlation with rain data is uniformly delayed (Lag −1). In addition, their water table rising, of between eight and ten meters, was the greatest detected. This trend proves the anthropogenic impact (Bloomfield et al. 2015), representing the ending phase of the GW rebound, triggered by the industrial decommissioning that started at the beginning of the 1990s (Bonomi 1999). The same explanation provided for the northern clusters could be provided even for C2, grouping MWs located at the transition belt between the northern clusters and C4. This latter cluster groups all the GW time-series located in the downtown belt, showing both a dampened magnitude of trend and degree of autocorrelation compared to the northern MWs. C1 includes all the southern MWs, with a part of them stretching up to the downtown area: this spatial distribution could depend both on a structural and anthropogenic factor. The structural factor is due to the constrained possibility of oscillations of the water table in this part of domain; the anthropogenic influence could be attributed to the GW exploitation for heat exchange:

GWHPs active in the downtown area, mainly inducing a thermal stress, could be considered as non-consumptive (García-Gil et al. 2016), as by using a system of catch and return wells the water withdrawn is usually returned to the shallow aquifer. At the same time, if only catch wells are adopted, this could contribute to limit the water table rising. C6 and C7 group all the MWs located in the western area: as discussed above, the fluctuating but constrained GW level trend of these MWs could be related both to the presence of lowland springs and local perched aquifers and to the land use, with irrigation activities conducted during the summer season.

Thus, also cluster analysis emphasized that, even within the same aquifer, and in a rather limited domain, significant differences in GW behaviour could be identified.

The outcomes of the data-driven approach have also been confirmed by the spatial analysis, applied to reconstruct the potentiometric maps of different GW conditions and to calculate the subsurface volumes influenced by these GW oscillations. In the North, where the highest trend magnitude (Fig. 6.4) and degree of correlation were detected (Fig. 6.7), the major GW hydraulic head variations have also been identified using GIS. Subsequently, a progressive dampening in water table oscillations has been registered moving both southward and westward, where a reduction in trend magnitude (Fig. 6.4) and degree of correlation (Fig. 6.7) was observed, while identifying a more rapid correlation with rainfall data (Fig. 6.8a). Moreover, the content of mobile water included in these subsurface volumes has been estimated. This information could be useful for stakeholders, as in GW rising phases part of this amount of water could represent a flooding threat to underground structures; for this reason, this water could be locally withdrawn to secure the infrastructure at risk, exploiting this resource for other needs (i.e. street washing, recreational uses).

6.5.2. Considerations on the data-driven approach

This agreement among the obtained results allowed this study to focus on the effectiveness of a data-driven approach. GW-level time-series have been analysed, applying different statistical techniques; each one was employed to investigate a specific hydrogeologic aspect: however, in the end, the final outcomes obtained always showed spatially coherent regions of GW behaviour. Thus, time-series analysis provided a deep insight into the main hydrogeologic features of the shallow GW system, highlighting fundamental properties that affect GW level dynamics (Bloomfield et al. 2015): applying them to support GW system conceptualization could guarantee both time- and cost-effective assistance to GW models (Obergfell et al. 2013), providing useful complementary information. Besides, even if for many GW questions an answer could be obtained only by structuring a spatial GW model (Anderson et al. 2015), time-series analysis can still have a relevant role (Bakker and Schaars 2019): for example, in data pre-processing and target definition.

In particular, through the approach developed in R to identify GW conditions, the highest number of reversal points was identified for the western and southern time-series (Table S6.2 of the ESM); this proved the absence of a clear significant trend, evidencing a more fluctuating behaviour if compared to the most visible rising and declining phases detectable in the northern and central sectors. This outcome is consistent with the hydrogeologic framework described through the Mann-Kendall test and Sen's slope estimator. Thus, the adopted approach turned out to be reliable in identifying the main GW conditions typical of the considered shallow aquifer, also identifying local situations.

As regards cross-correlation, combining GW-level time-series and precipitation data provided a better understanding of at least one natural forcing on GW trends (Kumar et al. 2009). The adoption of just one meteorological station was a direct consequence of data lacking and fragmentation, which is still a limiting factor as regards the potential use of Open Data information (Janssen et al. 2012). However, as the study area is a limited domain, located in the middle of an alluvial plain, a rather homogeneous rainfall trend over the area is supposable; thus, considering only one weather station was anyway believed enough to obtain reliable results. Depending on data availability, future perspectives could consider a higher number of meteorological stations to deepen this analysis.

Finally, grouping GW time-series through cluster analysis techniques, focusing on GW levels, constitutes an emerging research field (Naranjo-Fernández et al. 2020). In particular, its application represents an element of novelty for the study area: in fact, in this domain statistical techniques have been mostly applied for GW chemicals (Alberti et al. 2016; Azzellino et al. 2019; Pollicino et al. 2019) and thermal issues (Previati and Crosta 2021b), but not for quantitative analysis. As well, the adopted approach allowed one to accurately pinpoint the potential features influencing GW levels (i.e. geology, precipitation, withdrawals, land use), thus evidencing more defined local GW conditions. Moreover, their application in an urban planning framework is supposed to guarantee better policy outcomes. To the best of the authors' knowledge, this is the first time that data-driven analysis of GW levels have been adopted in supporting UIs management, and this approach could help stakeholders in effectively designing the already planned urban underground development that will take place in the next years for the city of Milan, considering also GW aspects.

6.5.3. Decision management

In view of the previous results, that showed a similar spatial zoning, four management areas (MAs) have been identified (Fig. 6.11). Each area showed a local hydrogeologic behaviour, thus needing different management policies in urban GW management and urban planning. In order to elaborate effective guidelines for the management and construction of new public car parks, an already defined spatial methodology has been previously adopted to evaluate how their interference with the water table in terms of flooding (not submerged, possibly critical, submerged) has varied over time. The methodology has been fine-tuned with respect to a previous work (Sartirana et al. 2020), introducing a threshold value that allows one to identify potentially submerged infrastructures (i.e. possibly critical structures). Given the total number of 126 car parks, 35 car parks are located in MA1; 54 and 30 car parks are respectively sited in MA2 and MA3, while only 7 are in MA4. The results of the spatial relationship between public car parks and the water table have been summed up at Table 6.2 and are visible at Fig. 6.11. The MA for each public car park is visible at Table S6.1 of the ESM.

Table 6.2. Conditions of public car parks in the proposed management areas (MAs) at the analysed GW conditions.

MA	GW period	Public Car Parks Condition		
		Not Submerged	Possibly Critical	Submerged
MA1	Sep07	35	-	-
	Mar15	29	5	1
	Sep19	35	-	-
MA2	Sep07	39	4	11
	Mar15	12	8	34
	Sep19	28	3	23
MA3	Sep07	12	7	11
	Mar15	8	2	20
	Sep19	9	4	17
MA4	Sep07	4	-	3
	Mar15	2	3	2
	Sep19	1	2	4

Thus, car park submersion mainly occurred in MA2, followed by MA3. This depends also on the depth of these structures: in the downtown area (MA2) car parks can reach up to six floors (i.e. 20 meters of depth); in contrast, in the northern sector (MA1) car parks have a medium depth of two-three floors (i.e. 8-11 meters of depth), while one floor (i.e. five meters) is typical in the western sector (MA4). Finally, car parks located in MA3 range from one-two floors in the southernmost part, up to five floors in the northernmost part, at the border with MA2 (Sartirana et al. 2020). Thus, MA3 also presented recurring impacted car parks, due to both the number of floors and the proximity of the water table to the ground level (Fig. 6.2). Finally, MA1 did not show any impact for Sep07 (Fig. 6.11a) and Sep19 (Fig. 6.11c), while some parks resulted as being possibly critical with respect to flooding in Mar15 (Fig. 6.11b), as a consequence of the steep water table rise occurring in the northern sector. Even if the unsaturated thickness is high (Fig. 6.2), adopting proper management measures would be suggested. As for MA4, the worst condition has been detected in Sep19, because of the seasonal water table fluctuations in this sector (Fig. 6.9b), determining a local GW level maximum at the end of the summer.

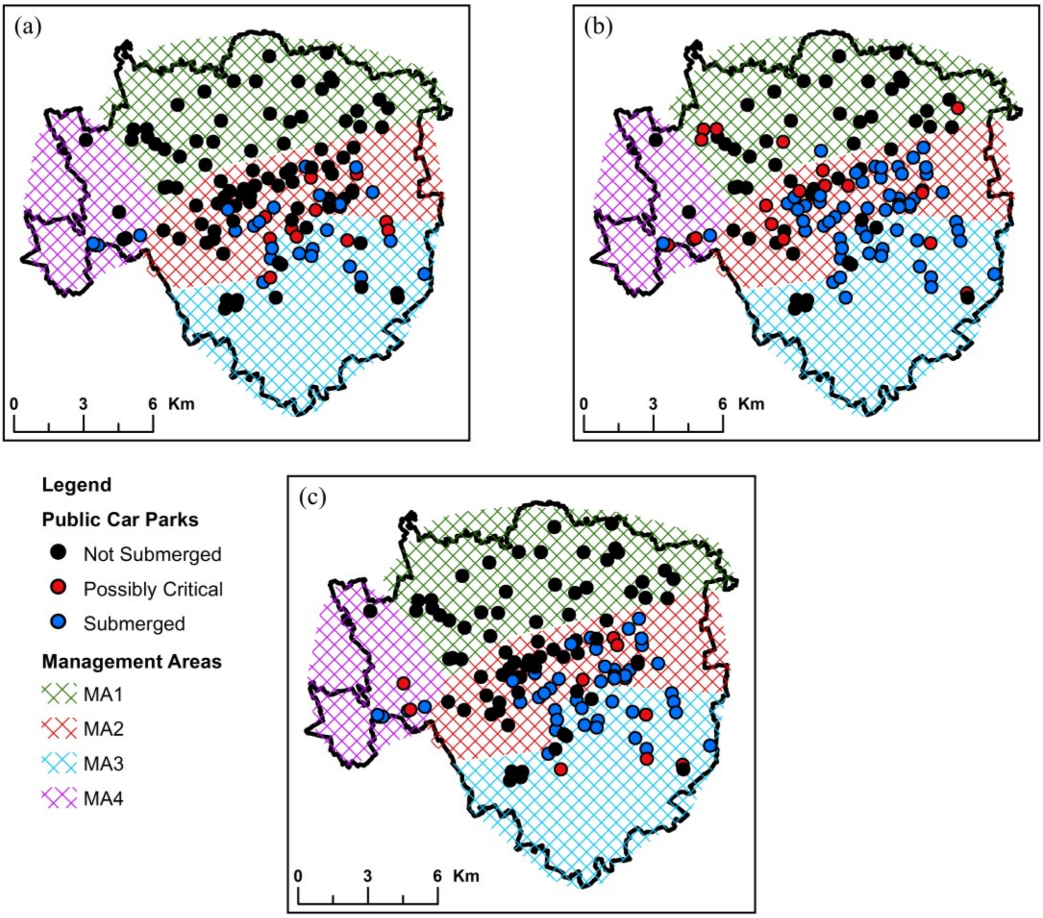

Fig. 6.11. Management areas (MAs) and public car park interaction with the water table at **a)** Sep07, **b)** Mar15 and **c)** Sep19. In order to obtain a clear representation, public car parks have been represented as points instead of polygons.

As a consequence of these results, a list of suggested guidelines regarding the construction of new public car parks has been elaborated. These guidelines, together with the hydrogeologic features and the possibility of submersion for each MA, are summarized in Table 6.3.

Table 6.3. Main hydrogeologic conditions, submersion risks and suggested guidelines for the identified management areas (MAs).

MA	**Hydrogeology**	**Submersion possibility**	**Suggested guidelines**
MA1	Wide range of thickness of the unsaturated zone; steep water table rise	Intense GW rebound: possible submersion supposing a further future GW-level rise	-Construction of new underground car parks with waterproofing techniques -Favour a horizontal subsurface sprawl of the car parks instead of deep structures (i.e. two floors as suggested depth)
MA2	Constrained water table rise (anthropogenic control)	Submersion facilitated by the depth of structures	-Construction of new underground car parks with waterproofing techniques -Adoption of pumping systems to locally control the GW rise: drainage and reinjection systems or GWHPs -3D numerical model to assess the impact of both the car parks and pumping systems on GW (i.e. avoid aquifer fragmentation or alter the GW budget of the flow system) -Installation of MWs close to the built structures to regularly

MA	Hydrogeology	Submersion possibility	Suggested guidelines
			monitor the hydraulic head
MA3	Constrained water table rise (geological control)	-Submersion facilitated by the depth of infrastructure (close to MA2) - Dependent on the water table close to the ground level (southern sector)	-Construction of new underground car parks with waterproofing techniques -Favour a horizontal subsurface sprawl of the car parks instead of deep structures, in particular in the southern sector (i.e. one floor as suggested depth)
MA4	Seasonal fluctuations of the water table; absence of a clear rising trend	Dependent on the water table close to the ground level	-Construction of new underground car parks with waterproofing techniques -Favour a horizontal subsurface sprawl of the car parks instead of deep structures (i.e. one floor as suggested depth)

In the past, some underground structures have been designed without waterproofing, neglecting the possibility of a GW rebound. Consequently, in the last decades, there have been flooding episodes in some public car parks (Sartirana et al. 2020). For this reason, a general guideline on the adoption of waterproofing techniques for new UIs has been proposed, acting as a reminder for the administrators. Based on local hydrogeologic conditions, a suggested number of floors has been provided for new public car parks for MA1, MA3, and MA4. A maximum of two floors has been indicated only for MA1, aiming to avoid possible interactions with the water table. A similar proposal has not been developed for MA2, as the majority of the economic activities are located in the city centre. This supposes a high demand for new infrastructure due to socio-economic needs (Bobylev 2009), and considers that the already in-place structures are developed as multi-storey, specific guidelines have been elaborated considering an interaction with the water table. In particular, pumping systems, including the adoption of GWHPs, could be favoured to control the water table rise, regulating the withdrawals based on regular monitoring of the interaction between GW and the UIs. Moreover, in order to assess the impact of the UIs on GW (Attard et al. 2017), local 3D numerical models should be developed. In this way, a sustainable and integrated management scheme will be developed, balancing the needs of both a secure GW resource and UIs.

6.6. Conclusions and Future Perspectives

This work aimed at proposing a data-driven approach to support decision-based management for urban planning of new UIs, focusing on public car parks; to do so, time-series analysis of GW-level time-series of the shallow aquifer beneath the city of Milan has been conducted. As interaction with GW has been observed in the last decades, resulting in the adoption of targeted management strategies in the urban planning framework becoming necessary. In particular, this study has allowed this paper to:

1. Define a workflow of different statistical and geospatial techniques that allows one to evaluate the spatio-temporal patterns of the GW levels for the studied shallow aquifer, proving the effectiveness of a data-driven approach.

2. Identify portions of the study area showing different GW conditions, mainly attributable to local hydrogeologic settings. Indeed, even in spatially limited domains, a thorough monitoring network could guarantee a broad insight into GW processes. Thus, different GW management strategies should be adopted according to specific hydrogeologic situations.

3. Provide to the decision makers a (site-specific) methodology to adequately design and handle the planned underground development of the city of Milan,

also considering GW aspects. In particular, as a main outcome of this study, four areas of GW/UIs integrated management options have been identified, where different guidelines for managing and designing new underground public car parks should be adopted.

This approach could be complementary to GW numerical modelling, in order to properly design urban GW management strategy. Indeed, analysing GW-level time-series could allow one to improve the definition of the conceptual model, and to identify local hydrogeologic conditions to be further studied through the development of a specific numerical model. Future perspectives will consider the realization of different GW scenarios, simulating possible climate change effects, to evaluate the dynamics of the interferences between GW and the underground structures, thus updating when required the suggested guidelines. The adopted methodology could be extended worldwide to other urban areas that have a well-structured GW monitoring network, are impacted by an existing interaction between GW and the UIs, and that may face future underground development.

Supplementary Materials: The online version contains supplementary materials available at https://doi.org/10.1007/s10040-022-02494-5

Funding: This research did not receive external funding.

Acknowledgments: The authors are grateful to Metropolitana Milanese S.p.A for providing piezometric data for groundwater-level time-series reconstructions. The authors would like to thank the associate editor, Hamid Kardam Moghaddam and another anonymous reviewer for their comments, which helped to improve this article.

References

Alberti L, Azzellino A, Colombo L, Lombi S (2016) Use of cluster analysis to identify tetrachloroethylene pollution hotspots for the transport numerical model implementation in urban functional area of Milan, Italy. Int Multidiscip Sci GeoConference SGEM 1:723–729

Anand B, Karunanidhi D, Subramani T, Srinivasamoorthy K, Suresh M (2020) Long-term trend detection and spatiotemporal analysis of groundwater levels using GIS techniques in Lower Bhavani River basin, Tamil Nadu, India. Environ Dev Sustain 22(4):2779–2800. https://doi.org/10.1007/s10668-019-00318-3

Anderson MP, Woessner WW, Hunt RJ (2015) Applied groundwater modeling: simulation of flow and advective transport. Academic press

ARPA Lombardia (2021) Agenzia Regionale per la Protezione dell'Ambiente [Regional Environmental Monitoring Agency]. https://www.arpalombardia.it/. (Accessed on 13 April 2021)

Attard G, Rossier Y, Winiarski T, Eisenlohr L (2017) Urban underground development confronted by the challenges of groundwater resources: Guidelines dedicated to the construction of underground structures in urban aquifers. Land use policy 64:461–469. https://doi.org/10.1016/j.landusepol.2017.03.015

Attard G, Winiarski T, Rossier Y, Eisenlohr L (2015) Review: Impact of underground structures on the flow of urban groundwater. Hydrogeol J 24(1):5–19. https://doi.org/10.1007/s10040-015-1317-3

Azzellino A, Colombo L, Lombi S, Marchesi V, Piana A, Merri A, Alberti L (2019) Groundwater diffuse pollution in functional urban areas: The need to define anthropogenic diffuse pollution background levels. Sci Total Environ 656:1207–1222. https://doi.org/10.1016/j.scitotenv.2018.11.416

Bakker M, Schaars F (2019) Solving Groundwater Flow Problems with Time Series Analysis: You May Not Even Need Another Model. Groundwater 57(6):826–833.

https://doi.org/10.1111/gwat.12927

Becker RA, Chambers JM, Wilks AR (1988) The New S Language. Wadsworth & Brooks/Cole. Comput Sci Ser Pacific Grove, CA

Beretta GP, Avanzini M, Pagotto A (2004) Managing groundwater rise: Experimental results and modelling of water pumping from a quarry lake in Milan urban area (Italy). Environ Geol 45(5):600–608. https://doi.org/10.1007/s00254-003-0918-7

Bernini A, Toure AL, Casagrandi R (2019) The time varying network of urban space uses in Milan. Appl Netw Sci 4(1). https://doi.org/10.1007/s41109-019-0245-x

Best KB, Miro ME, Kirpes RM, Kaynar N, Najera Chesler A (2021) Data-driven decision support tools for assessing the vulnerability of community water systems to groundwater contamination in Los Angeles County. Environ Sci Policy 124(July):393–400. https://doi.org/10.1016/j.envsci.2021.07.015

Bloomfield JP, Marchant BP (2013) Analysis of groundwater drought building on the standardised precipitation index approach. Hydrol Earth Syst Sci 17(12):4769–4787. https://doi.org/10.5194/hess-17-4769-2013

Bloomfield JP, Marchant BP, Bricker SH, Morgan RB (2015) Regional analysis of groundwater droughts using hydrograph classification. Hydrol Earth Syst Sci 19(10):4327–4344. https://doi.org/10.5194/hess-19-4327-2015

Bobylev N (2009) Mainstreaming sustainable development into a city's Master plan: A case of Urban Underground Space use. Land use policy 26(4):1128–1137. https://doi.org/10.1016/j.landusepol.2009.02.003

Bobylev N (2016) Transitions to a High Density Urban Underground Space. Procedia Eng 165:184–192. https://doi.org/10.1016/j.proeng.2016.11.750

Bonomi T (1999) Groundwater level evolution in the Milan area: Natural and human issues. IAHS-AISH Publ (259):195–202

Bonomi T (2009) Database development and 3D modeling of textural variations in heterogeneous, unconsolidated aquifer media: Application to the Milan plain. Comput Geosci 35(1):134–145. https://doi.org/10.1016/j.cageo.2007.09.006

Bonomi T, Cavallin A, De Amicis M, Rizzi S, Tizzone R, Trefiletti P (1998) Evoluzione della dinamica piezometrica nell'area milanese in funzione di alcuni aspetti socio-economici [Evolution of the piezometric dynamics in the Milan area as a function of some socio-economic aspects]. In: Atti della Giornata Mondiale dell'Acqua" Acque Sotterranee: Risorsa Invisibile". pp 9–17

Bonomi T, Del Rosso F, Fumagalli L, Canepa P (2010) Assessment of groundwater availability in the Milan Province aquifers. Mem Descr della Cart Geol d'Italia 90:31–40

Bonomi T, Fumagalli L, Dotti N (2009) Fenomeno di inquinamento da solventi in acque sotterranee sfruttate ad uso potabile nel nord-ovest della provincia di Milano [Phenomenon of solvent pollution in groundwater exploited for drinking use in the north-west of Milan province] G. Geol. Appl. 12:43–59

Bonomi T, Fumagalli L, Rotiroti M, Bellani A, Cavallin A (2014) The hydrogeological well database TANGRAM©: a tool for data processing to support groundwater assessment. Acque Sotter - Ital J Groundw 3(2). https://doi.org/10.7343/as-072-14-0098

Cavallin A, Bonomi T (1997) Application of a hydrogeological model to analyze and manage groundwater processes in the urban environment: a case study in the Milan area, Italy

Chae GT, Yun ST, Kim DS, Kim KH, Joo Y (2010) Time-series analysis of three years of groundwater level data (Seoul, South Korea) to characterize urban groundwater recharge. Q J Eng Geol Hydrogeol 43(1):117–127. https://doi.org/10.1144/1470-9236/07-056

Chaudhuri S, Ale S (2013) Characterization of groundwater resources in the Trinity and Woodbine aquifers in Texas. Sci Total Environ 452–453:333–348. https://doi.org/10.1016/j.scitotenv.2013.02.081

Chaudhuri S, Ale S (2014) Long-term (1930-2010) trends in groundwater levels in Texas: Influences of soils, landcover and water use. Sci Total Environ 490:379–390. https://doi.org/10.1016/j.scitotenv.2014.05.013

Cleveland RB, Cleveland WS, McRae JE, Terpenning I (1990) STL: A seasonal-trend decomposition. J Off Stat 6(1):3–73

Colombo L, Gattinoni P, Scesi L (2018) Stochastic modelling of groundwater flow for hazard assessment along the underground infrastructures in Milan (northern Italy). Tunn Undergr Sp Technol 79(May):110–120. https://doi.org/10.1016/j.tust.2018.05.007

de Brito Neto RT, Santos CAG, Mulligan K, Barbato L (2016) Spatial and temporal water-level variations in the Texas portion of the Ogallala Aquifer. Nat Hazards 80(1):351–365. https://doi.org/10.1007/s11069-015-1971-8

De Caro M, Crosta GB, Previati A (2020) Modelling the interference of underground structures with groundwater flow and remedial solutions in Milan. Eng Geol 272(May):105652. https://doi.org/10.1016/j.enggeo.2020.105652

De Luca DA, Destefanis E, Forno MG, Lasagna M, Masciocco L (2014) The genesis and the hydrogeological features of the Turin Po Plain fontanili, typical lowland springs in Northern Italy. Bull Eng Geol Environ 73(2):409–427. https://doi.org/10.1007/s10064-013-0527-y

Dinpashoh Y, Mirabbasi R, Jhajharia D, Abianeh HZ, Mostafaeipour A (2014) Effect of Short-Term and Long-Term Persistence on Identification of Temporal Trends. J Hydrol Eng 19(3):617–625. https://doi.org/10.1061/(asce)he.1943-5584.0000819

Ducci D, Sellerino M (2015) Groundwater Mass Balance in Urbanized Areas Estimated by a Groundwater Flow Model Based on a 3D Hydrostratigraphical Model: the Case Study of the Eastern Plain of Naples (Italy). Water Resour Manag 29(12):4319–4333. https://doi.org/10.1007/s11269-015-1062-3

Filimonau V, Barth JAC (2016) From Global to Local and Vice Versa: On the

Importance of the ‘Globalization’ Agenda in Continental Groundwater Research and Policy-Making. Environ Manage 58(3):491–503. https://doi.org/10.1007/s00267-016-0722-2

Frollini E, Preziosi E, Calace N, Guerra M, Guyennon N, Marcaccio M, Menichetti S, Romano E, Ghergo S (2021) Groundwater quality trend and trend reversal assessment in the European Water Framework Directive context: an example with nitrates in Italy. Environ Sci Pollut Res. https://doi.org/10.1007/s11356-020-11998-0

García-Gil A, Epting J, Ayora C, Garrido E, Vázquez-Suñé E, Huggenberger P, Gimenez AC (2016) A reactive transport model for the quantification of risks induced by groundwater heat pump systems in urban aquifers. J Hydrol 542:719–730. https://doi.org/10.1016/j.jhydrol.2016.09.042

García-Gil A, Vázquez-Suñe E, Schneider EG, Sánchez-Navarro JÁ, Mateo-Lázaro J (2015) Relaxation factor for geothermal use development - Criteria for a more fair and sustainable geothermal use of shallow energy resources. Geothermics 56:128–137. https://doi.org/10.1016/j.geothermics.2015.04.003

Gattinoni P, Scesi L (2017) The groundwater rise in the urban area of Milan (Italy) and its interactions with underground structures and infrastructures. Tunn Undergr Sp Technol 62:103–114. https://doi.org/10.1016/j.tust.2016.12.001

George DJ (1992) Rising groundwater: a problem of development in some urban areas of the Middle East. In: Geohazards. Springer, pp 171–182

Goovaerts P (1997) Geostatistics for natural resources evaluation. Oxford University Press on Demand

Hayashi T, Tokunaga T, Aichi M, Shimada J, Taniguchi M (2009) Effects of human activities and urbanization on groundwater environments: An example from the aquifer system of Tokyo and the surrounding area. Sci Total Environ 407(9):3165–3172. https://doi.org/10.1016/j.scitotenv.2008.07.012

Hernández MA, González N, Chilton J (1997) Impact of rising piezometric levels on Greater Buenos Aires due to partial changing of water services infrastructure

Hirsch RM, Slack JR, Smith RA (1982) Techniques of trend analysis for monthly water quality data. Water Resour Res 18(1):107–121

Isaaks EH, Srivastava RM (1989). An introduction to applied geostatistics. Oxford Univ Press New York

Istat (2011) L'italia del censimento. Struttura demografica e processo di rilevazione, Lombardia [Italy in the census. Demographic structure and survey process, Lombardy]

Janssen M, Charalabidis Y, Zuiderwijk A (2012) Benefits, Adoption Barriers and Myths of Open Data and Open Government. Inf Syst Manag 29(4):258–268. https://doi.org/10.1080/10580530.2012.716740

Judd AG (1980) The use of cluster analysis in the derivation of geotechnical classifications. Bull Assoc Eng Geol 17(4):193–211

Kendall MG (1948) Rank correlation methods.

Kitanidis PK (1997) Introduction to geostatistics: applications in hydrogeology. Cambridge university press

Kotchoni DOV, Vouillamoz JM, Lawson FMA, Adjomayi P, Boukari M, Taylor RG (2019) Relationships between rainfall and groundwater recharge in seasonally humid Benin: a comparative analysis of long-term hydrographs in sedimentary and crystalline aquifers. Hydrogeol J 27(2):447–457. https://doi.org/10.1007/s10040-018-1806-2

Koziatek O, Dragićević S (2017) iCity 3D: A geosimualtion method and tool for three-dimensional modeling of vertical urban development. Landsc Urban Plan 167(June):356–367. https://doi.org/10.1016/j.landurbplan.2017.06.021

Kumar S, Merwade V, Kam J, Thurner K (2009) Streamflow trends in Indiana: Effects of long term persistence, precipitation and subsurface drains. J Hydrol 374(1–2):171–183. https://doi.org/10.1016/j.jhydrol.2009.06.012

Lamé A (2013) Modélisation hydrogéologique des aquifères de Paris et impacts des aménagements du sous-sol sur les écoulements souterrains [Hydrogeological modeling of the Paris aquifers and impacts of subsoil development on underground flows]

Lasagna M, Mancini S, De Luca DA (2020) Groundwater hydrodynamic behaviours based on water table levels to identify natural and anthropic controlling factors in the Piedmont Plain (Italy). Sci Total Environ 716:137051. https://doi.org/10.1016/j.scitotenv.2020.137051

Li F, Feng P, Zhang W, Zhang T (2013a) An Integrated Groundwater Management Mode Based on Control Indexes of Groundwater Quantity and Level. Water Resour Manag 27(9):3273–3292. https://doi.org/10.1007/s11269-013-0346-8

Li HQ, Parriaux A, Thalmann P, Li XZ (2013b) An integrated planning concept for the emerging underground urbanism: Deep City Method Part 1 concept, process and application. Tunn Undergr Sp Technol 38:559–568. https://doi.org/10.1016/j.tust.2013.04.010

Li HQ, Li X, Parriaux A, Thalmann P (2013c) An integrated planning concept for the emerging underground urbanism: Deep City Method Part 2 case study for resource supply and project valuation. Tunn Undergr Sp Technol 38:569–580. https://doi.org/10.1016/j.tust.2013.04.009

Lotti F, Borsi I, Guastaldi E, Barbagli A, Basile P, Favaro L, Mallia A, Xuereb R, Schembri M, Mamo JA, Sapiano M (2021) Numerically enhanced conceptual modelling (NECoM) applied to the Malta Mean Sea Level Aquifer. Hydrogeol J 29(4):1517–1537. https://doi.org/10.1007/s10040-021-02330-2

Mann HB (1945) Nonparametric tests against trend. Econom J Econom Soc :245–259

Meggiorin M, Passadore G, Bertoldo S, Sottani A, Rinaldo A (2021) Techical report

Assessing the long-term sustainability of the groundwater resources in the Bacchiglione basin (Veneto , Italy) with the Mann – Kendall test: suggestions for higher reliability. :35–48. https://doi.org/10.7343/as-2021-499

Milan Metropolitan City (2019) Documento di piano Milano 2030 Visione, Costruzione, Strategie, Spazi [Milan 2030 plan document Vision, Construction, Strategies, Spaces]

Moritz S, Bartz-Beielstein T (2017) imputeTS: Time series missing value imputation in R. R J 9(1):207–218. https://doi.org/10.32614/rj-2017-009

Mudd GM, Deletic A, Fletcher TD, Wendelborn A (2004) A review of urban groundwater in Melbourne: Considerations for WSUD. In: WSUD 2004: Cities as Catchments; International Conference on Water Sensitive Urban Design, Proceedings of. Engineers Australia, p 428

Naranjo-Fernández N, Guardiola-Albert C, Aguilera H, Serrano-Hidalgo C, Montero-González E (2020) Clustering groundwater level time series of the exploited almonte-marismas aquifer in southwest Spain. Water (Switzerland) 12(4). https://doi.org/10.3390/W12041063

Neto DC, Chang HK, van Genuchten MT (2016) A Mathematical View of Water Table Fluctuations in a Shallow Aquifer in Brazil. Groundwater 54(1):82–91. https://doi.org/10.1111/gwat.12329

Obergfell C, Bakker M, Zaadnoordijk WJ, Maas K (2013) Deriving hydrogeological parameters through time series analysis of groundwater head fluctuations around well fields. Hydrogeol J 21(5):987–999 https://doi.org/10.1007/s10040-013-0973-4

Parriaux A, Blunier P, Maire P, Tacher L (2007) The DEEP CITY Project: A Global Concept for a Sustainable Urban Underground Management. 11th ACUUS Int Conf Sp Expand Front Athens, Greece :255–260

Pathak AA, Dodamani BM (2019) Trend Analysis of Groundwater Levels and

Assessment of Regional Groundwater Drought: Ghataprabha River Basin, India. Nat Resour Res 28(3):631–643. https://doi.org/10.1007/s11053-018-9417-0

Patle GT, Singh DK, Sarangi A, Rai A, Khanna M, Sahoo RN (2015) Time series analysis of groundwater levels and projection of future trend. J Geol Soc India 85(2):232–242

Peterson TJ, Western AW, Cheng X (2018) The good, the bad and the outliers: Automated detection of errors and outliers from groundwater hydrographs. Hydrogeol J 26(2):371–380 https://doi.org/10.1007/s10040-017-1660-7

Pettitt AN (1979) A non-parametric approach to the change-point problem. J R Stat Soc Ser C (Applied Stat 28(2):126–135

Pollicino LC, Colombo L, Alberti L, Masetti M (2021) PCE point source apportionment using a GIS-based statistical technique combined with stochastic modelling. Sci Total Environ 750:142366. https://doi.org/10.1016/j.scitotenv.2020.142366

Pollicino LC, Masetti M, Stevenazzi S, Colombo L, Alberti L (2019) Spatial statistical assessment of groundwater PCE (tetrachloroethylene) diffuse contamination in urban areas. Water (Switzerland) 11(6). https://doi.org/10.3390/w11061211

Previati A, Crosta GB (2021a) Regional-scale assessment of the thermal potential in a shallow alluvial aquifer system in the Po plain (northern Italy). Geothermics 90. https://doi.org/10.1016/j.geothermics.2020.101999

Previati A, Crosta GB (2021b) Characterization of the subsurface urban heat island and its sources in the Milan city area, Italy. Hydrogeol J 29(7):2487–2500. https://doi.org/10.1007/s10040-021-02387-z

Pulighe G, Lupia F (2019) Multitemporal geospatial evaluation of urban agriculture and (non)-sustainable food self-provisioning in Milan, Italy. Sustain 11(7). https://doi.org/10.3390/su11071846

R Core Team (2021) R: A language and environment for statistical computing

Regione Lombardia (2016) Piano di Tutela ed Uso delle Acque (PTUA) [Water Protection and Use Plan (PTUA)]

Regione Lombardia (2021a) Open Data Regione Lombardia https://dati.lombardia.it/ (Accessed on 15 July 2021)

Regione Lombardia (2021b) Geoportal of the Lombardy Region, Italy http://www.geoportale.regione.lombardia.it/ (Accessed on 1 June 2021)

Regione Lombardia & ENI Divisione AGIP (2002) Geologia degli acquiferi Padani della Regione Lombardia [Geology of the Padan aquifers of the Lombardy Region]

Rinderer M, van Meerveld HJ, McGlynn BL (2019) From Points to Patterns: Using Groundwater Time Series Clustering to Investigate Subsurface Hydrological Connectivity and Runoff Source Area Dynamics. Water Resour Res 55(7):5784–5806. https://doi.org/10.1029/2018WR023886

Sartirana D, Rotiroti M, Zanotti C, Bonomi T, Fumagalli L, De Amicis M (2020) A 3D geodatabase for urban underground infrastructures: implementation and application to groundwater management in Milan metropolitan area. ISPRS Int J Geo-Information 9(10). https://doi.org/10.3390/ijgi9100609

Scanlon BR, Reedy RC, Stonestrom DA, Prudic DE, Dennehy KF (2005) Impact of land use and land cover change on groundwater recharge and quality in the southwestern US. Glob Chang Biol 11(10):1577–1593. https://doi.org/10.1111/j.1365-2486.2005.01026.x

Sen PK (1968) Estimates of the regression coefficient based on Kendall's tau. J Am Stat Assoc 63(324):1379–1389

Singh A, Shekhar C, Jeyaseelan SAT (2015) Spatio – temporal analysis of groundwater resources in Jalandhar district of Punjab state , India. Sustain Water Resour Manag 1(3):293–304. https://doi.org/10.1007/s40899-015-0022-7

Sottani A, Meggiorin M, Ribeiro L, Rinaldo A (2020) Comparison of two methods for optimizing existing groundwater monitoring networks: application to the

Bacchiglione Basin, Italy. :8759

Sterling R, Admiraal H, Bobylev N, Parker H, Godard J-P, Vähäaho I, Rogers CDF, Shi X, Hanamura T (2012) Sustainability issues for underground space in urban areas. Proc Inst Civ Eng Des Plan 165(4):241–254

Stevenazzi S, Masetti M, Beretta GP (2017) Groundwater vulnerability assessment: from overlay methods to statistical methods in the Lombardy Plain area. Acque Sotter - Ital J Groundw 6(2). https://doi.org/10.7343/as-2017-276

Tabari H, Nikbakht J, Shifteh Some'e B (2012) Investigation of groundwater level fluctuations in the north of Iran. Environ Earth Sci 66(1):231–243. https://doi.org/10.1007/s12665-011-1229-z

Tamburini A, Menichetti M (2020) Groundwater circulation in fractured and karstic aquifers of the Umbria-Marche Apennine. Water (Switzerland) 12(4). https://doi.org/10.3390/W12041039

Triki I, Trabelsi N, Hentati I, Zairi M (2014) Groundwater levels time series sensitivity to pluviometry and air temperature: A geostatistical approach to Sfax region, Tunisia. Environ Monit Assess 186(3):1593–1608. https://doi.org/10.1007/s10661-013-3477-8

Un-Habitat (2012) State of the World's Cities 2008/9: Harmonious Cities. Routledge

Vähäaho I (2016) An introduction to the development for urban underground space in Helsinki. Tunn Undergr Sp Technol 55:324–328. https://doi.org/10.1016/j.tust.2015.10.001

Vázquez-Suñé E, Sánchez-Vila X, Carrera J (2005) Introductory review of specific factors influencing urban groundwater, an emerging branch of hydrogeology, with reference to Barcelona, Spain. Hydrogeol J 13(3):522–533. https://doi.org/10.1007/s10040-004-0360-2

Vázquez-Suñé E, Sánchez-Vila X, Carrera J, Marizza M, Arandes R (1997) Rising groundwater levels in Barcelona: evolution and effects on urban structures. In:

Groundwater in the Urban Environment. pp 267–271

Ward Jr JH (1963) Hierarchical grouping to optimize an objective function. J Am Stat Assoc 58(301):236–244

Webster R, Oliver MA (2001) Cross-correlation, co-regionalization, and co-kriging. Geostatistics Environ Sci Chichester, UK, John Wiley Sons

Wilkinson W (1985) Rising groundwater levels in London and possible effects on engineering structures. Proc 18th Congr Int Assoc Hydrogeol Cambridge :145–157

Electronic Supplementary Material

Data-driven decision management of urban underground infrastructure through groundwater-level time-series cluster analysis: the case of Milan (Italy)

Davide Sartirana[1]*, Marco Rotiroti[1], Tullia Bonomi[1], Mattia De Amicis[1], Veronica Nava[1], Letizia Fumagalli[1] and Chiara Zanotti[1]

[1]Department of Earth and Environmental Sciences, University of Milano-Bicocca, Piazza Della Scienza 1, 20126 Milan, Italy

*corresponding author: d.sartirana1@campus.unimib.it

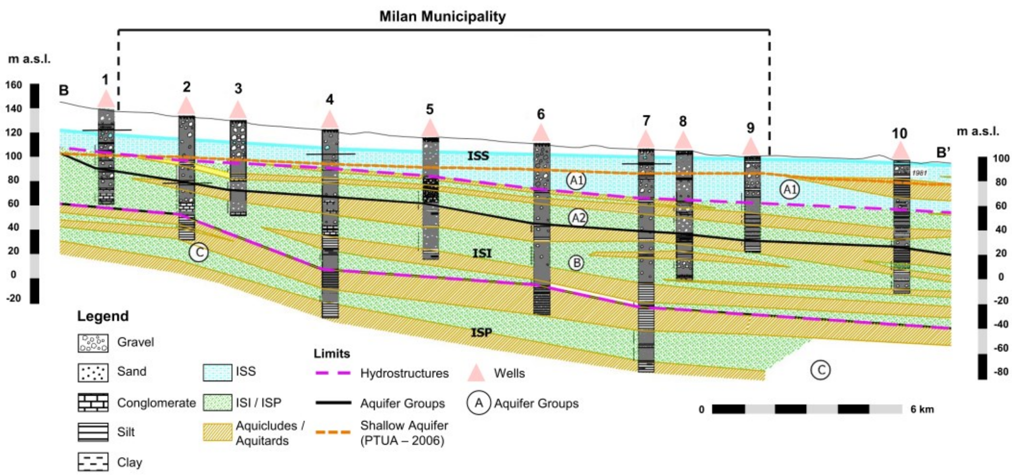

Fig. S6.1. Geological profile of N-S cross section BB' of the study area, modified from Regione Lombardia (2016). The aquifer group classification from Regione Lombardia & ENI (2002) is also provided. For its location see Fig. 6.1b of the main article.

Table S6.1. List and main features of the underground car parks located in the study area. Modified from Sartirana et al., (2020). MA stands for management area.

Name	Bottom (m a.s.l.)	Depth (m)	Area × 10^3 (m^2)	Volume × 10^3 (m^3)	Floors	MA
Accursio	115.6	14	4.55	63.7	4	1
Alghero	122.72	5	2.12	10.6	1	1
Balla	125.58	8	2.65	21.2	2	1
Betti	123.7	8	5.69	45.52	2	1
Bicocca P7	122.1	11	5.67	62.37	3	1
Bicocca P8	125.5	8	6.67	53.36	2	1
Capecelatro/Pessano	116.35	8	5.05	40.4	2	1
Carafa/Conte Verde	120.2	11	3.3	36.3	3	1
Caroli/Ricordo	121.53	8	3.77	30.16	2	1
Cechov	122.54	8	2.92	23.36	2	1
Cervi/Assietta	130.11	8	8.05	64.4	2	1
Cilea 100	126.83	8	4.37	34.96	2	1
De Lemene	120.6	8	2.29	18.32	2	1
Don Calabria	116.85	8	6.4	51.2	2	1
Emo	116.23	11	2.76	30.36	3	1
Gandhi/Perlasca	128.2	8	4.31	34.48	2	1
Govone	110.19	17	1.6	27.2	5	1
Grado	118.77	8	1.68	13.44	2	1
Graf/De Pisis Ovest	128.9	8	5.94	47.52	2	1
Lampugnano	119.85	8	3.78	30.24	2	1

Name	Bottom (m a.s.l.)	Depth (m)	Area × 10^3 (m^2)	Volume × 10^3 (m^3)	Floors	MA
Marmolada	124.4	11	3.36	36.96	3	1
Monte Baldo	117.22	8	3.1	24.8	2	1
Muttoni/Quarenghi	124.8	8	3.99	31.92	2	1
Ojetti	124.16	8	7.03	56.24	2	1
Osculati/Camerino	125.14	11	0.45	4.95	3	1
Populonia/Valassina	117.68	11	8.68	95.48	3	1
Prinetti/Vida	114.2	11	3.25	35.75	3	1
Riccione	120.95	11	1.91	21.01	3	1
Salmoiraghi/Stuparich	115.37	11	1.76	19.36	3	1
San Giusto/Val Poschiavina	116.7	8	5.56	44.48	2	1
Sarca/Nota	123.99	8	4.4	35.2	2	1
Suzzani	129.85	8	3.56	28.48	2	1
Toce/Boltraffio	115.33	11	4.55	50.05	3	1
Trechi	132.14	8	3.97	31.76	2	1
Veglia/Caserta	120.9	8	22.28	178.24	2	1
Adda	102	20	0.81	16.2	6	2
Ampere/Compagni	104.5	14	2	28	4	2
Arduino	112.9	11	5.67	62.37	3	2
Aretusa Nord	110.75	11	4.39	48.29	3	2
Bazzini	102.2	17	1.49	25.33	5	2
Benedetto Marcello	106.53	14	3.05	42.7	4	2

Name	**Bottom (m a.s.l.)**	**Depth (m)**	**Area × 10^3 (m^2)**	**Volume × 10^3 (m^3)**	**Floors**	**MA**
Carducci Olona	101.2	17	3.42	58.14	5	2
Caterina da Forlì	108.97	11	10.35	113.85	3	2
Cesariano	111.5	11	4.54	49.94	3	2
Ciclamini/Margherite	111.5	8	3	24	2	2
Correggio Est	107.81	14	1.03	14.42	4	2
Correggio Ovest	106.95	14	2.75	38.5	4	2
Costa/Loreto	106.9	14	1.97	27.58	4	2
Dateo Nord	99.8	17	1.94	32.98	5	2
Dateo Sud	102.8	14	2.11	29.54	4	2
Donati/Redaelli	110.01	8	9.53	76.24	2	2
Etiopia	111.66	8	0.5	4	2	2
Fratelli Bandiera	103.5	14	2.81	39.34	4	2
Giotto	107.05	14	4.49	62.86	4	2
Giulio Cesare	109.2	14	4.42	61.88	4	2
Gramsci	110.2	14	4.3	60.2	4	2
Leoncavallo	108	14	2.54	35.56	4	2
Leone XIII	115.35	8	7.4	59.2	2	2
Lucerna	113.39	8	4	32	2	2
Majno	101.86	17	2.05	34.85	5	2
Manuzio	103.56	17	2.27	38.59	5	2
Mascagni	102.2	14	4.63	64.82	4	2

Name	Bottom (m a.s.l.)	Depth (m)	Area × 10³ (m²)	Volume × 10³ (m³)	Floors	MA
Meda	102.85	17	2.1	35.7	5	2
Moisè Loria/Stromboli	101.5	17	3	51	5	2
Moscova	107	14	7.32	102.48	4	2
Murani	101.6	14	3.38	47.32	4	2
Novelli	103.2	14	1.17	16.38	4	2
Numa Pompilio	100.7	17	4.07	69.19	5	2
Ozanam	105.63	14	4.6	64.4	4	2
Piazza Diaz	108.5	11	2.4	26.4	3	2
Po	105.2	14	6.87	96.18	4	2
Puccini	101.33	20	1.68	33.6	6	2
Quinto Alpini	106.47	14	1.66	23.24	4	2
Rio de Janeiro	105.7	11	2.27	24.97	3	2
Rio de Janeiro/Andrea del Sarto	105.7	11	2.64	29.04	3	2
Risorgimento nord	96.9	20	1.43	28.6	6	2
Risorgimento Sud	102.8	14	2.11	29.54	4	2
Romagnoli/Bertieri	107.34	11	2.11	23.21	3	2
Rossetti	115.2	8	2.88	23.04	2	2
Sammartini/Lunigiana	112.3	11	3.49	38.39	3	2
Sant'Ambrogio	102	17	7.41	125.97	5	2

Name	Bottom (m a.s.l.)	Depth (m)	Area × 10^3 (m^2)	Volume × 10^3 (m^3)	Floors	MA
Savona Tolstoj	110.67	5	1.08	5.4	1	2
Solera Mantegazza	107.85	14	2.92	40.88	4	2
Tommaseo	103.89	17	3.15	53.55	5	2
Viganò	110.61	14	2.19	30.66	4	2
Vittor Pisani	107.58	14	8.78	122.92	4	2
Volontari	108.8	14	1.3	18.2	4	2
Washington/Piemonte	100.35	20	3.02	60.4	6	2
XXV Aprile	105.2	17	5.07	86.19	5	2
Avezzana	98.07	11	2.04	22.44	3	3
Bacchiglione/Scheiwiller	99.9	11	3.35	36.85	3	3
Balilla/Zamenhof	105.66	8	2.4	19.2	2	3
Bellosio/Facchinetti	102.46	8	3.71	29.68	2	3
Bibbiena/Centro Civico	105.65	8	3.86	30.88	2	3
Bordighera/Alzaia Naviglio Pavese	102.56	11	3.32	36.52	3	3
Cardinal Ferrari	101.53	14	2.24	31.36	4	3
Cascina Bianca	106.2	5	7.88	39.4	1	3
Ciceri Visconti	101.47	11	4.16	45.76	3	3
Conca del Naviglio	101.92	14	2.43	34.02	4	3
Dalmazia	101.75	8	2.09	16.72	2	3

Name	Bottom (m a.s.l.)	Depth (m)	Area × 10^3 (m^2)	Volume × 10^3 (m^3)	Floors	MA
De Nicola/San Vigilio	106.46	5	4.78	23.9	1	3
De Pretis/San Vigilio	106.4	5	4.52	22.6	1	3
De Pretis/Voltri	106.89	5	4.73	23.65	1	3
Erculea	100.91	17	1.3	22.1	5	3
Feltrinelli	101.83	5	8.3	41.5	1	3
Giulio Romano	96.45	17	2.48	42.16	5	3
Isimbardi	102.9	8	2.64	21.12	2	3
Maffei	100.9	14	3.41	47.74	4	3
Manusardi	100.25	14	2.12	29.68	4	3
Menotti Serrati	98.94	5	7.5	37.5	1	3
Monte Popera/Piana	101.12	5	2.8	14	1	3
Monte Velino/Cadibona	102.83	8	7.05	56.4	2	3
Montemartini/Fabio Massimo	101.38	8	7.16	57.28	2	3
Pavia	99.84	14	3.38	47.32	4	3
Sabotino	96.91	17	2.47	41.99	5	3
San Barnaba	105.4	11	7.45	81.95	3	3
Spaventa/Meda	104.44	8	5.46	43.68	2	3
Trani/Malipiero/Mecenate	100.1	8	5.92	47.36	2	3
Vittadini	99.23	14	3.63	50.82	4	3

Name	Bottom (m a.s.l.)	Depth (m)	Area × 10^3 (m^2)	Volume × 10^3 (m^3)	Floors	MA
Betulle Est	118.01	5	4.6	23	1	4
Betulle Ovest	118.2	5	2.49	12.45	1	4
Broggini	119.07	5	2.17	10.85	1	4
Nikolajevka	113.4	8	4.64	37.12	2	4
Silla	131.3	5	5.82	29.1	1	4
Valsesia Est	116.45	5	3.42	17.1	1	4
Valsesia Ovest	116.6	5	1.96	9.8	1	4
Total parks: 126				5,157		

Time-series reversal points: R Script

#Packages uploading

library(imputeTS) *#to be used for interpolating time-series missing values*

library(utils) *# to export the final list of identified reversal points for each monitoring well (MW)*

#Data loading (.csv format)

db<-read.table("MWs_dataset.csv", header=T, sep=";", dec=",") *#file setting: the first column contains Date; the remaining columns contain MWs time-series; each row contains the MWs observations at a given Date*

```
#Set Date
db$Date<-as.Date(db$Date,format = c("%d/%m/%Y")) # set Date column in Date format


#Interpolating Missing Values
db_notNA<-na_interpolation(db) #Create a new database linearly interpolating missing values


#Reversal Points Identification
results <- NULL #Initialize results
count <- 1
for (i in 1:ncol(db_notNA)){  #for is used to set a cycle, thus iterating the procedure for all the MWs
  sel_db<-(db_notNA[,i]) #select columns
  ts_db<-ts(sel_db, start=2005, frequency=2) #set data as time-series
  stl_db<-stl(ts_db, s.window="periodic") # Decompose a time series into seasonal, trend and irregular components using loess
  trend_db<-stl_db$time.series[,"trend"] #Analyse only the trend component
  shape_smooth <- diff(sign(diff(trend_db, na.pad = T))) #Determine the sign of the difference between successive      couples of data
index_smooth<-which(shape_smooth!=0,arr.ind = T)+1 #Determine the position of reversal points
  results[[count]] <- index_smooth
```

```
  names(results)[[count]] <- names(db_notNA)[i]

  count <- count + 1

  print(results)

}

capture.output(print(results), file = "Identified_ReversalPoints.txt") #Export a .txt file containing all the identified Reversal Points for each MW
```

Table S6.2. Summary of GW reversal points (RPs) for the analysed monitoring wells (MWs) in the study area.

MW	Location	GW Min.	GW Max.	GW Loc. Max.	GW Loc. Min.	No. of RPs
MW1	Downtown	sep-07	mar-12	sep-12	sep-14	6
MW2	East	mar-07	NCI	NCI	mar-18	8
MW3	North	sep-07	sep-11	sep-12	sep-15	4
MW4	North	mar-08	sep-11	sep-12	sep-15	4
MW5	North	sep-07	sep-11	sep-12	mar-15	6
MW6	North	mar-08	sep-11	sep-12	mar-15	4
MW7	South	sep-07	NCI	NCI	sep-14	10
MW8	Downtown	sep-07	sep-11	sep-12	mar-15	7
MW9	East	sep-06	mar-11	mar-12	mar-15	6
MW10	South	mar-07	NCI	NCI	sep-16	7
MW11	East	sep-07	sep-11	sep-12	mar-15	4
MW12	East	sep-06	mar-11	mar-12	sep-15	7
MW13	West	mar-07	mar-11	sep-12	sep-14	4
MW14	East	sep-06	NCI	NCI	mar-14	10

MW	Location	GW Min.	GW Max.	GW Loc. Max.	GW Loc. Min.	No. of RPs
MW15	East	mar-07	sep-11	mar-12	sep-15	8
MW16	South	NCI	NCI	NCI	NCI	8
MW17	South	sep-07	mar-10	mar-12	sep-14	9
MW18	South	mar-07	NCI	NCI	mar-14	8
MW19	North	mar-08	sep-11	sep-12	mar-15	4
MW20	West	mar-07	NCI	NCI	sep-13	10
MW21	South	mar-07	NCI	NCI	sep-14	9
MW22	North	mar-07	sep-11	sep-12	sep-14	6
MW23	Downtown	sep-06	sep-11	sep-12	mar-15	7
MW24	North	sep-07	sep-11	sep-12	mar-15	4
MW25	Downtown	NCI	NCI	NCI	mar-14	8
MW26	Downtown	mar-07	NCI	NCI	sep-14	10
MW27	South	mar-07	NCI	NCI	mar-14	11
MW28	South	mar-07	NCI	NCI	mar-15	11
MW29	North	mar-08	sep-11	sep-12	mar-15	6
MW30	North	mar-07	sep-11	sep-12	mar-15	6
MW31	Downtown	mar-07	NCI	NCI	mar-15	10
MW32	Downtown	mar-07	NCI	NCI	sep-14	6
MW33	East	mar-07	mar-11	mar-12	mar-15	7
MW34	North	mar-08	sep-11	sep-12	mar-15	4
MW35	East	sep-06	mar-11	sep-12	NCI	10
MW36	South	NCI	NCI	NCI	NCI	10

MW	Location	GW Min.	GW Max.	GW Loc. Max.	GW Loc. Min.	No. of RPs
MW37	West	NCI	NCI	NCI	NCI	10
MW38	North	mar-07	NCI	NCI	mar-14	7
MW39	West	sep-06	NCI	NCI	mar-14	10
MW40	West	NCI	NCI	NCI	NCI	8
MW41	North	sep-07	sep-11	sep-12	mar-15	9
MW42	Downtown	mar-07	NCI	NCI	mar-14	7
MW43	West	NCI	NCI	NCI	NCI	13
MW44	East	sep-06	NCI	NCI	sep-14	7
MW45	West	NCI	NCI	NCI	NCI	14
MW46	Downtown	sep-06	sep-09	mar-12	mar-15	8
MW47	East	mar-07	mar-11	mar-12	sep-15	6
MW48	North	sep-07	sep-11	sep-12	mar-15	4
MW49	South	NCI	sep-09	mar-11	mar-15	9
MW50	East	mar-07	mar-11	sep-12	sep-18	6
MW51	Downtown	sep-07	sep-11	sep-12	sep-14	6
MW52	Downtown	sep-07	sep-11	sep-12	sep-14	4
MW53	Downtown	mar-06	mar-11	sep-11	sep-16	6
MW54	North	mar-08	sep-11	sep-12	mar-15	4
MW55	North	sep-07	sep-11	sep-12	sep-15	4
MW56	North	sep-07	sep-11	sep-12	mar-15	6
MW57	East	sep-07	sep-11	mar-12	sep-15	5
MW58	West	sep-07	mar-11	sep-12	sep-14	8

MW	Location	GW Min.	GW Max.	GW Loc. Max.	GW Loc. Min.	No. of RPs
MW59	Downtown	sep-07	mar-11	sep-12	mar-15	8
MW60	Downtown	sep-07	mar-11	sep-12	mar-15	9
MW61	Downtown	sep-07	sep-11	sep-12	sep-15	10
MW62	Downtown	sep-07	sep-11	sep-12	mar-16	6
MW63	East	mar-07	sep-11	mar-12	sep-16	8
MW64	North	mar-08	sep-11	sep-12	mar-15	4
MW65	North	sep-07	sep-11	mar-12	mar-15	6
MW66	South	sep-07	mar-12	mar-13	sep-14	8
MW67	Downtown	sep-07	sep-11	sep-12	mar-15	7
MW68	Downtown	sep-07	sep-11	sep-12	mar-15	6
MW69	Downtown	sep-07	sep-11	sep-12	mar-16	10
MW70	South	sep-07	mar-12	sep-12	mar-15	8
MW71	South	sep-07	sep-11	mar-12	sep-15	6
MW72	South	mar-07	NCI	NCI	sep-15	9
MW73	Downtown	mar-07	NCI	NCI	mar-15	6
MW74	Downtown	mar-07	sep-09	sep-10	mar-15	6
MW75	West	sep-06	NCI	NCI	sep-15	14
MW76	North	mar-07	sep-11	sep-12	mar-15	4
MW77	Downtown	mar-07	sep-11	sep-12	mar-15	6
MW78	Downtown	sep-07	sep-11	sep-12	mar-15	6
MW79	Downtown	sep-07	sep-11	sep-12	sep-14	6
MW80	West	sep-07	mar-11	sep-12	mar-15	8

MW	Location	GW Min.	GW Max.	GW Loc. Max.	GW Loc. Min.	No. of RPs
MW81	West	mar-08	sep-11	sep-12	mar-14	10
MW82	North	sep-07	sep-11	sep-12	sep-14	4
MW83	North	sep-07	sep-11	sep-12	mar-15	4
MW84	North	mar-08	mar-12	sep-12	mar-15	4
MW85	North	mar-08	mar-12	sep-12	mar-15	6
MW86	Downtown	sep-07	sep-11	sep-12	sep-15	7
MW87	South	mar-07	sep-11	sep-12	sep-15	7
MW88	East	mar-06	NCI	NCI	NCI	10
MW89	North	sep-07	sep-11	sep-12	sep-14	4
MW90	West	mar-06	NCI	NCI	NCI	7
MW91	North	mar-08	sep-11	sep-12	mar-15	4
MW92	North	sep-07	sep-11	sep-12	mar-15	4
MW93	West	mar-06	NCI	NCI	NCI	9
MW94	West	sep-07	mar-11	mar-12	mar-14	6
MW95	North	sep-07	sep-11	sep-12	sep-15	4

*NCI stands for Not Clearly Identifiable.

ESM References

Regione Lombardia (2016) Piano di Tutela ed Uso delle Acque (PTUA) [Water Protection and Use Plan (PTUA)]

Regione Lombardia & ENI Divisione AGIP (2002) Geologia degli acquiferi Padani della Regione Lombardia [Geology of the Padan aquifers of the Lombardy Region]

Sartirana D, Rotiroti M, Zanotti C, Bonomi T, Fumagalli L, De Amicis M (2020) A 3D geodatabase for urban underground infrastructures: implementation and application to groundwater management in Milan metropolitan area. ISPRS Int J Geo-Information 9(10). https://doi.org/10.3390/ijgi9100609

Chapter 7: GW/UIs interactions

Quantifying Groundwater Infiltrations into Subway Lines and Underground Car Parks using MODFLOW-USG

Davide Sartirana[1]*, Chiara Zanotti[1], Marco Rotiroti[1], Mattia De Amicis[1], Mariachiara Caschetto[1], Agnese Redaelli[1], Letizia Fumagalli[1] and Tullia Bonomi[1]

[1]Department of Earth and Environmental Sciences, University of Milano-Bicocca, Piazza Della Scienza 1, 20126 Milan, Italy

*corresponding author: d.sartirana1@campus.unimib.it

This chapter is largely based on the following paper: *Water* **2022**, *14*(24), 4130; https://doi.org/10.3390/w14244130

Keywords: urban hydrogeology; rising groundwater levels; shallow aquifer; 3D geodatabase; horizontal flow barrier; Milan; Italy

Abstract

Urbanization is a worldwide process that recently has culminated in wider use of the subsurface, determining a significant interaction between groundwater and underground infrastructures. This can result in infiltrations, corrosion, and stability issues for the subsurface elements. Numerical models are the most applied tools to manage these situations. Using MODFLOW-USG and combining the use of HFB and DRN packages, this study aimed at simulating underground infrastructures (i.e. subway lines and public car parks) and quantifying their infiltrations. This issue has been deeply investigated to evaluate water inrush during tunnel construction, but problems also occur with regard to the operation of tunnels. The methodology has involved developing a steady-state groundwater flow model, calibrated against a maximum groundwater condition, for the western portion of Milan city (Northern Italy, Lombardy Region). Overall findings pointed out that the most impacted areas are sections of subway tunnels already identified as submerged. This spatial coherence with historical information could act both as validation of the model and a step forward, as infiltrations resulting from an interaction with the water table were quantified. The methodology allowed for the

improvement of the urban conceptual model and could support the stakeholders in adopting proper measures to manage the interactions between groundwater and the underground infrastructures.

7.1. Introduction

Urban hydrogeology is a specific branch of research (Vázquez-Suñé et al. 2005; Epting et al. 2008) that has been constantly developed in recent years as a consequence of rapid urbanization phenomena that have been witnessed in most parts of the world (Arshad and Umar 2020). Considering that 70% of the world population is expected to live in urban areas by 2050 (Un-Habitat 2012), urbanization can be defined as a world-wide process (La Vigna 2022). Thus, it is reasonable to think that in the next few years a huge effort will be allocated to research into urban hydrogeology (Schirmer et al. 2013).

Overexploitation and deterioration of urban water resources act as the main consequences of this rapid urbanization (Calderhead et al. 2012). To put a brake on urban sprawl, a vertical urban development has occurred, determining an augmented use of urban underground (Parriaux et al. 2006; Li et al. 2013a; Li et al. 2013b; Vähäaho 2016; Koziatek and Dragićević 2017). However, the construction of ever-deeper structures (Bobylev 2009) can impact groundwater (GW) with regards to flow, quality, and thermal issues (Attard et al. 2015; La Vigna 2022; Noethen et al. 2022).

With respect to GW flow, different cities around the world have observed rising water table levels, as a consequence of the deindustrialization process, that have generated some interference between GW and underground infrastructures (UIs) such as basements, car parks, and subway lines (Wilkinson 1985; Hernández et al. 1997; Vazquez-sune and Sanchez-vila 1999; Hayashi et al. 2009; Lamé 2013; Ducci and Sellerino 2015; Colombo et al. 2017; Allocca et al. 2021). Numerical GW flow modeling was widely adopted as the main tool to evaluate the barrier effect of UIs to flow patterns, GW budget (Attard et al. 2015), and the possible side effects on the underground elements (i.e. corrosion and stability issues).

Concerning engineering issues, GW inflow into tunnels has been predicted in urban areas by adopting analytical solutions (El Tani 2003), synthetic modeling (Butscher 2012), and steady-state numerical modeling on real cases (Nikvar Hassani et al. 2016; Farhadian et al. 2017) to properly design the tunnel drainage system during the construction phase. In fact, water inrush is a challenging issue to face, causing negative impacts on tunnel stability, generating subsidence damage (Butscher 2012; Xia et al. 2018), heavy financial losses, and losing construction time (Nikvar Hassani et al. 2016; Nikvar Hassani et al. 2018).

At the same time, the problem of damages in operating tunnels, as water seepage or lining cracking, requires consideration (Li et al. 2008; Gao et al. 2019; Guo et al. 2021; Ai et al. 2022). Despite the lower water amounts penetrating inside the UIs over a long period, GW could determine severe issues, such as temporary unusability, which require waterproofing works and lead to economic losses. Thus, quantifying infiltrations could help to assess proper mitigation strategies (Golian et al. 2018), supporting the stakeholders in the complex task of urban GW management. To do so, among the different approaches applied in the literature, GW infiltrations into subsurface elements have been evaluated by modeling the UIs by means of the DRN package (Zaidel et al. 2010; Lagudu et al. 2015; Golian et al. 2018). Recently, a single model layer was developed by Golian et al. 2021 to restore GW levels after tunneling. In this work, an unsealed and a sealed underground tunnel were modeled using RIV and HFB packages, respectively. The latter has been applied in various fields of GW modeling: from coastal areas to model slurry walls containing seawater intrusion (Abd-Elaty et al. 2022; Abd-Elaty and Zelenakova 2022), to geophysical modeling to simulate faults (Chaussard et al. 2014; Medici et al. 2021), to urban contexts in industrial sites (Bonomi et al. 2022), or to evaluate the impact of UIs on GW levels (Bonomi and Bellini 2003; Boukhemacha et al. 2015).

The existence of 3D GDBs, gathering information on underground structures (Di Salvo et al. 2020; Sartirana et al. 2020) and frequently scattered over many institutions and stakeholders (Vázquez-Suñé et al. 2005; Parriaux et al. 2007; Delmastro et al. 2016; Moghadam et al. 2016), could support the adoption of these packages to properly model

UIs. In this way, it should be possible to precisely define their relationship with the water levels, thus improving the urban conceptual model. y

Based on these assumptions, the aim of this study has been to quantify GW infiltrations into different categories of UIs (i.e. subway lines and underground car parks), considering different UI conditions (i.e. intact, saturated, and leaky walls). The methodology that has been applied involves developing a local 3D GW numerical flow model for the western area of Milan metropolitan city (Lombardy, Northern Italy). Through this model, the most critical portions of the subsurface network suffering from GW infiltrations have been evaluated. Interactions with the water table and possible infiltrations in subway line M4 (to be inaugurated in 2023) and two public car parks that are currently under construction were also analyzed.

By means of this model, the stakeholders would be able to design management solutions to secure the infrastructures from being flooded in the future. The model has been realized as steady-state with MODFLOW-USG (Panday et al. 2013) and calibrated using a trial and error approach against a GW maximum condition that was defined in a previous work as documented by Sartirana et al. 2022. HFB and DRN packages have been coupled to model the UIs, reproducing their geometries and volumes through the adoption of grid refinement, contributing to the quantification of GW infiltrations into subsurface elements. In particular, the top and the bottom of the UIs were modeled through the HFB package; to the best of the authors' knowledge, this application of the HFB package could represent an improvement in modeling the UIs. In fact, the relation between GW and the UIs along the vertical sides of a model cell could be thus considered. Moreover, as for Milan city, this is the first time that car parks have been considered in a 3D GW numerical flow model, while being studied for the adoption of GW-level time-series clustering to suggest targeted guidelines for the construction of new underground public car parks (Sartirana et al. 2022).

The methodology presented here could be implemented for other urban realities, serving as a way of managing a documented interaction between GW and the UIs that may lead to a planned subsurface infrastructure development with possibly great potential for an integrated management strategy.

7.2. Urban conceptual model of the study area

The study area covers 100 km² inside the Milan metropolitan area (Fig. 7.1). Human activities have always characterized this area, especially through industrial and agricultural activities that are still conducted in the western and southern areas of Milan (Bonomi et al. 2009; Pulighe and Lupia 2019). The city hosts 1.4 million inhabitants (Istat 2011) and is currently undergoing an important urban transformation (Boscacci et al. 2017). It is located in the middle of the Po Valley, whose hydrogeologic structure has been deeply examined both in the past (Regione Lombardia & ENI Divisione AGIP 2002) and recently (Regione Lombardia 2016). Three main hydrostructures were identified: a shallow hydrostructure (ISS), an intermediate (ISI), and a deep (ISP) hydrostructure. Within the model domain, an ISS has a medium thickness of 40 m with a bottom surface ranging from 100 m above sea level (a.s.l.) (to the North) to about 60 m a.s.l. (to the South). It hosts a shallow aquifer (Fig. 7.2) (i.e. Aquifer Group A1, Regione Lombardia and ENI Divisione AGIP 2002, where all the UIs are located. This aquifer is not exploited for drinking needs. Sands and gravels mainly characterize this hydrostructure. The same lithologies, but with an increasing presence of silty and clayey horizons, constitute the ISI, that mostly corresponds to Aquifer Groups A2 and B of Regione Lombardia and ENI Divisione AGIP 2002. An ISP, having a more uncertain lithological composition, was not modeled within this study.

Industrial needs triggered an extensive GW withdrawal since the early 1960s. Consequently, the water table reached its maximum depth of more than 30 m in the northern part of the city around 1975, thus determining the minimum GW levels due to significant water exploitation (Bonomi et al. 1998; Bonomi 1999). During the same time frame, some UIs (car parks, subway lines M1 and M2) were built, sometimes without proper lining methods, without consideration for a possible future GW level rise. Subsequently, since the beginning of the 1990s, the decommissioning of many industrial sites, mainly located in the northern sector of the city, generated a rise in GW level, determining flooding episodes for these oldest and shallowest subway lines and for some underground car parks built starting from the middle of the 1980s (Gattinoni and Scesi 2017; De Caro et al. 2020). Consequently, the most recent and deepest subway lines (M3, M4 to be inaugurated in 2023, and M5) have been designed with lining systems. As for underground car parks, 126 public car parks are now listed in the city (Sartirana et al. 2022): 65 out of 126 are located in the model domain. The construction of two new underground car parks (Fig. 7.1b) is currently taking place close to the Gelsomini and Frattini stations of subway line M4. These car parks are named Brasilia (placed just northward of the stations) and Scalabrini (to the South of the stations), respectively; both have been designed to be two floors deep (i.e. 8 m depth as calculated by Sartirana et al. 2020).

The water table rise occurred differently among different areas of the town, with a maximum rise of about 10–15 m in the North, and a more dampened effect in the other sectors (Sartirana et al. 2022). Particularly, a low significant rising trend was evidenced in the West and South, respectively, due to local geological conditions and the hydraulic gradient that constrains the water table close to the ground level, thus reducing the water table oscillations.

In the downtown area, an increasing presence of open-loop GW heat pumps (GWHPs) for geothermal needs (Fig. 7.1b), together with the presence of a huge number of UIs, could induce an anthropogenic control on water table rising; due to extraction and injection wells systems, the water withdrawn is usually returned to the shallow aquifer, thus determining a non-consumptive use of the resource (García-Gil et al. 2016). These systems sometimes discharge exploited water to surface water bodies to control the GW rise.

Public-supply well fields withdraw water used for drinking needs, and have screens to tap the semi-confined and confined aquifer units. A total of 261 wells, belonging to 13 well fields, are located inside the considered domain.

The construction of new underground car parks takes place in the framework of the adoption of the Plan of Government for the Territory (PGT) (Milan Metropolitan City

2019), that regulates further subsurface occupation as a measure against excessive soil consumption. In this context, numerical modeling, possibly combined with the application of other techniques aimed at better understanding the urban conceptual model (Sartirana et al. 2022), could represent a valid tool to coordinate urban underground development, thus supporting stakeholders in their decision-making process.

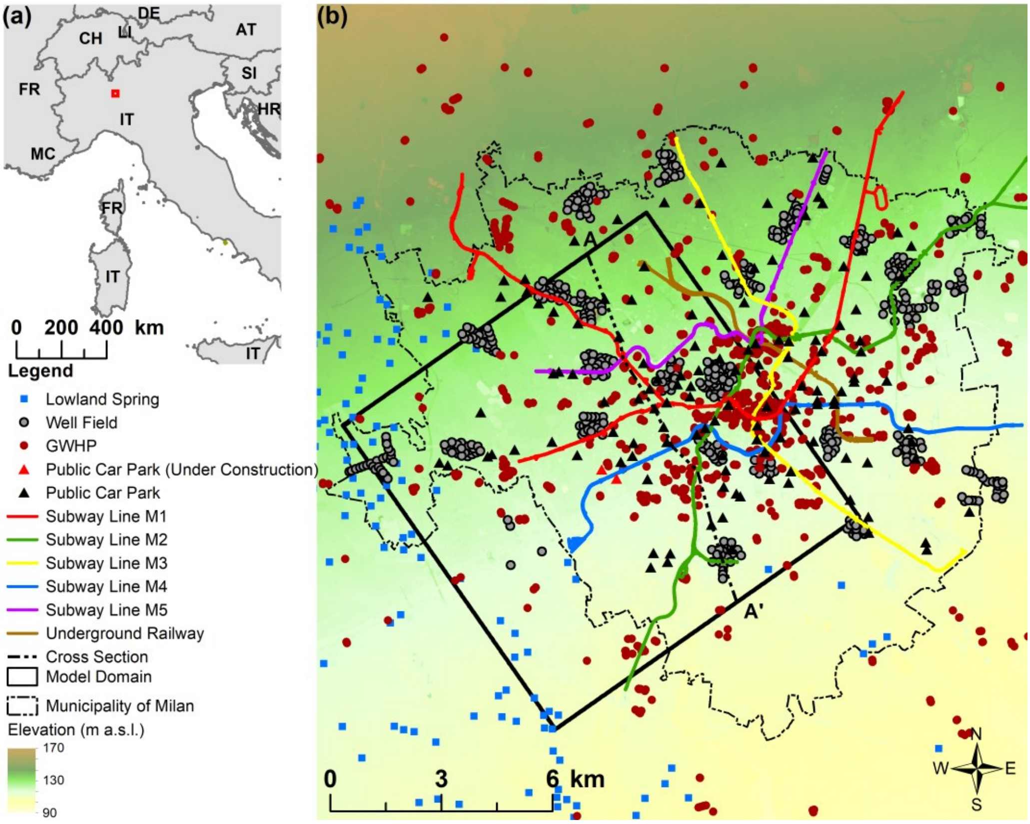

Fig. 7.1. a) Geographical setting of the study area; **b)** main hydrogeologic features (lowland springs) and anthropogenic elements: subway line network, underground public car parks, well fields and GW heat pumps (GWHPs); line AA' points out the location of the cross-section that is visible in Fig. 7.2. Color coding for the subway lines respects the color coding used by the subway managing company. Public car parks have been represented as triangles to differentiate them from wells. (Image readapted from Sartirana et al. 2022).

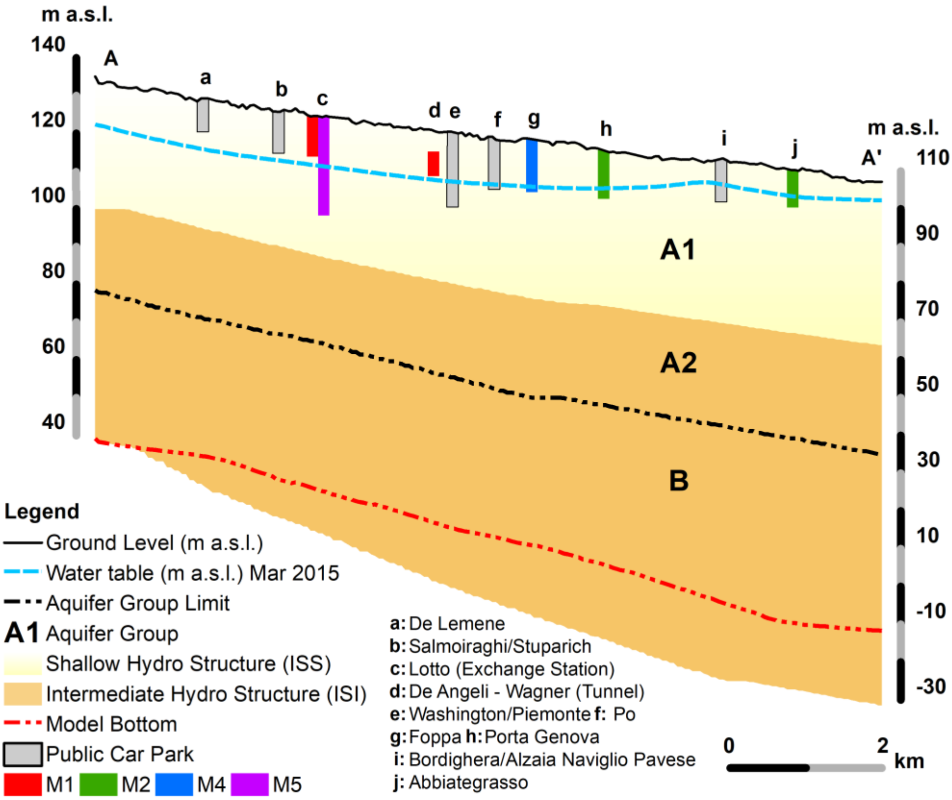

Fig. 7.2. Hydrogeologic schematic cross sections AA' (N-S) of the study area, showing the location of some UIs and their relation with the GW condition of Mar 2015 (Sartirana et al., 2022). For their location in map please refer to Fig. 7.1.

7.3. Materials and Methods

The numerical model was built considering an already existing urban conceptual model (Sartirana et al. 2022), integrating its contents, when possible, with Open Data information (Regione Lombardia 2021a). The core of the methodology was the modelling of the UIs (See section 7.3.1.2.1 "Underground infrastructures modelling") to evaluate GW infiltrations. Different scenarios of conductance were realized to quantify infiltrations simulating different wall conditions; the results have been examined in order to discuss possible strategies to manage GW/UIs interactions.

7.3.1. Numerical Model

A steady-state numerical flow model was developed using MODFLOW-USG (Panday et al. 2013), and Groundwater Vistas 8 (Rumbaugh and Rumbaugh 2020) was used as the graphical user interface.

7.3.1.1. Grid Discretization

The model grid (Fig. 7.3) was composed of 1,668,348 cells and was horizontally structured by applying a quadtree refinement: cell dimension ranges were from 100 m in the peripheral areas, up to 12.5 m around subway lines and public car parks (i.e. fourth level of refinement); in proximity to public car parks currently under construction, a fifth quadtree level of refinement was applied (i.e. 6.25 m) (Fig. 7.3a). The grid was rotated by 35° from the offset (X = 1,509,407; Y = 5,026,235; Monte Mario Italy 1; ESPG: 3003) to be perpendicular to the general NW–SE GW flow direction of the domain (Bonomi et al. 1998; Beretta et al. 2004).

The vertical discretization (Fig. 7.3c) consisted of 18 layers. The first 8 layers, with an average thickness of three meters, included all the UIs lying in the shallow aquifer (layers 1–10, ISS/Aquifer Group A1); layers 11 to 14 had a medium thickness of seven meters to model the first portion of the ISI (Aquifer Group A2). Layers 15 to 17 (with a medium thickness of 6 m) were adopted to represent the aquitard (AQ), while the last layer, with a medium thickness of 20 m, aimed at modeling the final portion of the ISI (Aquifer Group B).

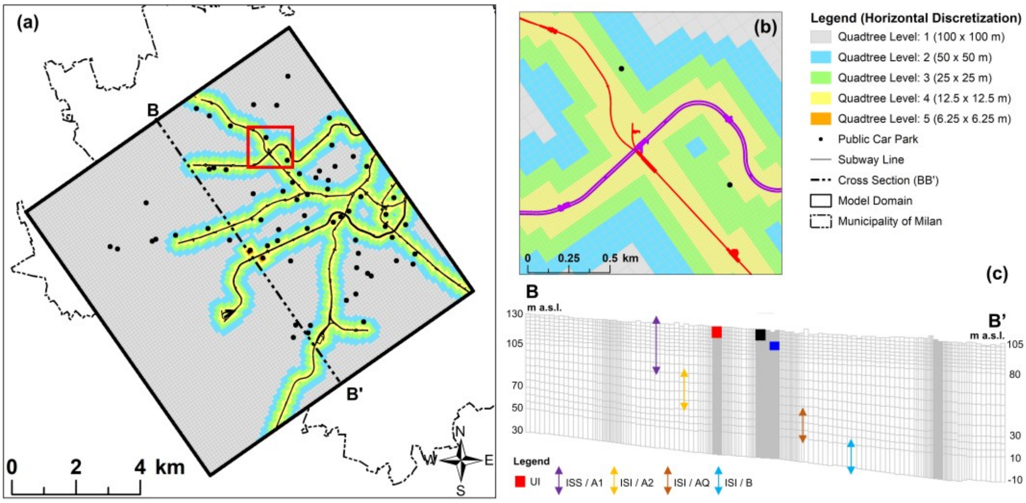

Fig. 7.3. a) Grid horizontal discretization; the red rectangle points to the sector area represented in Fig. 7.3b; **b)** example of quadtree refinement close to Lotto exchange station (see Fig. 7.2); **c)** grid vertical discretization. Please note that for Fig. 7.3b, the same colour coding of Fig. 7.1b has been used for subway lines.

7.3.1.2. Boundary conditions

Boundary conditions (Fig. 7.4), used to outline the hydrogeologic system, were represented through Neumann and Cauchy conditions:

- General Head Boundary (GHB) was used to model the initial heads along the borders around the study area, at their real distance from the analysed domain. As for their hydraulic head values, the initial information was taken from a piezometric map of March 2015 (Mar15) for the study area (Sartirana et al. 2022). In addition, the main quarries located inside the domain (Fig. 7.4) have been represented as GHBs.

- WELL (WEL) was used to model the 261 public wells and 785 GW heat pumps (GWHPs) described in Section 7.2. Information on well discharge was readapted from De Caro et al. 2020 with regard to public wells, and from Regione Lombardia 2021a for GWHPs. Finally, a further 384 private wells fell within the analysed domain: as their well discharge was mostly unknown, a discharge value of −432 m^3/d was initially attributed to these wells.

- Recharge (RCH): 5 zones, based on land use, were identified from the geographic database Dusaf 6.0 (Regione Lombardia 2021b); their values were calculated as the contribution of precipitations, irrigations, and runoff. The initial values for each zone were calculated starting from the precipitation data of Paderno Dugnano rain gauge (located just northward of the city of Milan), monitored by the regional environmental protection agency (ARPA Lombardia 2021). Precipitations amounted to 1496.2 mm/yr for the twelve months before Mar15, the period chosen for model calibration. Absence of infiltration was considered for urban areas and for surface water elements (i.e. quarries), while a 20% of infiltration was attributed to the other recharge areas; moreover, an additional contribution from recharge infiltration was attributed to irrigational areas.

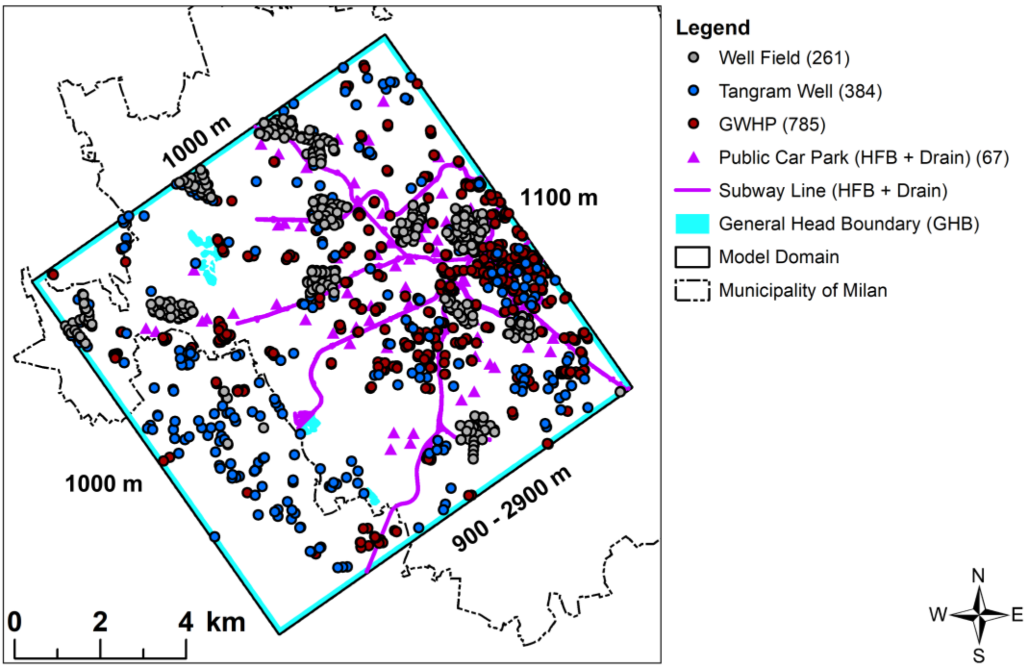

Fig. 7.4. Model boundary conditions. GHBs' distance from the model area has been indicated. Please note that color coding of the infrastructural elements (subway lines and underground public car parks) refers to the HFB package color in Groundwater Vistas 8. Public car parks have been represented as triangles to differentiate them from wells.

7.3.1.2.1. Underground Infrastructures Modelling

The underground railway (Fig. 7.1b) occupies only a small portion of the north-western area; thus, it was not considered within the study. All the UIs (Fig. 7.4) were conceptualized and modeled by coupling the HFB (Hsieh and Freckleton 1993) and the DRN (Harbaugh 2005) packages. The capabilities of both packages were combined to properly simulate and evaluate the exchange between the UIs and the surrounding aquifer. HFB offers the ability to isolate individual components to consider how water is passed between an engineered element such as a subway line and the aquifer. On the other hand, the DRN package enables the modeler to assign a head inside the engineered structures. In this case, the DRN package was adopted to simulate a fictitious water-collection system within the UIs. Combining the capabilities of these two packages is the core of the proposed methodology. To support and validate the adopted methodology, the model domain was discretized into 187 zones: the aquifer of interest, and all the UIs' elements. Thus, water exchanged between neighbouring zones, based on the MODFLOW solution (Harbaugh 1990; Toscani et al. 2022), was quantified.

To properly model the depth of the UIs, information regarding the UIs' bottom and the diameter of the subway tunnels has been obtained from an already-existing 3D GDB of the subsurface elements for the study area (Sartirana et al. 2020). Subsequently, the following rule was adopted as the main constraint to model the UIs: if an UI occupied a layer of more than 50% of its thickness, the UI was then represented inside that layer; otherwise, if this constraint was not respected, the UI was then modeled in the overlying layer.

The wall usually goes along any of the four horizontal sides of each cell, but in MODFLOW-2005 there is no option to specify a vertical barrier. Notwithstanding, the adoption of MODFLOW-USG allowed for wider flexibility in using the HFB package, as the barrier could be aligned along any face of the unstructured grid (Panday et al. 2013); thus, HFB cells could also be placed at the intersection between two nodes sharing the same X and Y coordinates, in contiguous layers. This enabled the reproduction not only of the lateral sides, but also the top and the bottom of all the subsurface elements.

To do so, the initial information about the lateral sides of the UIs was integrated by "manually" compiling the HFB package, adding the position of the top/bottom of the UIs.

The drainage network was placed inside the UI and positioned at the bottom layer of each section of the UI. The drain head (i.e. drain elevation) was fixed as equal to the bottom elevations of the UI. In this way, the possible GW inflow into the UIs could be drained, quantifying the amount of water to be withdrawn to dry the infrastructure. The conceptual model of the adopted approach to simulate the UIs network is represented in Fig. 7.5.

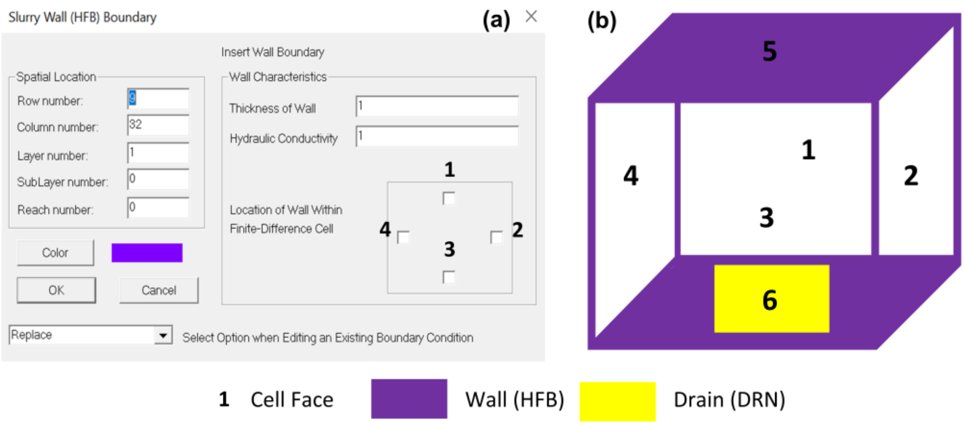

Fig. 7.5. a) Traditional application scheme for HFBs cell; insertion mask taken from Groundwater Vistas 8; **b)** conceptual model of the adopted approach to model all the UIs.

At the exchange stations, lines were positioned at their real depth, thus properly separating the deepest and more recent lines (i.e. M3, M4, and M5) from the shallowest and older ones (M1 and M2).

Conductance, which can be defined as the ratio between hydraulic conductivity (K) and the wall thickness (d), is the single parameter that controls the ability of the wall to transmit water. The absence/presence of lining systems was represented through different conductance values. With regard to the wall thickness, a value of 1 m was considered representative of all the modeled UIs.

The drainage system was assumed to provide no resistance to GW flow, imposing a value of conductance higher than the wall conductance and the aquifer conductivity (Zaidel et al. 2010; Butscher 2012).

7.3.1.3. Further modelling aspects

The hydraulic conductivity parametrization was readapted from a previous project on the study area developed within the same research group (Bonomi et al. 2010), where the lithological information, stored within the Tangram database (Bonomi et al. 2014) in the form of stratigraphic data and pumping tests, was numerically coded and interpolated into GOCAD software using the kriging method (Paradigm 2009). Initial values to the continuous distribution of hydraulic conductivity were assigned from Tangram reference tables. A refined investigation was conducted which analyzed 3 cross-sections built along public-supply well fields from Airoldi and Casati 1989, to infer the spatial distribution of fine materials (i.e. clay lenses).

With regard to calibration, sensitivity analysis using different multiplying factors (from 0.5 to 1.5) and a "trial and error" method were adopted to calibrate the steady-state model, focusing on GHB values and conductance, aquifer recharge (3 out of 5 zones), hydraulic conductivity, and well discharge. As for the hydraulic conductivity, the calibration effort was mostly focused on adjusting the conductivity values and the spatial distribution of fine materials (i.e. clay lenses), acting on the initial continuous distribution. A total of 30 head targets, representing field water table measurements, were considered, showing an uneven distribution over the entire domain, with a limited amount of information for the western sector. The calibration process was conducted against the maximum GW condition of Mar15, the highest in the last 30 years (Sartirana et al. 2022), evaluating the goodness of the obtained results and analyzing the model statistics (i.e. residual sum of squares, scaled RMSE). In this way, the most critical situation for the UIs should be considered; this is also recommended for UIs currently under construction.

7.3.2. Decision management support

Different scenarios were analyzed to quantify GW infiltrations into UIs. Further engineering aspects, such as possible subsidence issues due to the drainage effect, or potential negative effects determined by buoyancy as a result of the aquifer pressure (i.e. uplift risks), were not considered within the aims of the project.

The conductance value for waterproofed subway lines (Table 7.1) was defined from the literature references (Dassargues 1997; Bonomi and Bellini 2003; Attard et al. 2016). Different conductance values (S1–S3) were tested for subway lines M1 and M2 due to a higher uncertainty; considering the absence of lining systems, the conductance was modified simulating possible deteriorations due to a prolonged interaction with the water table over time. In fact, infiltrations may be regarded as a gradual process, ranging from an unsaturated to a saturated flow induced by GW flow (Wang et al. 2017). Since for public car parks' conductance no information was available, it was decided to attribute the lowest conductance value to all car parks.

The most impacted locations of S1–S3 were then analyzed, locally increasing the conductance value of the HFB cells to simulate possible wall fractures. A focus was provided only for subway lines M1, M2, and car parks, as historically they have shown the most revealed interference. To reproduce fractures, wall conductance was only modified close to the infiltration area, increasing the initial value of four order magnitudes, as considered in studies on fractured rocks (Huang et al. 2021). The change in the conductance was applied to the minimum model dimension (i.e. one cell). In this way, it was possible to compare the amounts of infiltration of intact and leaky walls.

Table 7.1. Conductance value for all the considered scenarios.

UI	Waterproofed	Initial Conductance (m²/d) (S1-S2-S3)	Fractures Conductance (m²/d) (S4-S5-S6)
M1	No	1.16×10^{-11} / 10^{-10} / 10^{-9}	1.16×10^{-7} / 10^{-6} / 10^{-5}
M2	No	1.16×10^{-11} / 10^{-10} / 10^{-9}	1.16×10^{-7} / 10^{-6} / 10^{-5}
M3	Yes	1.16×10^{-13}	1.16×10^{-13}
M4	Yes	1.16×10^{-13}	1.16×10^{-13}
M5	Yes	1.16×10^{-13}	1.16×10^{-13}
Car Parks	---	1.16×10^{-13}	1.16×10^{-9}

The identified infiltrations were then analysed to discuss some management proposals with regard to the design of dewatering systems in the most critical locations of the subsurface network, and also proposing the implementation of monitoring systems to manage possible infiltration issues in advance.

7.4. Results

7.4.1. Model calibration and statistics

The final values of GHBs were 127 m a.s.l. for the northern GHB and 102.2 m a.s.l. for the southern, while the western and the eastern boundaries varied from 126 to 103 m a.s.l. and from 124 to 103 m a.s.l. from North to South, respectively. Calibrated values of hydraulic conductivity ranged from 235 to 1.15×10^{-3} m/d, as visible in Fig. 7.6.

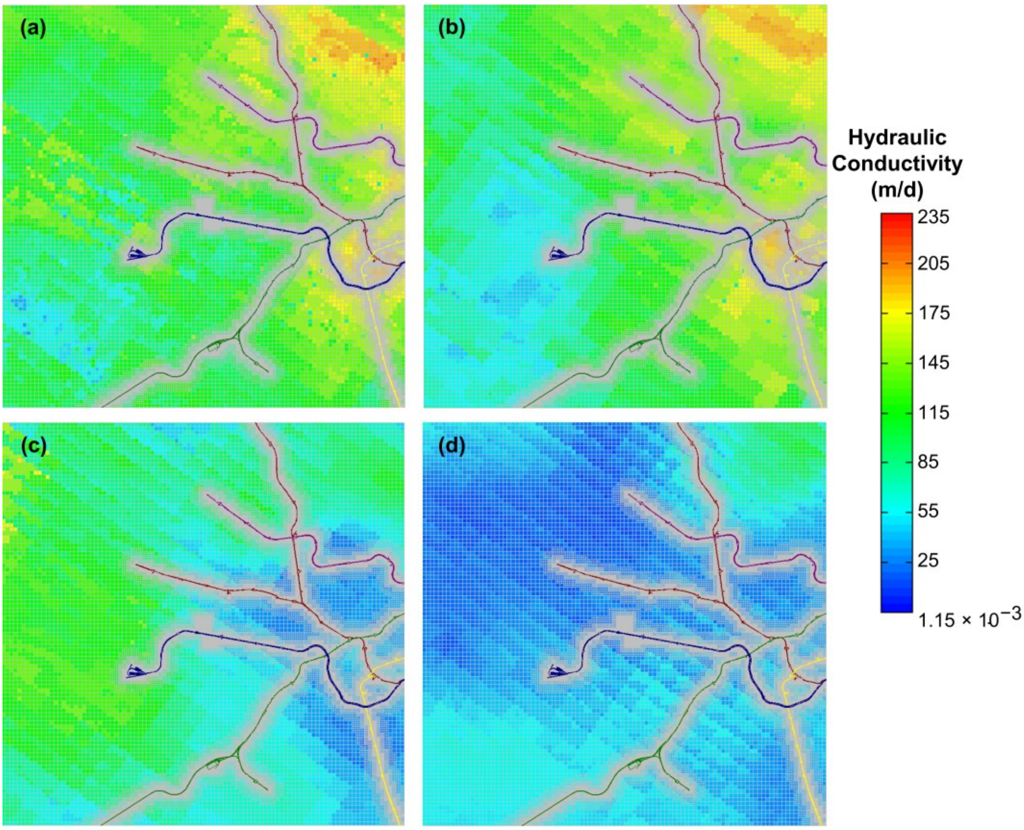

Fig. 7.6. Hydraulic conductivity values for layers **a)** 1 **b)** 4 **c)** 11 **d)** 14. Please note that subway line tracks are plotted inside all layers to provide refence points, since the grid is not rotated in these images.

Final recharge values, and their spatial distribution, are represented in Fig. 7.7. Finally, well discharge was reduced by 25% for the GWHPs and private wells, while for well fields, the reduction, when applied, ranged from 25% up to 50% (for the southernmost well field) of the initial value. The reduction of GWPHs' discharge could be due to the fact that the initial value is the one authorized from the local water supplier, which is generally higher than the effective well discharge.

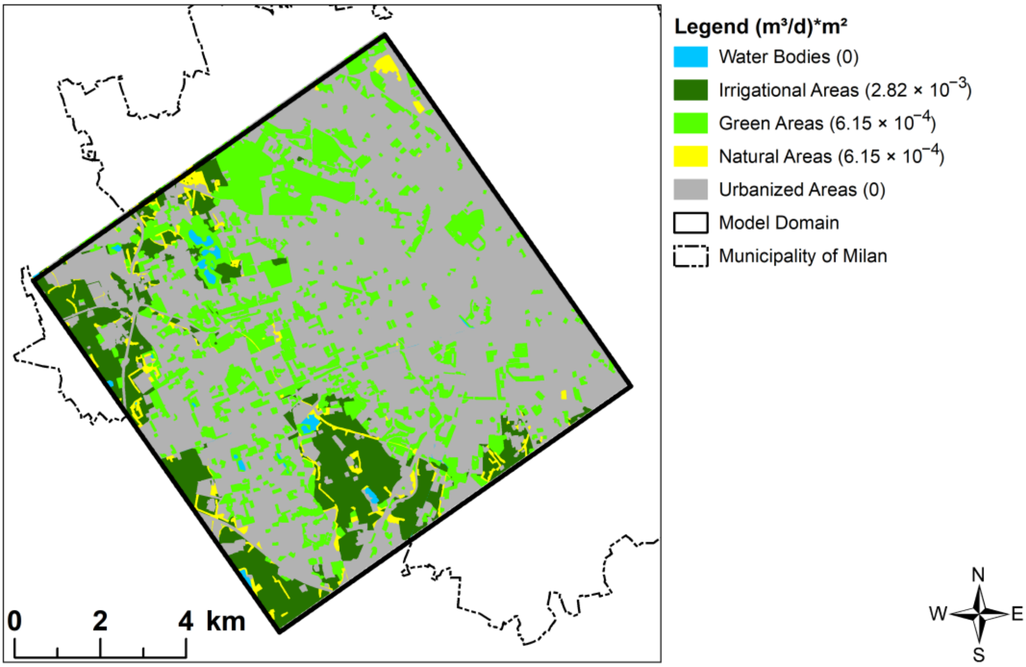

Fig. 7.7. Areal distribution of the 5 recharge zones; final recharge values are provided in legend.

With regard to the calibration, the calibrated model generally provided good statistics (Table 7.2, Figs. 7.8 and 7.9) for most of the 30 head targets considered. The most critical targets were located in the western and southernmost portions of the domain, quite far from the subsurface network that was the main focus of the study. Although these values could represent some modeling issues for some local areas of the domain, the scaled RMSE (4.6%) respects the international criteria that indicate the goodness of a solution in a scaled RMSE to be less than 8% (Middlemis et al. 2000; Feinstein et al. 2010).

Table 7.2. Model statistics for the considered head targets. Statistics refer to S1.

Statistical Parameter	Target Value
Absolute Residual Mean	0.32
Residual Sum of Squares (RSS)	21.8
RMSE	0.85

Statistical Parameter	Target Value
Minimum Residual	−1.15
Maximum Residual	2.16
Range of Observations	18.39
Scaled RMSE (nRMSE)	0.046

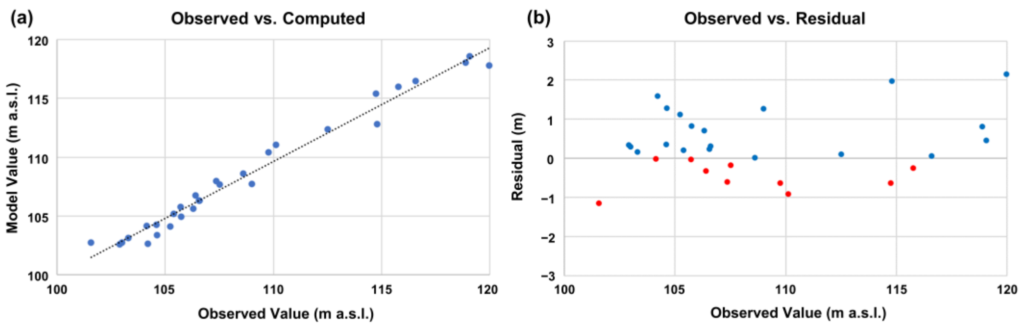

Fig. 7.8. Comparison of **a)** observed (m a.s.l.) vs computed (m a.s.l.) values and **b)** observed values (m a.s.l.) vs residuals (m).

The potentiometric map for the shallow aquifer is represented in Fig. 7.9. From the visualization of the head targets, it is visible that the water table is generally well represented close to the subsurface network, thus allowing for proper assessment of GW/UI interactions and the consequent infiltrations. In the eastern part of the models, located close to Milan's downtown area, the contour lines' behaviour is influenced by the pumping effect of both public well fields and GWHPs (Fig. 7.4).

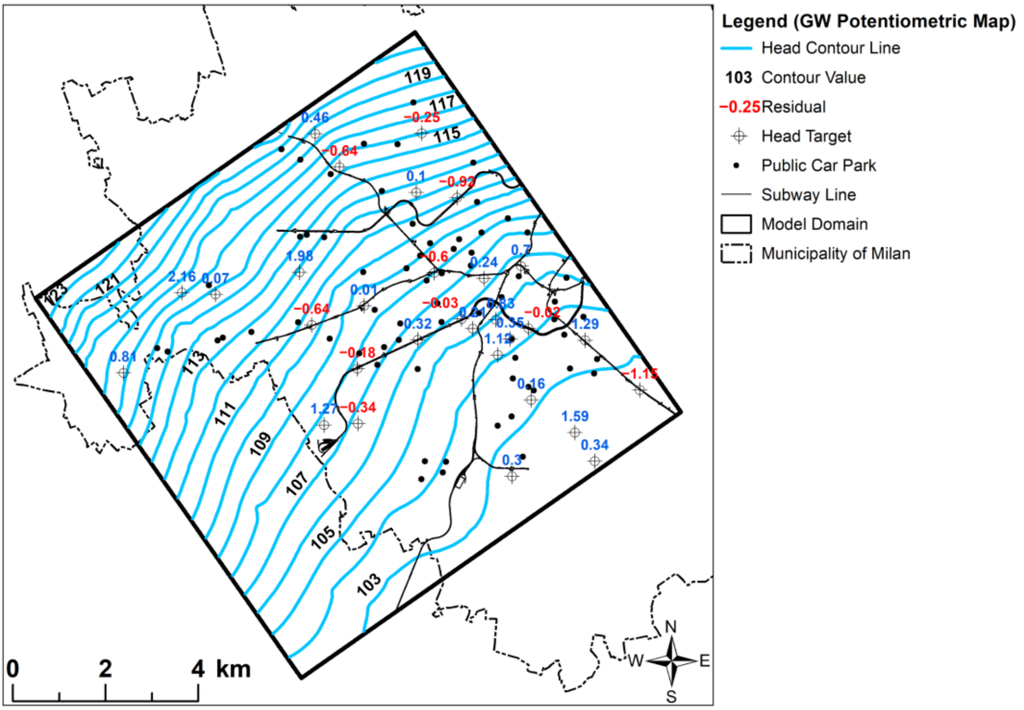

Fig. 7.9. GW potentiometric map of the study area.

Model mass balance (Table 7.3) evidences the importance of well discharge inside the domain, both for the outflows and the inflows; the latter are exclusively due to the injection wells of GWHP systems. The water amounts withdrawn by the drains indicate the GW infiltration into the UIs; despite being a limited amount of water, quantification of the water amounts is important to compare them with the results of the other scenarios in the framework of urban underground management. Model percentage discrepancy is considered to be low (4.59×10^{-5}). A good coherence was detected between the drain outflows and the mass balance with neighbouring zones (i.e. surrounding aquifer and the UIs), thus validating the obtained results.

Table 7.3. Model mass balance.

Mass Balance	Inflow (m³/d)	Outflow (m³/d)	% Error
GHB	419,633.07	72,039.06	
Wells	115,743.33	515,438.32	
Drain	---	2.93×10^{-5}	
Recharge	52,101.25	---	
Total	587,477.65	587,477.38	4.59×10^{-5}

7.4.2. Modelling scenarios

GW inflow for all the UIs was calculated, and results are summarized in Fig. 7.10. As can be seen in Fig. 7.10, an absence of inflow was detected for some subway line branches, as the water table level was lower than the bottom of the UIs. Particularly, these inflow gaps were visible in the North, along subway line M1, and in the central portion of the domain, close to Cadorna exchange station (C-ES) (subway lines M1 and M2). The tunnel sections more exposed to GW inflows are the westmost stretch of M1, towards Bisceglie Station (M1-a), and the stretches close to Uruguay station (M1-b) and between QT8 and Lotto (M1-c) for line M1; and the sections from Porta Genova to Sant'Agostino station (M2-a) and from Lanza to Moscova (M2-b) for subway line M2. Due to their major depth, subway lines M3 and M4 were completely submerged by the water table, which also occurred for subway line M5 (Table 7.4). With regard to public car parks, 34 out of 67 resulted in infiltration; in the central area, Washington/Piemonte (P-a) and Carducci (P-b) turned out to be among the most impacted infrastructures, while, for example, Betulle Est was impacted in the West (P-c). Critical sections for M1 and M2 were already identified as areas where a historical interaction (i.e. submersion) with the water table was evidenced (Colombo 1999; Sartirana et al. 2020). In particular, Sant'Agostino (M2-a) was impacted for both GW minimum and maximum conditions.

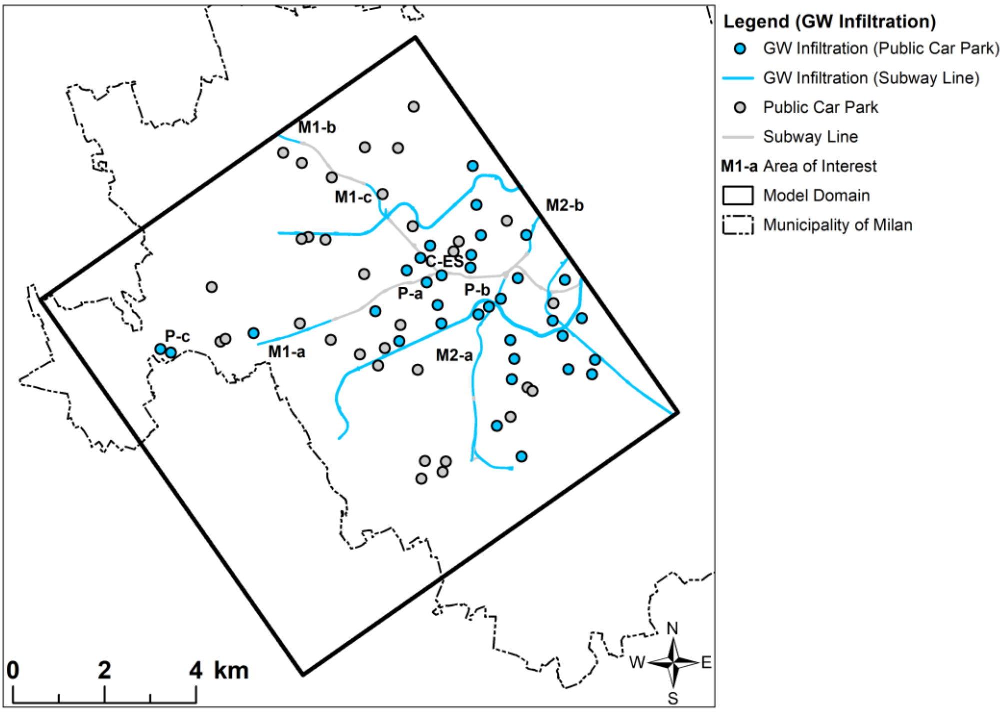

Fig. 7.10. Areas showing GW infiltrations into UIs.

As summarized in Table 7.4, GW inflows for S1-S3 are limited, with low orders of magnitude. The highest values of inflows ($10^{-5}/10^{-3}$ order of magnitude) were detected for the oldest subway lines M1 and M2, modeled with higher conductance values to simulate the absence of waterproofing systems and a progressive saturation of the walls over time. As for the deepest lines, such small values are attributable to the low conductance representing lining systems. The spatial distribution of these infiltrations is different, as for shallow lines the infiltrations are detected only at certain spots, as visible in Fig. 7.10, thus evidencing local but more critical situations to manage.

Table 7.4. GW inflows into UIs (m³/d) for S1–S3. Please remember that for M3, M4, M5, and parks, K was always set equal to 1.16×10^{-13} m/d. Percentage below the water table is intended as the sections of UIs where the bottom of the infrastructure is lower than the hydraulic head.

UI Category	**Amount of infiltration (m³/d)**			**% below the water table**
	S1 (K = 1.16 × 10^{-11}m/d)	S2 (K = 1.16 × 10^{-10} m/d)	S3 (K = 1.16 × 10^{-9} m/d)	
M1	3.70×10^{-6}	5.83×10^{-5}	4.23×10^{-4}	8.37
M2	2.00×10^{-5}	2.34×10^{-4}	2.27×10^{-3}	71.38
S1-S3 (K = 1.16 × 10^{-13} m/d)				
M3	6.24×10^{-7}			100
M4	1.94×10^{-6}			100
M5	2.70×10^{-6}			100
Car Parks	3.00×10^{-7}			50.75

At the most critical points highlighted in S1–S3 (Fig. 7.10) for subway lines M1 and M2, and for some public car parks, locally punctual wall fractures have been simulated to quantify the variation in GW infiltrations. Wall fractures have been simulated on the vertical sides of the UIs. The results of these spots are summarized in Table 7.5. As is visible, the most critical effects, also considering the features of the UIs (i.e. depth, volume), have been identified for M2-a, around Sant'Agostino station. The infiltration for these points generally increased linearly to one or two orders of magnitude.

Table 7.5. Comparison of GW inflows into UIs (m³/d) for the initial scenario (S1–S3, intact walls) and their corresponding final scenario (S4–S6, leaky walls). Please remember that, for car parks, K was always set equal to 1.16×10^{-13} m/d for S1–S3 and to 1.16×10^{-9} m/d for wall fractures in S4–S6. S means station, T means tunnel, P means park. Depth (m) has been provided for subway stations and parks, as they are designed from the ground field; as for tunnels, since they are not designed from the ground field, thickness was provided rather than depth.

Type	Name	Thickness/ Depth (m)	Volume x 10³ (m³)	Amount of Infiltration (m³/d) (S1/S4)	Amount of Infiltration (m³/d) (S2/S5)	Amount of Infiltration (m³/d) (S3/S6)
S	Bisceglie (M1-a)	11.93	33.49	1.13×10^{-7} / 4.35×10^{-6}	1.12×10^{-6} / 4.35×10^{-5}	2.04×10^{-4} / 4.35×10^{-4}
T	Bisceglie – Inganni (M1-a)	6.5	42.88	2.04×10^{-6} / 2.71×10^{-5}	2.04×10^{-5} / 2.71×10^{-4}	4.30×10^{-5} / 2.71×10^{-3}
S	Inganni (M1-a)	10.92	26.77	3.98×10^{-7} / 1.14×10^{-5}	3.98×10^{-6} / 1.15×10^{-4}	1.20×10^{-4} / 1.15×10^{-3}
T	Bonola – Uruguay (M1-b)	6.5	42.81	1.75×10^{-7} / 4.05×10^{-6}	2.43×10^{-6} / 4.50×10^{-5}	1.81×10^{-5} / 3.94×10^{-4}
T	QT8 – Lotto (M1-c)	6.5	71.89	9.92×10^{-7} / 1.06×10^{-6}	9.34×10^{-6} / 1.77×10^{-5}	9.34×10^{-5} / 1.17×10^{-4}
T	Romolo – Porta Genova (M2-a)	7	55.77	5.67×10^{-6} / 2.37×10^{-5}	5.67×10^{-5} / 2.37×10^{-4}	5.33×10^{-4} / 2.71×10^{-3}

Type	Name	Thickness/ Depth (m)	Volume x 10^3 (m^3)	Amount of Infiltration (m^3/d) (S1/S4)	Amount of Infiltration (m^3/d) (S2/S5)	Amount of Infiltration (m^3/d) (S3/S6)
T	Porta Genova – Sant'Agostino (M2-a)	7	37.05	5.34×10^{-6} / 5.86×10^{-5}	5.34×10^{-5} / 5.86×10^{-4}	8.04×10^{-5} / 5.86×10^{-3}
S	Sant'Agostino (M2-a)	17.35	23.77	8.24×10^{-7} / 5.29×10^{-5}	8.24×10^{-6} / 5.29×10^{-4}	2.64×10^{-4} / 5.29×10^{-3}
T	Lanza – Moscova (M2-b)	7	36.41	1.03×10^{-6} / 6.03×10^{-6}	1.03×10^{-5} / 6.03×10^{-5}	2.84×10^{-5} / 6.02×10^{-4}
P	Washington Piemonte	20	60.38	$1.72 \times 10^{-8}/1.49 \times 10^{-6}$		
P	Carducci Olona	17	58.14	$1.32 \times 10^{-8}/4.82 \times 10^{-7}$		
P	Betulle Est	5	23.02	$2.56 \times 10^{-9}/3.04 \times 10^{-7}$		

As for the two public car parks under construction (Fig. 7.1b), an absence of infiltration was detected in both cases, with respect to the considered GW maximum condition, due to a lack of interaction with the water table (Fig. 7.11) which was contrastingly evidenced for the close branches of subway line M4.

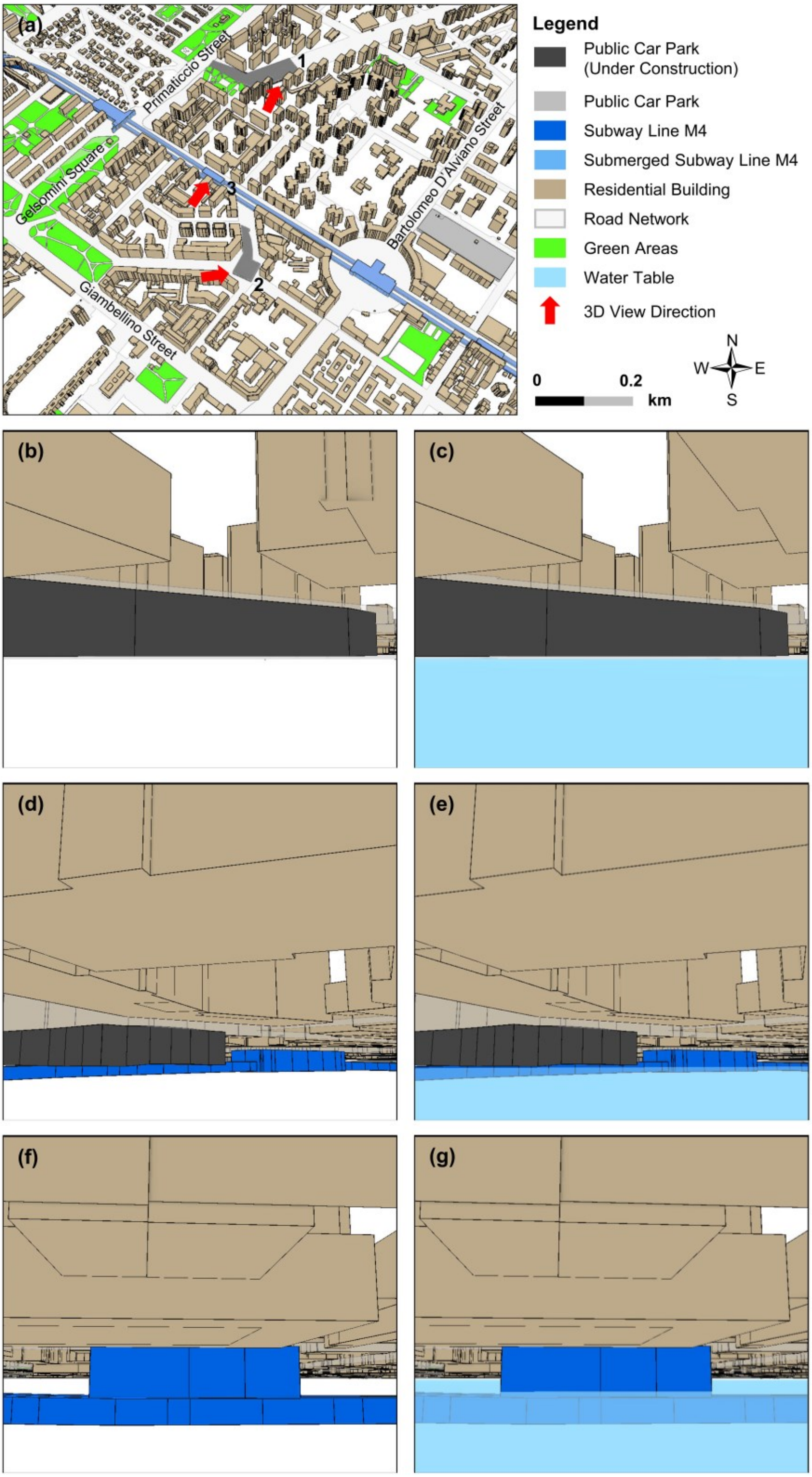
(a)
Primaticcio Street
Gelsomini Square
Giambellino Street
Bartolomeo D'Alviano Street
1
2
3
Legend
Public Car Park (Under Construction)
Public Car Park
Subway Line M4
Submerged Subway Line M4
Residential Building
Road Network
Green Areas
Water Table
3D View Direction
0
0.2
km
N
W
E
S
(b)
(c)
(d)
(e)
(f)
(g)

Fig. 7.11. a) 3D geographical setting of the area close to the car parks currently under construction. The car parks and the subway line M4 are visible below the road network; the names of some roads are indicated to provide more geographic details. Three-dimensional underground reconstruction of **b)** Brasilia car park, **d)** Scalabrini car park, **f)** Lorenteggio 124 intervention point. GW/UIs interaction for **c)** Brasilia car park, **e)** Scalabrini car park, **g)** Lorenteggio 124 intervention point. **b)** and **c)** refer to point 1 in Fig. 7.11 **a)**; **d,e)** refer to point 2 in Fig. 7.11 **a)**; **f,g)** refer to point 3 in Fig. 7.11 **a)**. Transparency has been adopted to represent the volumes submerged by the water table; as visible in **c)** and **e,g)** this occurs only for subway line M4, and not for public car parks. The red arrows indicate the viewpoints and the view directions adopted in the 3D visualization of the subsurface elements. Images were realized using ArcGIS Pro.

7.5. Discussion

Managing GW/UIs interaction in urban areas is a challenging issue. Different problems can arise regarding GW quality, quantity and thermal issues (Schirmer et al. 2013; Attard et al. 2015; La Vigna 2022; Noethen et al. 2022), but also stability, erosion and infiltration for UIs are some further topics to consider. With regard to GW infiltration into UIs, the scientific literature deals both with water inrush calculation during the construction of tunnels (Nikvar Hassani et al. 2016; Farhadian et al. 2017) and problems regarding already-operating underground tunnels (Guo et al. 2021; Ai et al. 2022); in this study, a local scale numerical model was developed for the western sector of Milan city, applying a methodology to quantify GW infiltrations into completed and operative UIs.

7.5.1. Modelling scenarios

Model results in terms of calibration were generally acceptable (Table 7.2, Figs. 7.8 and 7.9). However, some head targets did not show an optimal result. This happened for a couple of targets in the north-western portion of the domain, and for one target in the South. In the North-West, not far from the critical targets, the behaviour of the water table is presumably influenced by a multitude of local situations. The proximity of a group of quarries and a public-supply well field with high discharge (Fig. 7.4), and the presence of clay lenses determining the existence of perched aquifers with seasonal oscillations (Bonomi et al. 2009; Sartirana et al. 2022) make predictions more uncertain. This response could highlight the presence of local mechanisms, possibly uniformed by the targets, that have been neglected. In this sense, the model provides a guide for future data collection, that could allow the improvement of the appropriateness of the conceptual model (Bredehoeft 2005). In addition, acquiring further data could contribute to making more effective predictions, thus improving the model use in supporting management decisions (Lotti et al. 2021).

Identifying the areas more exposed to infiltrations is important to predicting future risks due to a more severe water inrush; thus, adopting strategies to ensure these infrastructures are preserved is vital (Shi et al. 2018; Wang et al. 2019). Some of the impacted areas (i.e. M1-a, M1-b, M1-c, M2-a) have already been identified as critical in previous works (Colombo 1999; Sartirana et al. 2020). In this case, only a qualitative GW/UIs interaction was detected through a GIS methodology. This spatial coherence among the results could be considered as a validation of the numerical model. At the same time, model findings could represent a step forward in the definition of the urban conceptual model; through this approach, GW infiltrations resulting from GW/UI interactions could be estimated. As for M2-a, P-a, and P-b, the highest depth of downtown infrastructures (Table 7.5) plays a key role in influencing GW/UI interactions. This is due both to a high population density, thus requiring more space for subsurface infrastructures (Bobylev 2016), and to the adoption of specific construction methods; as an example, Sant'Agostino station was built with two overlapping pipes (De Caro et al. 2020). As for the western sector, the complex geological situation explained above could be a possible driver of the infiltrations both for subway lines (M1-a) and underground car parks (P-c), despite their limited depth (Table 7.5). To counteract this situation, in the framework of creating a more sustainable and resilient city (La Vigna 2022), some residential constructions have been designed with superficial car parks occupying the first floors of the buildings. With regard to public car parks, the new buildings currently under construction have been designed as two floors deep; at this time, this results in an absence of impact even considering a GW maximum condition (Fig. 7.11). However, prolonged monitoring should be useful to cope the evolution of

GW/UIs interactions. Finally, in the North, a reduced GW/UIs interaction is attributable to a wide unsaturated thickness of the shallow aquifer (Sartirana et al. 2022), with the water table located around 10-12 m from the ground.

7.5.2. Considerations on the adopted modelling approach

The applied modeling strategy aimed to quantitatively evaluate the interaction between the GW system and the subsurface structures. With regard to the calibration process, it is not tied to the prediction of interest; in fact, it is based on head targets whose hydraulic measures are not directly connected to the final goal (i.e. GW infiltrations into UIs). The information content on which the head targets are based is not informative about the degree of connection between the UIs and the water table. In technical terms, the K of the walls is completely in the null space and outside the solution space of the model. This does not mean that the calibration is useless, but it does mean that the model could not be so much a predictive tool as a way to understand a phenomenon (inflow across leaky walls) in general terms. The geometry of the UIs is realistic (Sartirana et al. 2020), but one can only make hypotheses about the permeability of the intact and leaky walls that are not in any way informed by the calibration. To limit this uncertainty, a literature analysis was conducted to choose the initial conductance values for subsurface impervious structures (Attard et al. 2016) and the conductance to simulate isolated fractures (Huang et al. 2021). Moreover, an ensemble of scenarios (Ferré 2017) was defined to deal with non-lined systems, testing different conductance values. In this way, stakeholders are enabled to visualize a range of impacts and they could consider them to apply different management options (Wu and Lee 2015; Castilla-Rho 2017). As for S1–S3 (Table 7.4), GW infiltrations are very limited, especially for waterproofed subway lines; thus, the model allowed for the gaining of insights into the conductance values that are needed to simulate an almost impermeable element.

Anyway, obtaining good calibration results was crucial, since they allow GW/UI interactions to be well represented and, consequently, they allow the obtaining of a more reliable estimate of the infiltrations originated by the relationship between the aquifer and the subsurface infrastructures. As visible in Figs. 7.8 and 7.9, this is mostly true for this specific case, especially for the targets located in the central part of the domain that lie in proximity of the main UIs' elements.

Using MODFLOW-USG as numerical code allowed the refining of the grid horizontally, therefore properly representing the UIs. Moreover, through the implementation of the unstructured grid, the key numerical computations could be limited within the required bounds (Panday et al. 2013), making the simulations less computationally intensive. Above all, the adoption of MODFLOW-USG was pivotal to model the UIs, as it allowed the HFB package to be used to represent not only the cells' lateral sides, but also the top and the bottom of the UIs. In this way, the subsurface elements could be modeled with their real depth and volumes, thus refining previous applications of the HFB package to simulate UIs fully penetrating single-layered models (Bonomi and Bellini 2003; Boukhemacha et al. 2015; Golian et al. 2021); hence, a precise estimate of further modeling aspects (i.e. evaluation of the barrier effect on GW flow paths) should also be guaranteed. In MODFLOW-USG, to reduce numerical instability, desaturated cells (i.e. dry cells) are not inactivated, so there could be a small amount of flow from one cell to another. The adoption of the DRN package helped to solve this possible issue, especially in the upper portion of the domain where unsaturated aquifer was present. As a drain is activated only when the hydraulic head is at least equal to the drain elevation, it was possible to unravel where an effective infiltration was present. The choice of the DRN package also came after its previous applications to quantifying flooding episodes during the construction of tunnels (Lagudu et al. 2015; Golian et al. 2018). Through the developed methodology, modeling GW/UI interactions could be enhanced. In fact, combining the use of HFB, DRN, and mass balance zones to quantify infiltrations depending on different conductance values is possible, instead of deactivating cells of impervious structures. Thus, a step forward could be taken in the development of the urban conceptual model, supporting previous approaches conducted within the same domain (Colombo et al. 2018; Previati et al. 2022), or in other areas (Attard et al. 2017) where different aspects of GW/UI interactions have been investigated but GW infiltrations into subsurface elements were not quantified.

The methodology has been tested on a steady-state numerical model. Future applications on transient numerical models would be possible depending on long-term data collections (Naranjo 2017); this could raise awareness about infiltration issues, supporting a deeper interpretation of GW/UIs interactions and making the model a useful management tool to make long-term predictions (Bredehoeft 2005).

7.5.3. Decision management

The infiltration issue of UIs in Milan city is historical. Different episodes have been documented over time (Colombo 1999; Gattinoni and Scesi 2017; Sartirana et al. 2020), leading both to economic and management problems for Metropolitana Milanese Spa, the subway managing company. For example, the section between Piola and Lambrate stations, along subway line M2 (outside the numerical model domain), was closed during summer 2019 to complete lining works because of GW infiltrations, thus forcing the use of surface public transport. Although the water inflow is small with respect to water inrush into subway tunnels during their construction (Xia et al. 2018; Huang et al. 2021; Liu et al. 2022), this situation could trigger further issues over a long time period (i.e. corrosion of foundations), resulting in a decline of the subway system efficiency; thus, this problem should not be underestimated.

To ensure sustainable development of GW/UI interactions, effective engagement of the stakeholders should be of great value (Blunier et al. 2007; Admiraal and Cornaro 2016; Di Salvo et al. 2017). Open communication is needed to raise awareness about the importance of data to describe the system and conceptualize and develop a model (Castilla-Rho 2017; Peeters 2017) with increased predictive capabilities. For this specific case, monitoring, estimation, and control are essential aspects for tunnel management (Liu et al. 2022). Having access to existing infiltration measures, if available, or implementing monitoring of the punctual inflows along the tunnels or for car parks would also improve the calibration process; in this way, model uncertainty would be reduced, thus strengthening the usefulness of hydrogeologic models for decision-making bodies (Bredehoeft 2005; Lotti et al. 2021). The collection of field data could focus on the most critical sectors highlighted (i.e. M1-a, M2-a) by the model results. Amongst these areas, dewatering solutions could be adopted to manage the issue, thus contributing to preserving the status of the subway network, avoiding the development of more serious issues as occurred for the surrounding areas of Piola and Lambrate stations. In particular, the historical issues of Sant'Agostino station, also due to the adoption of specific construction methods (De Caro et al. 2020), impose an increased degree of attention for this limited branch of subway line M2.

However, applying these solutions would be a consequence of effective GW infiltrations into UIs. A move away from reacting and correcting measures, focusing on preventive actions (Schirmer et al. 2013) to secure the UIs, should be evaluated. In a previous work by Sartirana et al. 2022, underground car parks were classified as possibly critical for different GW conditions if the difference between the reference plan (i.e. bottom) of the UI and the water table was less than one meter. To avoid infiltration issues, activating localized pumping when a certain threshold is locally exceeded would be a possible measure (Carneiro and Carvalho 2010). To do so, early warning monitoring solutions, such as integrating GIS, BIM, and GPS techniques (Du et al. 2015; Lyu et al. 2019), with continuous online data measurements should be implemented in proximity of the most critical UIs.

Moreover, GW is not only an annoyance for its side effects, but it is also a heritage (Schirmer et al. 2013) in urban frameworks; therefore, further management strategies could be proposed. For example, as GW is a valuable energy reservoir (Noethen et al. 2022; Previati et al. 2022), increasing the adoption of GWHP systems, possibly only due to extraction wells, could keep the water table levels controlled close to the UIs, thus not only limiting the infiltration issues but also exploiting the thermal potential of these subsurface elements (Bayer et al. 2019).

Finally, in the framework of the goals of the Plan of Government for the Territory, this local-scale urban model could help the decision makers to understand and manage the relation between new UIs and water table levels, testing possible urban underground development scenarios.

7.6. Conclusions

This work aimed to adopt a methodology to quantify GW infiltrations into UIs (subway lines and public car parks) with the view of assisting urban underground management. In this sense, the realization of a local-scale, urban numerical model allowed the following:

1. Verification of the usefulness of the applied methodology to model the UIs, quantifying GW infiltrations through the combination of HFB and DRN packages. In particular, the adoption of MODFLOW-USG allowed the use of the HFB package to model the top and the bottom of the UIs, thus considering the interaction with the water table along the vertical direction as well. The existence of a 3D GDB of the UIs for the city of Milan helped to accurately model the UIs' depth.
2. Identification of the UIs sectors more exposed to GW infiltrations under different conductance scenarios (from intact to leaky walls), providing a qualitative and quantitative overview intended for both the municipality decision makers and the subway managing company. The westmost stretch of subway line M1 and the sector around Sant'Agostino station for line M2 were among the most critical areas. Moreover, for the first time, public car parks have been deeply considered in a 3D GW flow numerical model for the city of Milan. GW infiltrations were detected both for deep car parks in the central portion of the domain and shallow car parks in the western sectors. This resulted in an improvement of the already-existing urban conceptual model of the area.
3. Support for the decision makers in designing possible dewatering systems, also proposing early warning monitoring systems and proactive solutions to secure the UIs from potential GW infiltration damages.

The overall findings of this study could provide a useful tool to the stakeholders to properly design new UIs in the framework of the planned underground development of the city. In this sense, the numerical model could be used to realize different GW scenarios, testing their effects on the designed UIs. Furthermore, modeling their tops and bottoms through the HFB package could improve the evaluation of their barrier effect on GW flow paths. For future applications, reasoning the combination of the HFB package with different third-type boundary conditions (i.e. River, GHB) to model other subsurface elements (i.e. sewer systems, buried channels, etc., to evaluate their leakance) could represent a challenging task. The methodology has been tested for the city of Milan—nonetheless it should be worth considering its application to other urban realities to enhance the analysis of GW/UI interactions.

Author Contributions: Conceptualization, D.S.; methodology, D.S. and T.B.; validation, M.R., M.D.A., L.F., and T.B; formal analysis, D.S. and C.Z.; data curation, D.S. and M.D.A.; writing—original draft preparation, D.S.; writing—review and editing, D.S., C.Z., M.R., M.D.A., M.C., A.R., L.F., and T.B.; visualization, D.S., C.Z., M.C., and A.R.; supervision, M.R., M.D.A., L.F., and T.B.; project administration, T.B. All authors have read and agreed to the published version of the manuscript.

Funding: This research did not receive any external funding.

Acknowledgments: The authors are grateful to Metropolitana Milanese S.p.a for providing both the altimetric profiles of the subway lines and the piezometric data that were used as information for model calibration. Moreover, the authors would like to warmly thank Daniel T. Feinstein of USGS and Gennaro Alberto Stefania for their support and suggestions during the development of the work. The authors would also like to thank the three anonymous reviewers for their comments, which helped to improve this article.

Conflicts of interest: The authors declare no conflicts of interest.

References

Abd-Elaty I, Pugliese L, Straface S (2022) Inclined Physical Subsurface Barriers for Saltwater Intrusion Management in Coastal Aquifers. Water Resour Manag 36(9):2973–2987. https://doi.org/10.1007/s11269-022-03156-7

Abd-Elaty I, Zelenakova M (2022) Saltwater intrusion management in shallow and deep coastal aquifers for high aridity regions. J Hydrol Reg Stud 40(January):101026. https://doi.org/10.1016/j.ejrh.2022.101026

Admiraal H, Cornaro A (2016) Engaging decision makers for an urban underground future. Tunn Undergr Sp Technol 55:221–223. https://doi.org/10.1016/j.tust.2015.08.009

Ai Q, Yuan Y, Jiang X, Wang H, Han C, Huang X, Wang K (2022) Pathological diagnosis of the seepage of a mountain tunnel. Tunn Undergr Sp Technol 128(July):104657. https://doi.org/10.1016/j.tust.2022.104657

Airoldi R, Casati P (1989) Le falde idriche del sottosuolo di Milano. Comune di Milano

Allocca V, Coda S, Calcaterra D, De Vita P (2021) Groundwater rebound and flooding in the Naples ' periurban area (Italy). https://doi.org/10.1111/jfr3.12775

ARPA Lombardia (2021) Agenzia Regionale per la Protezione dell'Ambiente [Regional Environmental Monitoring Agency]. [Regional Environmental Monitoring Agency]. https://www.arpalombardia.it/. (Accessed on 13 November 2021)

Arshad I, Umar R (2020) Status of urban hydrogeology research with emphasis on India. Hydrogeol J 28(2):477–490. https://doi.org/10.1007/s10040-019-02091-z

Attard G, Cuvillier L, Eisenlohr L, Rossier Y, Winiarski T (2016) Deterministic modelling of the cumulative impacts of underground structures on urban groundwater flow and the definition of a potential state of urban groundwater flow: example of Lyon, France. Hydrogeol J 24(5):1213–1229. https://doi.org/10.1007/s10040-016-1385-z

Attard G, Rossier Y, Winiarski T, Eisenlohr L (2017) Urban underground development confronted by the challenges of groundwater resources: Guidelines dedicated to the construction of underground structures in urban aquifers. Land use policy 64:461–469. https://doi.org/10.1016/j.landusepol.2017.03.015

Attard G, Winiarski T, Rossier Y, Eisenlohr L (2015) Review: Impact of underground structures on the flow of urban groundwater. Hydrogeol J 24(1):5–19. https://doi.org/10.1007/s10040-015-1317-3

Bayer P, Attard G, Blum P, Menberg K (2019) The geothermal potential of cities. Renew Sustain Energy Rev 106(February):17–30. https://doi.org/10.1016/j.rser.2019.02.019

Beretta GP, Avanzini M, Pagotto A (2004) Managing groundwater rise: Experimental results and modelling of water pumping from a quarry lake in Milan urban area (Italy). Environ Geol 45(5):600–608. https://doi.org/10.1007/s00254-003-0918-7

Blunier P, Tacher L, Parriaux A (2007) Systemic approach of urban underground resources exploitation. 11th ACUUS Int Conf - Undergr Sp Expand Front :43–48

Bobylev N (2009) Mainstreaming sustainable development into a city's Master plan: A case of Urban Underground Space use. Land use policy 26(4):1128–1137. https://doi.org/10.1016/j.landusepol.2009.02.003

Bobylev N (2016) Transitions to a High Density Urban Underground Space. Procedia Eng 165:184–192. https://doi.org/10.1016/j.proeng.2016.11.750

Bonomi T (1999) Groundwater level evolution in the Milan area: Natural and human issues. IAHS-AISH Publ (259):195–202

Bonomi T, Bellini R (2003) The tunnel impact on the groundwater level in an urban area: a modelling approach to forecast it. RMZ - Materials and Geoenvironment 50(1):45–48

Bonomi T, Cavallin A, De Amicis M, Rizzi S, Tizzone R, Trefiletti P (1998) Evoluzione della dinamica piezometrica nell'area milanese in funzione di alcuni aspetti socio-economici [Evolution of the piezometric dynamics in the Milan area as a function of some socio-economic aspects]. In: Atti della Giornata Mondiale dell'Acqua" Acque Sotterranee: Risorsa Invisibile". pp 9–17

Bonomi T, Del Rosso F, Fumagalli L, Canepa P (2010) Assessment of groundwater availability in the Milan Province aquifers. Mem Descr della Cart Geol d'Italia 90:31–40

Bonomi T, Fumagalli L, Dotti N (2009) Fenomeno di inquinamento da solventi in acque sotterranee sfruttate ad uso potabile nel nord-ovest della provincia di Milano [Phenomenon of solvent pollution in groundwater exploited for drinking use in the north-west of Milan province] G. Geol. Appl. 12:43–59

Bonomi T, Fumagalli L, Rotiroti M, Bellani A, Cavallin A (2014) The hydrogeological well database TANGRAM©: a tool for data processing to support groundwater assessment. Acque Sotter - Ital J Groundw 3(2). https://doi.org/10.7343/as-072-14-0098

Bonomi T, Sartirana D, Toscani L, Stefania GA, Zanotti C, Rotiroti M, Redaelli A, Fumagalli L (2022) Modeling groundwater/surface-water interactions and their effects on hydraulic barriers, the case of the industrial area of Mantua (Italy). Acque Sotter - Ital J Groundw 11(2):43–55. https://doi.org/10.7343/as-2022-569

Boscacci F, Camagni R, Caragliu A, Maltese I, Mariotti I (2017) Collective benefits of an urban transformation: Restoring the Navigli in Milan. Cities 71(July):11–18. https://doi.org/10.1016/j.cities.2017.06.018

Boukhemacha MA, Gogu CR, Serpescu I, Gaitanaru D, Bica I (2015) A hydrogeological conceptual approach to study urban groundwater flow in Bucharest city, Romania. Hydrogeol J 23(3):437–450. https://doi.org/10.1007/s10040-014-1220-3

Bredehoeft J (2005) The conceptualization model problem - Surprise. Hydrogeol J 13(1):37–46. https://doi.org/10.1007/s10040-004-0430-5

Butscher C (2012) Steady-state groundwater inflow into a circular tunnel. Tunn Undergr Sp Technol 32:158–167. https://doi.org/10.1016/j.tust.2012.06.007

Calderhead AI, Martel R, Garfias J, Rivera A, Therrien R (2012) Pumping dry: An increasing groundwater budget deficit induced by urbanization, industrialization, and climate change in an over-exploited volcanic aquifer. Environ Earth Sci 66(7):1753–1767. https://doi.org/10.1007/s12665-011-1398-9

Carneiro J, Carvalho JM (2010) Groundwater modelling as an urban planning tool: Issues raised by a small-scale model. Q J Eng Geol Hydrogeol 43(2):157–170. https://doi.org/10.1144/1470-9236/08-028

Castilla-Rho JC (2017) Groundwater Modeling with Stakeholders: Finding the Complexity that Matters. 55(5). https://doi.org/10.1111/gwat.12569

Chaussard E, Bürgmann R, Shirzaei M, Fielding EJ, Baker B (2014) Predictability of hydraulic head changes and characterization of aquifer-system and fault properties from InSAR-derived ground deformation. J Geophys Res Solid Earth 119(8):6572–6590

Colombo A (1999) Milano e l'innalzamento della falda. Cave e Cantieri 2:26–36

Colombo L, Gattinoni P, Scesi L (2017) Influence of underground structures and infrastructures on the groundwater level in the urban area of Milan, Italy. Int J Sustain Dev Plan 12(1):176–184. https://doi.org/10.2495/SDP-V12-N1-176-184

Colombo L, Gattinoni P, Scesi L (2018) Stochastic modelling of groundwater flow for hazard assessment along the underground infrastructures in Milan (northern Italy). Tunn Undergr Sp Technol 79(May):110–120. https://doi.org/10.1016/j.tust.2018.05.007

Dassargues A (1997) Groundwater modelling to predict the impact of tunnel on the behavior of water table aquiefer in urban condition. Groundw. Urban Enviroment, Process. Manag. Chitt. et.al. 225–230

De Caro M, Crosta GB, Previati A (2020) Modelling the interference of underground structures with groundwater flow and remedial solutions in Milan. Eng Geol 272(May):105652. https://doi.org/10.1016/j.enggeo.2020.105652

Delmastro C, Lavagno E, Schranz L (2016) Underground urbanism: Master Plans and Sectorial Plans. Tunn Undergr Sp Technol 55:103–111. https://doi.org/10.1016/j.tust.2016.01.001

Di Salvo C, Ciotoli G, Pennica F, Cavinato GP (2017) Pluvial flood hazard in the city of Rome (Italy). J Maps 13(2):545–553. https://doi.org/10.1080/17445647.2017.1333968

Di Salvo C, Mancini M, Cavinato GP, Moscatelli M, Simionato M, Stigliano F, Rea R, Rodi A (2020) A 3d geological model as a base for the development of a conceptual groundwater scheme in the area of the colosseum (Rome, Italy). Geosci 10(7):1–26. https://doi.org/10.3390/geosciences10070266

Du H, Du J, Huang S (2015) GIS, GPS, and BIM-based risk control of subway station construction. In: ICTE 2015. pp 1478–1485

Ducci D, Sellerino M (2015) Groundwater Mass Balance in Urbanized Areas Estimated by a Groundwater Flow Model Based on a 3D Hydrostratigraphical Model: the Case Study of the Eastern Plain of Naples (Italy). Water Resour Manag 29(12):4319–4333. https://doi.org/10.1007/s11269-015-1062-3

El Tani M (2003) Circular tunnel in a semi-infinite aquifer. Tunn Undergr Sp Technol 18(1):49–55. https://doi.org/10.1016/S0886-7798(02)00102-5

Epting J, Huggenberger P, Rauber M (2008) Integrated methods and scenario development for urban groundwater management and protection during tunnel road construction: A case study of urban hydrogeology in the city of Basel, Switzerland. Hydrogeol J 16(3):575–591. https://doi.org/10.1007/s10040-007-0242-5

Farhadian H, Nikvar Hassani A, Katibeh H (2017) Groundwater inflow assessment to Karaj Water Conveyance tunnel, northern Iran. KSCE J Civ Eng 21(6):2429–2438. https://doi.org/10.1007/s12205-016-0995-2

Feinstein DT, Hunt RJ, Reeves HW (2010) Regional groundwater-flow model of the Lake Michigan Basin in support of Great Lakes Basin water availability and use studies. U. S. Geological Survey

Ferré TPA (2017) Revisiting the Relationship Between Data, Models, and Decision-Making. Groundwater 55(5):604–614. https://doi.org/10.1111/gwat.12574

Gao CL, Zhou ZQ, Yang WM, Lin CJ, Li LP, Wang J (2019) Model test and numerical simulation research of water leakage in operating tunnels passing through intersecting faults. Tunn Undergr Sp Technol 94(July):103134. https://doi.org/10.1016/j.tust.2019.103134

García-Gil A, Epting J, Ayora C, Garrido E, Vázquez-Suñé E, Huggenberger P, Gimenez AC (2016) A reactive transport model for the quantification of risks induced by groundwater heat pump systems in urban aquifers. J Hydrol 542:719–730. https://doi.org/10.1016/j.jhydrol.2016.09.042

Gattinoni P, Scesi L (2017) The groundwater rise in the urban area of Milan (Italy) and its interactions with underground structures and infrastructures. Tunn Undergr Sp Technol 62:103–114. https://doi.org/10.1016/j.tust.2016.12.001

Golian M, Abolghasemi M, Hosseini A, Abbasi M (2021) Restoring groundwater levels after tunneling: a numerical simulation approach to tunnel sealing decision-making. Hydrogeol J 29(4):1611–1628. https://doi.org/10.1007/s10040-021-02315-1

Golian M, Teshnizi ES, Nakhaei M (2018) Prediction of water inflow to mechanized tunnels during tunnel-boring-machine advance using numerical simulation. Hydrogeol J 26(8):2827–2851. https://doi.org/10.1007/s10040-018-1835-x

Guo Y, Wang H, Jiang M (2021) Efficient Iterative Analytical Model for Underground Seepage around Multiple Tunnels in Semi-Infinite Saturated Media. J Eng Mech 147(11):1–17. https://doi.org/10.1061/(asce)em.1943-7889.0001999

Harbaugh AW (1990) A computer program for calculating subregional water budgets using results from the U.S. Geological Survey Modular Three-Dimensional Finite-Difference Ground-Water Flow Model

Harbaugh AW (2005) MODFLOW-2005, the US Geological Survey modular ground-water model: the ground-water flow process. US Department of the Interior, US Geological Survey Reston, VA

Hayashi T, Tokunaga T, Aichi M, Shimada J, Taniguchi M (2009) Effects of human activities and urbanization on groundwater environments: An example from the aquifer system of Tokyo and the surrounding area. Sci Total Environ 407(9):3165–3172. https://doi.org/10.1016/j.scitotenv.2008.07.012

Hernández MA, González N, Chilton J (1997) Impact of rising piezometric levels on Greater Buenos Aires due to partial changing of water services infrastructure

Hsieh PA, Freckleton JR (1993) Documentation of a computer program to simulate horizontal-flow barriers using the U.S. Geological Survey's modular three-dimensional finite-difference ground-water flow model. Reston, VA

Huang Z, Zhao K, Li X, Zhong W, Wu Y (2021) Numerical characterization of groundwater flow and fracture-induced water inrush in tunnels. Tunn Undergr Sp Technol 116(July):104119. https://doi.org/10.1016/j.tust.2021.104119

Istat (2011) L'italia del censimento. Struttura demografica e processo di rilevazione, Lombardia [Italy in the census. Demographic structure and survey process, Lombardy]

Koziatek O, Dragićević S (2017) iCity 3D: A geosimualtion method and tool for three-dimensional modeling of vertical urban development. Landsc Urban Plan 167(June):356–367. https://doi.org/10.1016/j.landurbplan.2017.06.021

Lagudu S, Rao VVSG, Nandan MJ, Khokar C (2015) Application of MODFLOW for groundwater Seepage Problems in the Subsurface Tunnels. J Ind Geophys Union 19(4):422–432

La Vigna F (2022) Review: Urban groundwater issues and resource management, and their roles in the resilience of cities. Hydrogeol J 30(6):1657–1683. https://doi.org/10.1007/s10040-022-02517-1

Lamé A (2013) Modélisation hydrogéologique des aquifères de Paris et impacts des aménagements du sous-sol sur les écoulements souterrains [Hydrogeological modeling of the Paris aquifers and impacts of subsoil development on underground flows]

Li HQ, Parriaux A, Thalmann P, Li XZ (2013a) An integrated planning concept for the emerging underground urbanism: Deep City Method Part 1 concept, process and application. Tunn Undergr Sp Technol 38:559–568. https://doi.org/10.1016/j.tust.2013.04.010

Li HQ, Li X, Parriaux A, Thalmann P (2013b) An integrated planning concept for the emerging underground urbanism: Deep City Method Part 2 case study for resource supply and project valuation. Tunn Undergr Sp Technol 38:569–580. https://doi.org/10.1016/j.tust.2013.04.009

Li X, Zhang W, Li D, Wang Q (2008) Influence of underground water seepage flow on surrounding rock deformation of multi-arch tunnel. J Cent South Univ Technol 15(1):69–74

Liu JQ, Sun YK, Li CJ, Yuan HL, Chen WZ, Liu XY, Zhou XS (2022) Field monitoring and numerical analysis of tunnel water inrush and the environmental changes. Tunn Undergr Sp Technol 122(June 2021):104360. https://doi.org/10.1016/j.tust.2021.104360

Lotti F, Borsi I, Guastaldi E, Barbagli A, Basile P, Favaro L, Mallia A, Xuereb R, Schembri M, Mamo JA, Sapiano M (2021) Numerically enhanced conceptual modelling (NECoM) applied to the Malta Mean Sea Level Aquifer. Hydrogeol J 29(4):1517–1537. https://doi.org/10.1007/s10040-021-02330-2

Lyu HM, Shen SL, Zhou A, Yang J (2019) Perspectives for flood risk assessment and management for mega-city metro system. Tunn Undergr Sp Technol 84(October 2018):31–44. https://doi.org/10.1016/j.tust.2018.10.019

Medici G, Smeraglia L, Torabi A, Botter C (2021) Review of Modeling Approaches to Groundwater Flow in Deformed Carbonate Aquifers. Groundwater 59(3):334–351.

https://doi.org/10.1111/gwat.13069

Middlemis H, Merrick N, Ross JB (2000) Groundwater Flow Modelling Guideline. Prepared for Murray-Darling Basin Commission by Aquaterra Consulting Pty Ltd. Project No. 125

Milan Metropolitan City (2019) Documento di piano Milano 2030 Visione, Costruzione, Strategie, Spazi [Milan 2030 plan document Vision, Construction, Strategies, Spaces]

Moghadam ST, Delmastro C, Lombardi P, Corgnati SP (2016) Towards a New Integrated Spatial Decision Support System in Urban Context. Procedia - Soc Behav Sci 223:974–981. https://doi.org/10.1016/j.sbspro.2016.05.334

Naranjo RC (2017) Knowing Requires Data. 55(5). https://doi.org/10.1111/gwat.12553

Nikvar Hassani A, Farhadian H, Katibeh H (2018) A comparative study on evaluation of steady-state groundwater inflow into a circular shallow tunnel. Tunn Undergr Sp Technol 73(December 2017):15–25. https://doi.org/10.1016/j.tust.2017.11.019

Nikvar Hassani A, Katibeh H, Farhadian H (2016) Numerical analysis of steady-state groundwater inflow into Tabriz line 2 metro tunnel, northwestern Iran, with special consideration of model dimensions. Bull Eng Geol Environ 75(4):1617–1627. https://doi.org/10.1007/s10064-015-0802-1

Noethen M, Hemmerle H, Bayer P (2022) Sources, intensities, and implications of subsurface warming in times of climate change. Crit Rev Environ Sci Technol :1–23

Panday S, Langevin CD, Niswonger RG, Ibaraki M, Hughes JD (2013) MODFLOW – USG Version 1: An Unstructured Grid Version of MODFLOW for Simulating Groundwater Flow and Tightly Coupled Processes Using a Control Volume Finite-Difference Formulation. US Geol Surv (Techniques and Methods 6-A45):66

Paradigm (2009) Paradigm GOCAD 2009.1 User Guide. Paradigm, Houston, TX

Parriaux A, Blunier P, Maire P, Tacher L (2007) The DEEP CITY Project: A Global Concept for a Sustainable Urban Underground Management. 11th ACUUS Int Conf Sp Expand Front Athens, Greece :255–260

Parriaux A, Tacher L, Kaufmann V, Blunier P (2006) Underground resources and sustainable development in urban areas

Peeters LJM (2017) Assumption Hunting in Groundwater Modeling: Find Assumptions Before They Find You. 55(5). https://doi.org/10.1111/gwat.12565

Previati A, Epting J, Crosta GB (2022) The subsurface urban heat island in Milan (Italy) - A modeling approach covering present and future thermal effects on groundwater regimes. Sci Total Environ 810:152119. https://doi.org/10.1016/j.scitotenv.2021.152119

Pulighe G, Lupia F (2019) Multitemporal geospatial evaluation of urban agriculture and (non)-sustainable food self-provisioning in Milan, Italy. Sustain 11(7). https://doi.org/10.3390/su11071846

Regione Lombardia (2016) Piano di Tutela ed Uso delle Acque (PTUA) [Water Protection and Use Plan (PTUA)]

Regione Lombardia (2021a) Open Data Regione Lombardia https:// dati.lombardia.it/. (Accessed on 15 December 2021)

Regione Lombardia (2021b) Geoportal of the Lombardy Region, Italy. http://www.geoportale.regione.lombardia.it/. (Accessed on 1 December 2021)

Regione Lombardia & ENI Divisione AGIP (2002) Geologia degli acquiferi Padani della Regione Lombardia [Geology of the Padan aquifers of the Lombardy Region]

Rumbaugh J, Rumbaugh O (2020) Groundwater Vistas Version 7.24, Build 211. Environ Simulations Inc, Reinholds, PA

Sartirana D, Rotiroti M, Bonomi T, De Amicis M, Nava V, Fumagalli L, Zanotti C (2022) Data-driven decision management of urban underground infrastructure through groundwater-level time-series cluster analysis: the case of Milan (Italy). Hydrogeol J 30(4):1157–1177. https://doi.org/10.1007/s10040-022-02494-5

Sartirana D, Rotiroti M, Zanotti C, Bonomi T, Fumagalli L, De Amicis M (2020) A 3D geodatabase for urban underground infrastructures: implementation and application to groundwater management in Milan metropolitan area. ISPRS Int J Geo-Information 9(10). https://doi.org/10.3390/ijgi9100609

Schirmer M, Leschik S, Musolff A (2013) Current research in urban hydrogeology - A review. Adv Water Resour 51:280–291. https://doi.org/10.1016/j.advwatres.2012.06.015

Shi S, Xie X, Bu L, Li L, Zhou Z (2018) Hazard-based evaluation model of water inrush disaster sources in karst tunnels and its engineering application. Environ Earth Sci 77(4):1–13. https://doi.org/10.1007/s12665-018-7318-5

Toscani L, Stefania GA, Masut E, Prieto M, Legnani A, Gigliuto A, Ferioli L, Battaglia A (2022) Groundwater flow numerical model to evaluate the water mass balance and flow patterns in Groundwater Circulation Wells (GCW) with varying aquifer parameters. Acque Sotter - Ital J Groundw. https://doi.org/10.7343/as-2022-515

Un-Habitat (2012) State of the World's Cities 2008/9: Harmonious Cities. Routledge: Oxford, UK, 2012; ISBN 1136556729.

Vähäaho I (2016) An introduction to the development for urban underground space in Helsinki. Tunn Undergr Sp Technol 55:324–328. https://doi.org/10.1016/j.tust.2015.10.001

Vázquez-Suñé E, Sánchez-Vila X (1999) Groundwater modelling in urban areas as a tool for local authority management: Barcelona case study (Spain). Impacts Urban Growth Surf Water Groundw Qual Proc IUGG 99 Symp HS5 (259):65–72

Vázquez-Suñé E, Sánchez-Vila X, Carrera J (2005) Introductory review of specific factors influencing urban groundwater, an emerging branch of hydrogeology, with reference to Barcelona, Spain. Hydrogeol J 13(3):522–533.

https://doi.org/10.1007/s10040-004-0360-2

Wang X, Lei Q, Lonergan L, Jourde H, Gosselin O, Cosgrove J (2017) Heterogeneous fluid flow in fractured layered carbonates and its implication for generation of incipient karst. Adv Water Resour 107:502–516. https://doi.org/10.1016/j.advwatres.2017.05.016

Wang X, Li S, Xu Z, Li X, Lin P, Lin C (2019) An interval risk assessment method and management of water inflow and inrush in course of karst tunnel excavation. Tunn Undergr Sp Technol 92(July):103033. https://doi.org/10.1016/j.tust.2019.103033

Wilkinson W (1985) Rising groundwater levels in London and possible effects on engineering structures. Proc 18th Congr Int Assoc Hydrogeol Cambridge :145–157

Wu JS, Lee JJ (2015) Climate change games as tools for education and engagement. Nat Clim Chang 5(5):413–418. https://doi.org/10.1038/nclimate2566

Xia Q, Xu M, Zhang H, Zhang Q, Xiao XX (2018) A dynamic modeling approach to simulate groundwater discharges into a tunnel from typical heterogenous geological media during continuing excavation. KSCE J Civ Eng 22(1):341–350. https://doi.org/10.1007/s12205-017-0668-9

Zaidel J, Markham B, Bleiker D (2010) Simulating seepage into mine shafts and tunnels with MODFLOW. Ground Water 48(3):390–400. https://doi.org/10.1111/j.1745-6584.2009.00659.x

Chapter 8: Conclusions

Urban areas are intricate systems, where a multitude of resources are available. As regards the subsurface, four main resources can be identified: energy, materials, space and water. A strong interaction between GW and the UIs has been evidenced in the last decades, triggering management problems both for GW and the subsurface elements. For this reason, considering that urbanization is a worldwide process, an integrated management is needed to secure all the UIs.

Within this general framework, the main aim of this PhD project was to develop methodologies and tools in order to provide a deep understanding of the interactions between GW and the UIs for Milan metropolitan city. This task is relevant considering that, within the adoption of the Plan of Government of the Territory, a further subsurface development has been defined as a main goal to achieve.

To provide support to the decision makers, this work addressed three main topics concerning urban underground management. In particular:

1. the first topic concerned the implementation of a 3D GDB listing all the UIs located within the study area. For this specific purpose, a GIS methodology to gather all the available information was developed, using Open Data as the primary source of information. In this way, depending on data availability, the procedure can be tested and applied elsewhere in other urban domains; subsequently, the most critical areas showing a condition of submersion for the UIs (i.e. volumes of UIs lying below the water table) have been identified;

2. the second topic dealt with the application of data-driven techniques on GW time-series of the shallow aquifer. The investigation aimed at pinpointing the main factors influencing the water table behaviour, to identify areas having similar hydrogeologic features. Subsequently, management proposals for the construction of new UIs were defined for each of these hydrogeologic areas;

3. the third topic regarded the implementation of a local scale numerical model for the western portion of Milan city to further analyse GW/UIs interactions; in

particular, the main goal was to develop and test a methodology to quantify GW infiltrations into UIs.

The development of this work allowed for different considerations that are summarized in the following paragraphs.

8.1. Implementation of a 3D Geodatabase (GDB) for urban underground infrastructures (UIs)

Overall findings of this first part of the PhD project showed how the implementation of a 3D GDB for UIs in urban areas is time consuming. In fact, the development of the GIS methodology required different steps to generate the final outcome. However, this activity is essential in order to gather reliable information to develop GW numerical models.

The Topographic Database (DbT) was used as the main source of information. Using Open Data, superficial buildings having a possible subsurface development were both identified and quantified, thus storing information about private car parks. To do so, the presence of the dressing lines inside the DbT was pivotal. This constitutes an element of novelty, as no evidence in literature regarding this procedure has been detected before. In addition, as the DbT is developed following European Standards, this procedure could be replied elsewhere.

As for public car parks, only an Open Data list was available. To insert them in the GDB, a manual digitization of the perimeters of the parks was executed. Few elements present in the DbT (i.e. ventilation grilles) were used as markers for the digitization. Similarly, a manual process was conducted to digitize and store information for the subway lines. The digitization was realized according to their altimetric profiles that were provided by the subway managing company, thus obtaining a centimetric geometric accuracy.

Hence, the methodology evidenced the benefits deriving from using Open Data, also revealing how the information is still fragmented and scattered among the stakeholders, that sometimes ignore the presence of other management sectors. The heterogeneity of current available information shows the importance of standards for GDBs; to define them, engaging decision makers, favouring a continuous exchange of information between the stakeholders and the Universities could lead to beneficially support urban underground management. In this sense, the sharing of information with the subway managing company highlights how symbiotic relationships between stakeholders and research groups could lead to an efficient management of UIs information in urban environments.

The 3D GDB was designed as flexible and simple enough to be easily adopted for GW numerical models and other management purposes. The database structure allows also an easy integration of further information that could become available in the future, thus taking into account future urban planning changes.

As for modelling needs, the bottom and the volume of the UIs are two essential information. These data have been used to test the application of the GDB, identifying and estimating conditions of submersion of the UIs over the years. Main findings were coherent with the historical information of flooded areas for Milan city. This can act as a sort of validation of the methodology, also checking the reliability of the GDB.

Finally, the adoption of 3D maps could create awareness and commitment towards an urban underground future. This approach could help to move from a sectorial strategy, considering only a single UI, to a more integrated approach, providing a comprehensive planning framework. This could contribute to avoid jeopardizing the underground resources, thus providing valuable support to the decision makers in the framework of a long-term multi-use adoption of the subsurface.

8.2. Hydrodynamic characterization of the shallow aquifer to support underground management

Findings of the analysis conducted in this second part of the thesis demonstrated how GW time-series can be effectively interpreted by data-driven techniques. One of the main benefits of using these techniques is that they do not require an extensive approximation of the boundary parameters and the local geological conditions of the investigated domain. Notwithstanding, both univariate (i.e. autocorrelation) and bivariate (i.e. cross correlation) statistics proved to be self-sufficient and capable of extracting exhaustive information from all the available data.

The study was conducted on 95 monitoring wells, monitored over the 2005-2019 time's span. Two measures per year were available (March and September) for a total of 30 observations. This amount of information was fundamental to gain knowledge regarding the seasonality of some GW processes. Thus, it can be recommended as a minimum size to consider, when enough data are available. As for Milan, the monitoring network is undergoing a progressive downsizing over the years, presumably both for time and economic reasons. The application of data-driven techniques could support the decision makers in optimizing this shrinking process; reducing the dimension of the monitoring network could be accepted as long as not too much potential to capture the entire variability of the system is lost.

A similar spatial zoning of the results was obtained for all the statistical techniques, and was also confirmed by the water table reconstruction of different GW conditions that was realized by means of geospatial techniques.

To identify the GW conditions for the piezometric reconstruction, an R script was developed. The aim of this script was to deal with reversal points analysis, overcoming possible limitations that have been evidenced in literature for widely applied statistical tests (i.e. Pettitt test). The methodology proved to be efficient, as a good coherence among the results was obtained in identifying both GW minimum (September 2007) and maximum conditions (March 2015).

A clear rising trend has been detected in the northern portion of the area, where high values of autocorrelation and a lag response to precipitations are visible. Here, the water table is located 10-15 meters below the ground surface. Thus, the thickness of the unsaturated zone plays a contributory role in determining the degree of both correlation and autocorrelation, determining a higher memory of the GW system. Vice versa, the western and the southern monitoring wells respectively showed not significant, or low significant rising trends, low values of autocorrelation, but a more rapid response to precipitations. Here, geological evidences, as the presence of clay lenses, constrain the water table close to the ground surface, thus limiting its possibility of oscillation. Seasonal oscillations in the West, with peaks at September, are a tangible effect of the irrigation activities conducted during the summer. Thus, this area also shows a more rapid response to external drivers. As for the downtown, the piezometric trends are mostly influenced by the presence of an anthropogenic control that limits the water table rising due to an extensive, but mostly non-consumptive use of GWHPs and the presence of UIs. This meaningful classification proved that, even in a rather limited domain, significant differences in GW behaviour could be detected.

Hence, all these techniques allowed for a detailed description of this urban GW system, proving to be valuable tools to support the identification of the variables influencing the aquifer behaviour, highlighting also their spatial variability. The definition of targeted management proposals for the construction of new public car parks was thus facilitated by these results. To sum up, their application could be taken into account to support the development and refinement of the conceptual model in complex hydrogeologic systems as urban areas, providing also cost-effective assistance to the development of numerical models.

8.3. GW/ UIs interactions

Overall findings of this last part of the PhD project allowed to provide a preliminary estimate of GW infiltrations into UIs. This topic has been mostly investigated in literature to quantify flooding episodes during tunnels' construction, while only few studies deal with the quantification of GW infiltrations once the infrastructures are fully in operation. This may be due to the GW volumes involved in these interactions, that can differ of several orders of magnitude. However, even infiltrations must be considered as a threat for the UIs, as they could determine corrosion and stability issues over long periods. Within the framework of sustainability in urban areas, this could lead to undesired financial expenses. Historically, this problem has been already documented for the city of Milan, mainly triggered by the industrial decommissioning that caused the GW rebound. This evidences the importance of adopting a method to quantify GW infiltrations.

The key point of the methodology was the adoption of MODFLOW-USG as the code to develop the numerical model. The presence of grid nodes rather than rows and columns allowed to use the HFB package to set wall cells not only on the lateral sides, but also at the top and the bottom cells of subsurface elements. The wall conductance is the parameter that controls the infiltration. The combination with the DRN package, and an evaluation of the mass balance allowed then to quantify these infiltrations.

The absence of existing information about GW infiltrations limits the possibility of fully evaluating the reliability of the results. To make numerical models useful and predictive tools for urban GW management, a strict cooperation between the administrations and the researchers becomes crucial. However, in order to provide different scenarios to the stakeholders, walls conductance has been modified, especially for non-waterproofed subway lines, simulating a possible saturation over time. Also, walls fractures have been modelled to analyse possible side effects caused by this prolonged interaction with the water table.

The areas identified as critical in this study have been already classified in the past as areas where GW and UIs were interacting. As an example, the westmost stretch close to

Bisceglie station for subway line M1, and the surroundings of Sant'Agostino station for subway line M2 have been historically documented as critical in previous studies. Moreover, they have been also detected as submerged in the first part of this PhD project. This could have a double meaning: first, it could prove the effectiveness of the numerical model, as a good spatial coherence with historical results has been identified; in addition, the adopted methodology could represent a step forward in the definition of the urban conceptual model, moving from just identifying interactions to quantify the consequent infiltrations.

To sum up, the implementation of this local scale numerical model allowed to identify the most critical areas suffering GW infiltrations. In this way, different management solutions can be adopted to face this issue, in order to secure these infrastructures from being flooded in the future, protecting them from negative impacts as corrosion or stability issues. Finally, the adoption of the model could support the stakeholders to consider the relation between GW and the new UIs that will be designed in the framework of the future subsurface development.

8.4. Final remarks

In conclusion, the research work and the results of this PhD led to the following considerations:

1. 3D GDBs of UIs are important tools to understand the relation among all the subsurface resources and to create awareness and commitment to promote a more sustainable development of the urban underground.
2. Data-driven techniques can support the definition and improvement of the conceptual model in urban systems, highlighting the main natural and anthropogenic factors governing the water table behaviour.
3. Numerical models represent a valid instrument to manage the interactions between GW and UIs, as they guarantee the possibility of quantifying this phenomenon. Through their application, it can be possible to adopt management solutions to secure UIs.

On the whole, the combination of all these methodologies and tools can provide a deep knowledge of urban aquifer systems, thus bringing valuable support to stakeholders and decision makers to understand, manage and quantify GW/UIs interactions. An integrated approach, considering all the underground resources not as separate entities, is needed to properly manage the future urban underground development of the cities.

Appendix A: Articles and Presentations

Published articles

1. **Sartirana D,** Zanotti C, Rotiroti M, De Amicis M, Caschetto MC, Redaelli A, Fumagalli L, Bonomi T (2022). Quantifying groundwater infiltrations into subway lines and underground car parks using MODFLOW-USG. Water, 2022, 14(24), 4130. https://doi.org/10.3390/w14244130

2. Bonomi T, **Sartirana D,** Toscani L, Stefania GA, Zanotti C, Rotiroti M, Redaelli A, Fumagalli L (2022). Modeling groundwater/surface-water interactions and their effects on hydraulic barriers, the case of the industrial area of Mantua (Italy). *Acque Sotterranee - Italian Journal of Groundwater*, *11*(2), 43–55. https://doi.org/10.7343/as-2022-569

3. **Sartirana D,** Rotiroti M, Bonomi T, De Amicis M, Nava V, Fumagalli L, Zanotti C (2022). Data-driven decision management of urban underground infrastructure through groundwater-level time-series cluster analysis: the case of Milan (Italy). Hydrogeology Journal, 1-21. https://doi.org/10.1007/s10040-022-02494-5

4. **Sartirana D,** Rotiroti M, Zanotti C, Fumagalli L, Bonomi T, De Amicis M (2020). A 3D Geodatabase for urban underground infrastructures: implementation and application to groundwater management in Milan metropolitan area. ISPRS International Journal of Geo-Information. 2020; 9(10):609. https://doi.org/10.3390/ijgi9100609
5. Fumagalli L, Stefania GA, Zanotti C, **Sartirana D,** Di Martino GR, Perosa A, Valentini P, Rotiroti M, Bonomi T (2020). Multivariate statistical analysis and numerical modelling for the hydrogeological and hydrochemical characterization of a closed MSW landfill: the case study of Vizzolo-Predabissi. *Acque Sotterranee-Italian Journal of Groundwater*, *9*(1). https://doi.org/10.7343/as-2020-431

Communication to conferences

1. **Sartirana D,** Rotiroti M, Bonomi T, De Amicis M, Fumagalli L, Zanotti C (2021). Groundwater time-series analysis supporting urban underground infrastructures management: the Milan city (Italy) case study. XV Convegno Nazionale GIT. Session: "Metodi e Strumenti Data-Driven per la Gestione e Protezione delle Risorse Idriche Sotterranee". Ripatransone, 20-21 December 2021. http://hdl.handle.net/10281/392457 (Oral presentation).
2. Bonomi T, Fumagalli L, Toscani L, **Sartirana D,** Stefania GA, Zanotti C, Rotiroti M, Pena Reyes FA, Bonomi S, Spaggiari M, Bianchi A (2021). Modeling groundwater/surface-water interactions in an industrial area (Mantua, Italy). In Flowpath 2021 Conference Proceedings Book (pp.75-75). http://hdl.handle.net/10281/365532 (Poster).
3. Zanotti C, Fumagalli L, Rotiroti M, Caschetto MC, **Sartirana D,** Redaelli A, Bonomi T (2021). Hydrogeochemical characterization as a tool to perform risk assessment on wells, springs, and surface water intake in the scope of the Water Safety Plan. In Flowpath 2021 Conference Proceedings Book (pp.39-39). http://hdl.handle.net/10281/365522 (Oral presentation)
4. **Sartirana D,** Zanotti C, De Amicis M, Rotiroti M, Fumagalli L, Bonomi T (2021). Application of multivariate statistical techniques for groundwater spatio-temporal analysis: the case study of Milan metropolitan Area. In Flowpath 2021 Conference Proceedings Book (pp.74-74). http://hdl.handle.net/10281/365526 (Poster).
5. Zanotti C, Rotiroti M, Fumagalli L, Caschetto MC, **Sartirana D,** Bonomi T (2021). Hydrogeological and hydrochemical characterization to assess wells vulnerability in the scope of Water Safety Plans, a case study in Northern Italy. In EGU General Assembly 2021. https://doi.org/10.5194/egusphere-egu21-2106 (Oral Presentation).
6. Castelli C, De Amicis M, **Sartirana D,** De Vita D, Favini M, Convertini A (2021). Attività di formazione e prevenzione delle emergenze idrogeologiche in Regione Lombardia. XLII Conferenza Italiana di Scienze Regionali.

(https://www.aisre.it/wp-content/uploads/2021/09/2021-Abstract-book-06.pdf). (Abstract).

7. **Sartirana D,** De Amicis M, Bonomi T (2021). Interferenze falda – infrastrutture sotterranee: analisi per la città di Milano. Conferenza ESRI Italia 2021. Session: "Soluzioni per la gestione del rischio e delle emergenze". https://www.esriitalia.it/media/sync/SartiranaDavide_ConferenzaESRI_2021.pdf (Oral presentation).
8. Castelli C, De Amicis M, **Sartirana D,** De Vita D, Favini M (2020). Prevenzione e gestione di emergenze sismiche: i laboratori permanenti realizzati in Regione Lombardia, ID 9000, pag.255, XLI Conferenza scientifica annuale AISRe online– 2-4 September 2020 (https://aisre.it/images/Conferenza_2020_Lecce/2020-Abstract-book-03.pdf). (Abstract).